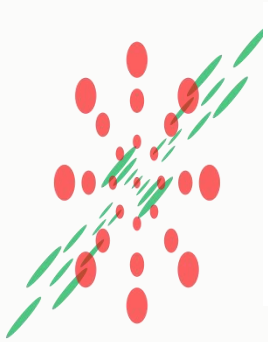

上智大学
SOPHIA UNIVERSITY

From heavy-ion to small systems and forward region: Effects from early stage dynamics

Shujun Zhao, Sophia University

Intersection of nuclear structure and high-energy nuclear collisions 2026

2026.04 Kyoto, Japan

Relativistic Heavy-Ion Collisions

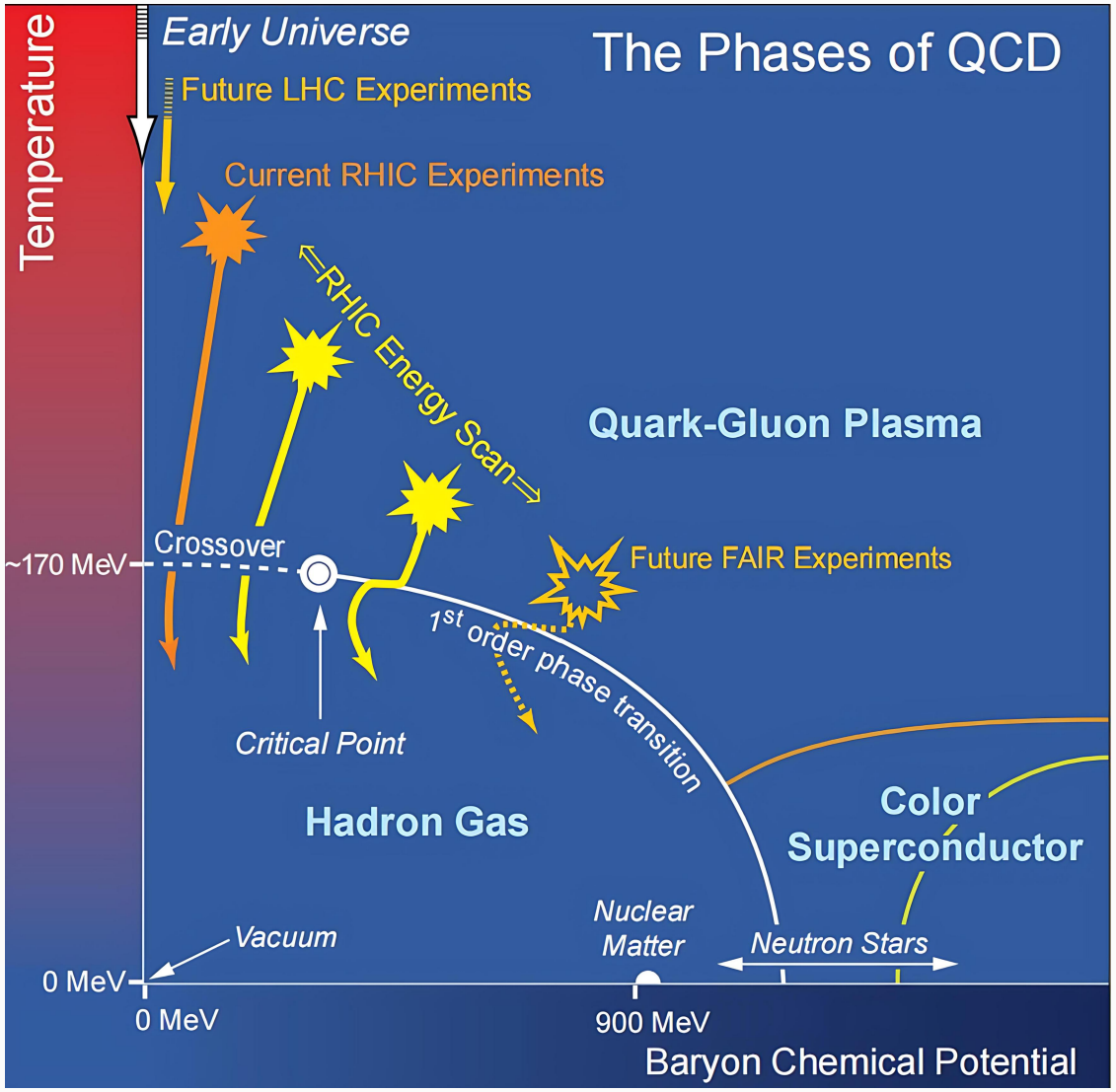

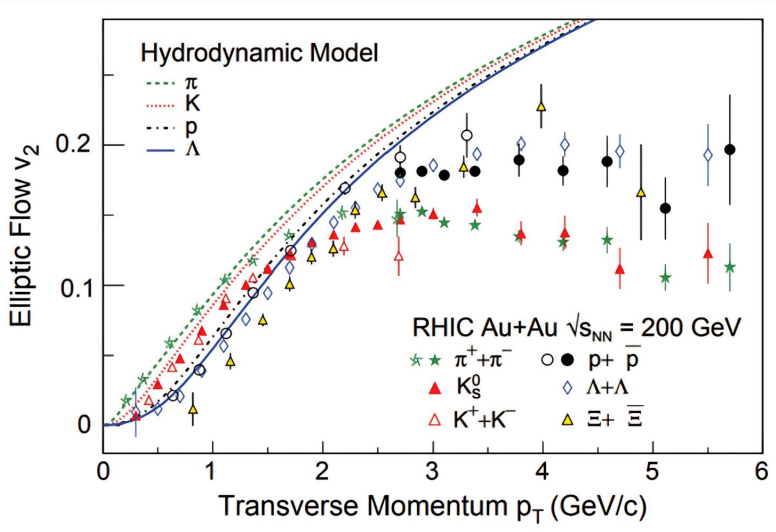

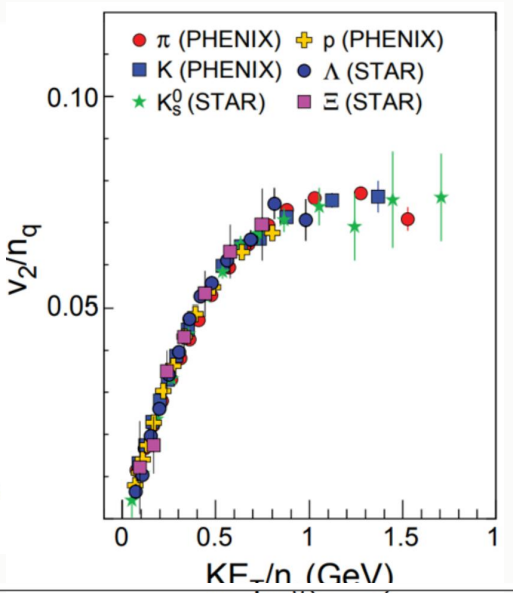

Hydrodynamic features of QGP

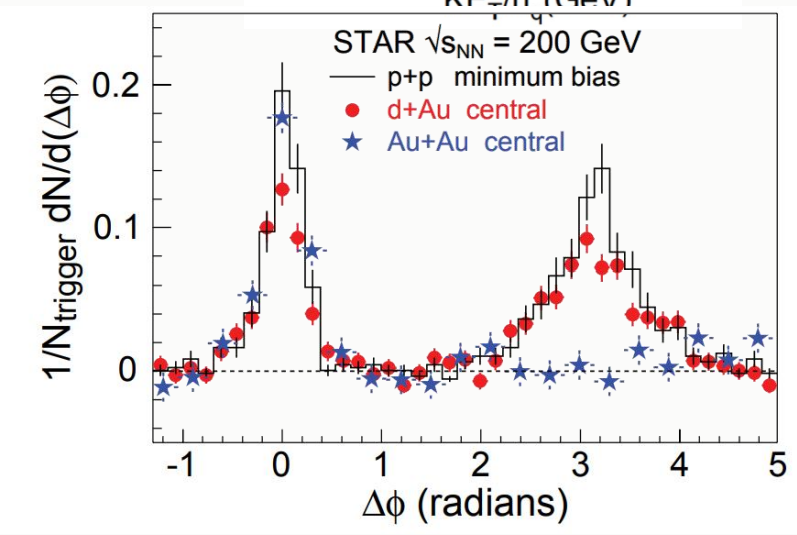

Relativistic Heavy-Ion Collisions

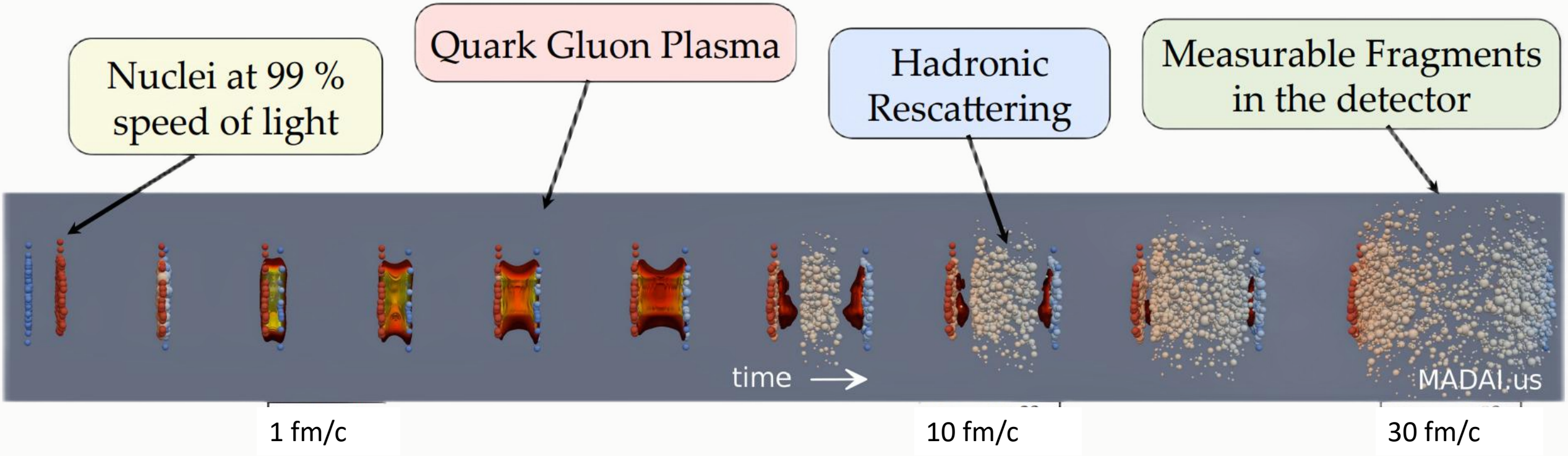

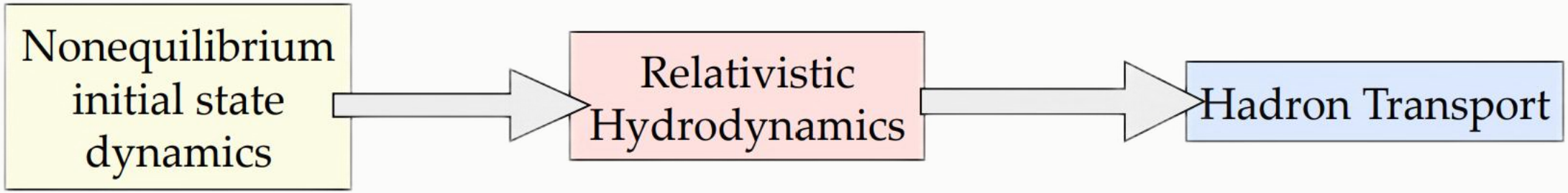

1. Hydrodynamization largely wash out details of pre-eq evolution
2. Pressure gradient driven expansion → Initial-Final stage mapping

Relativistic Heavy-Ion Collisions

Nuclear structure → Imaging → **Initial state** → $F = -\nabla P(\epsilon)$ hydro-response → **Final state**

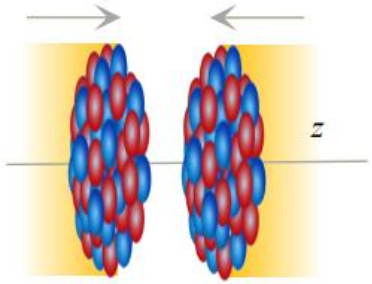

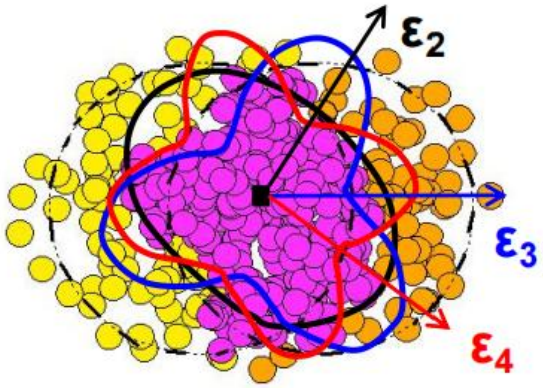

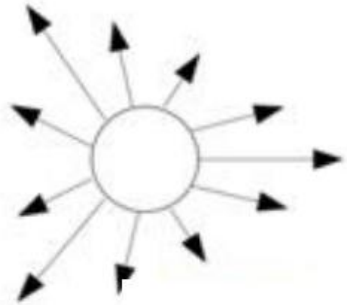

$$\rho(r,\theta,\phi) = \frac{\rho_0}{1+e^{(r-R(\theta,\phi))/a_0}}$$

$$R(\theta,\phi) = R_0(1+\beta_2[\cos\gamma Y_{2,0}(\theta,\phi) + \sin\gamma Y_{2,2}(\theta,\phi)] + \beta_3 Y_{3,0}(\theta,\phi))$$

- β_2 → Quadrupole deformation
- β_3 → Octupole deformation
- γ → Triaxiality
- a_0 → Surface diffuseness
- R_0 → Nuclear size

Initial Size $R_\perp^2 \propto \langle r_\perp^2 \rangle$ **Initial Shape** $\mathcal{E}_n \propto \langle r_\perp^n e^{in\phi} \rangle$

R_0 a_0 β_n

Radial Flow **Anisotropic Flow**

$$\frac{d^2N}{d\phi dp_T} = N(p_T)\left(\sum_n V_n e^{-in\phi}\right)$$

$$N_{ch} \propto N_{part} \quad \frac{\delta[p_T]}{[p_T]} \propto -\frac{\delta R_\perp}{R_\perp} \quad V_n \propto \mathcal{E}_n$$

High energy Heavy-Ion Collisions:

Large multiplicity and boost invariance; approximate linear response in each event

Precise constrain on the nuclear structures

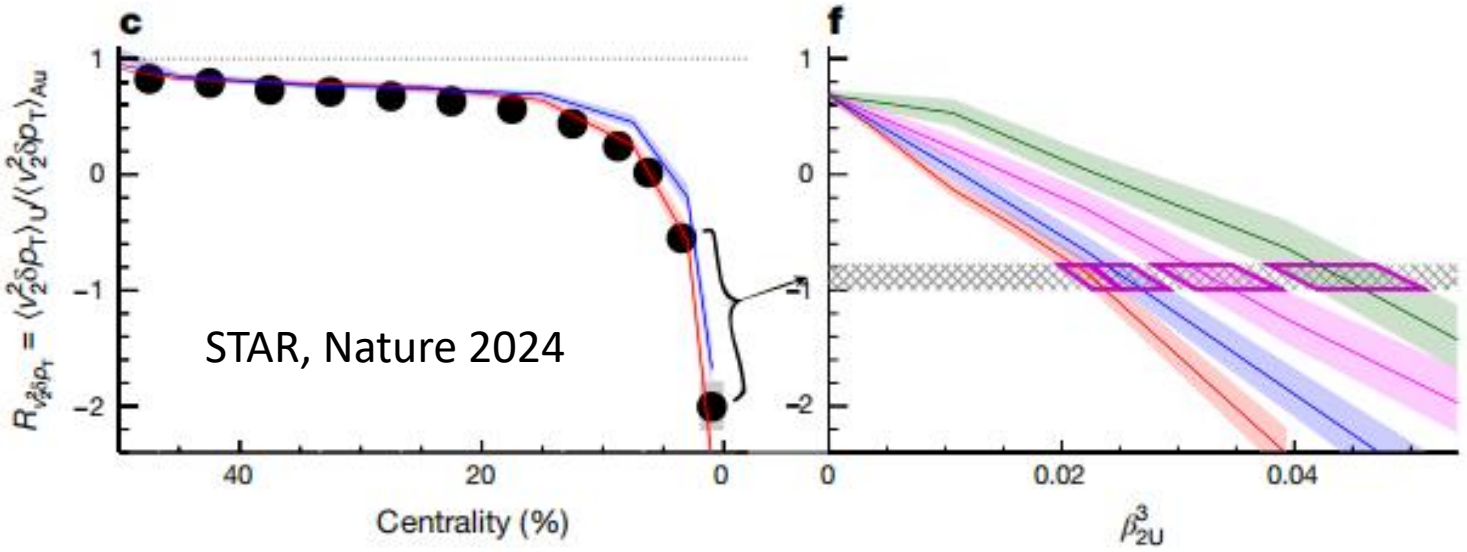

Rept.Prog.Phys. 88 (2025) 10, 108601

H. Li, H. Xu, F. Wang, et. al.
PRL 125 222301

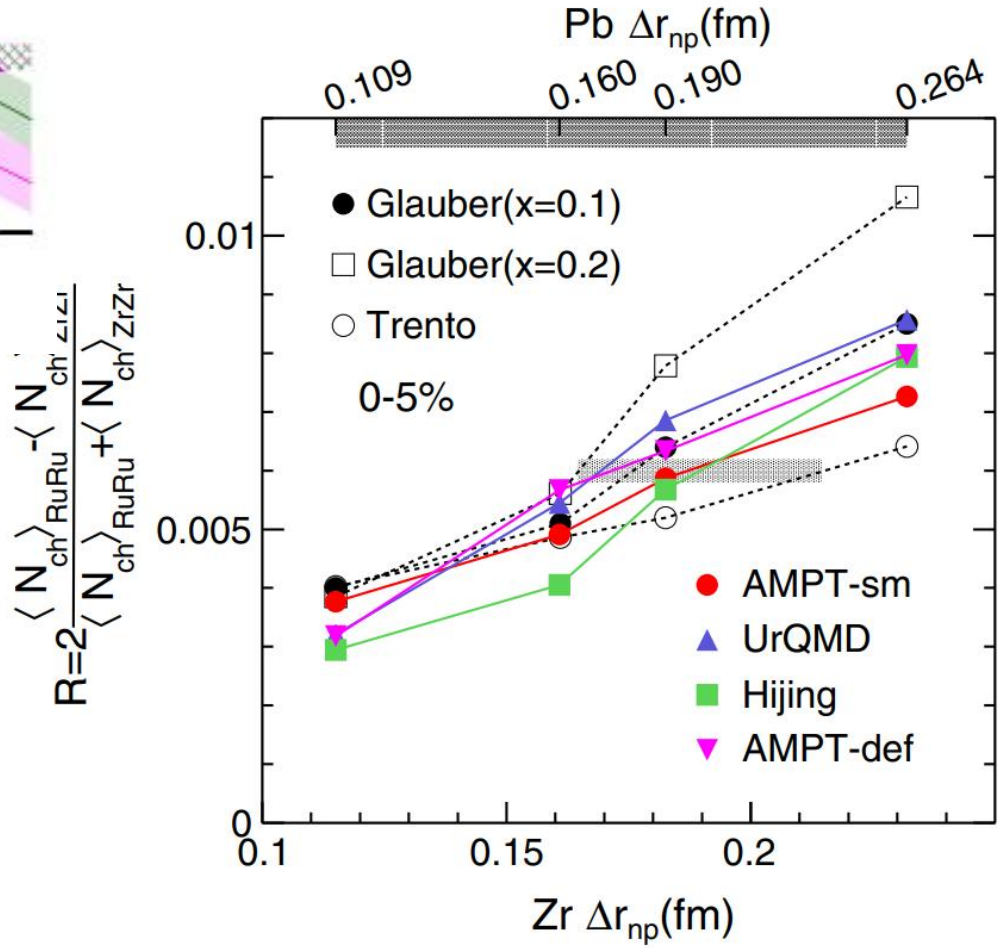

Quantitative level constrain can be reached for calibrating the heavy nucleus structure.

Validity of hydrodynamics can be reflected accordingly.

Heavy-Ion

Light-Ion

p+p

Hybrid model valid

May valid?

?

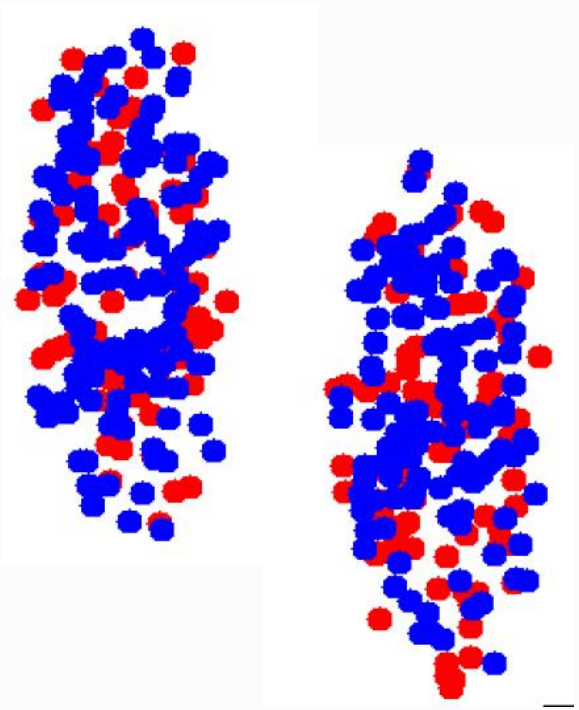

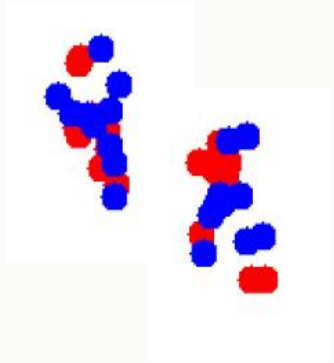

Applying Hydrodynamics in Small Systems

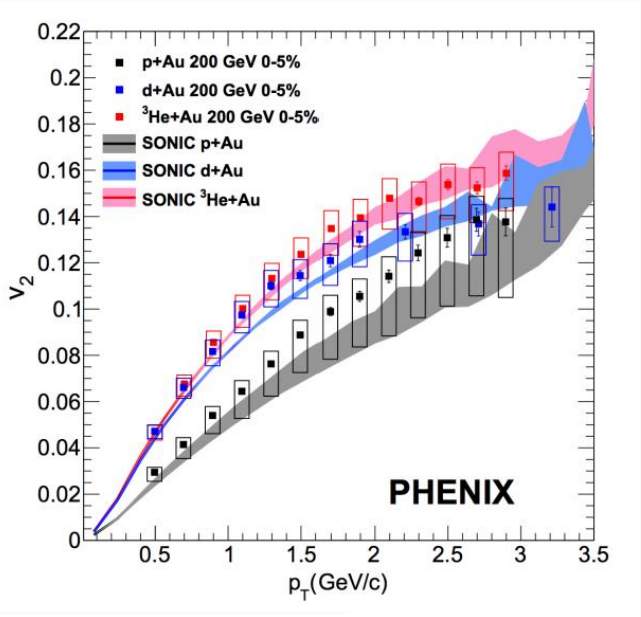

J. Carlson, et. al. Phys. Rev. Lett. 113 (2014) no. 11, 112301,

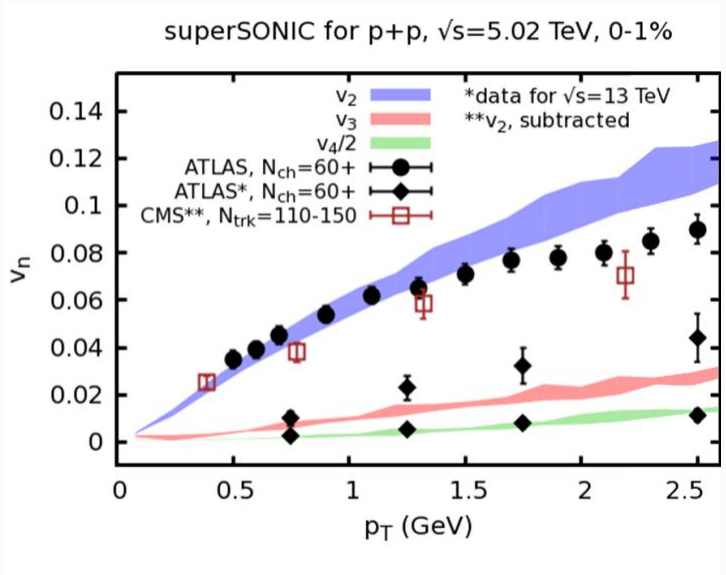

Weller, et. al. Phys.Lett.B 774 (2017) 351-356

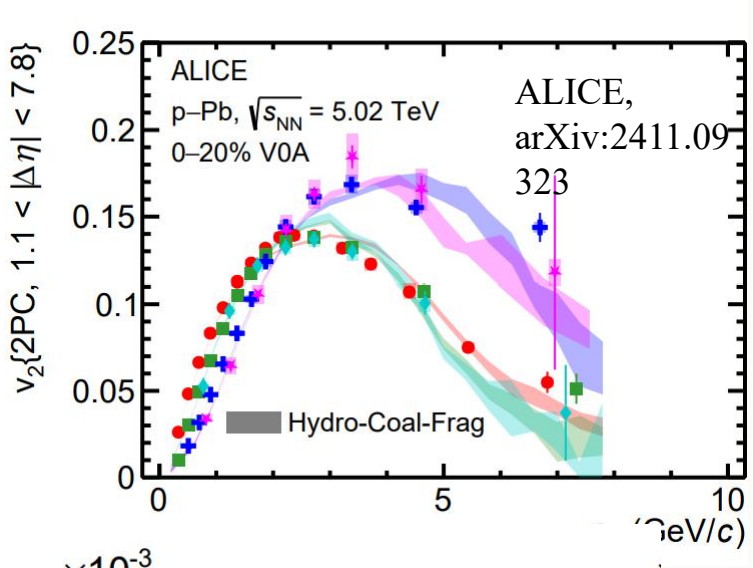

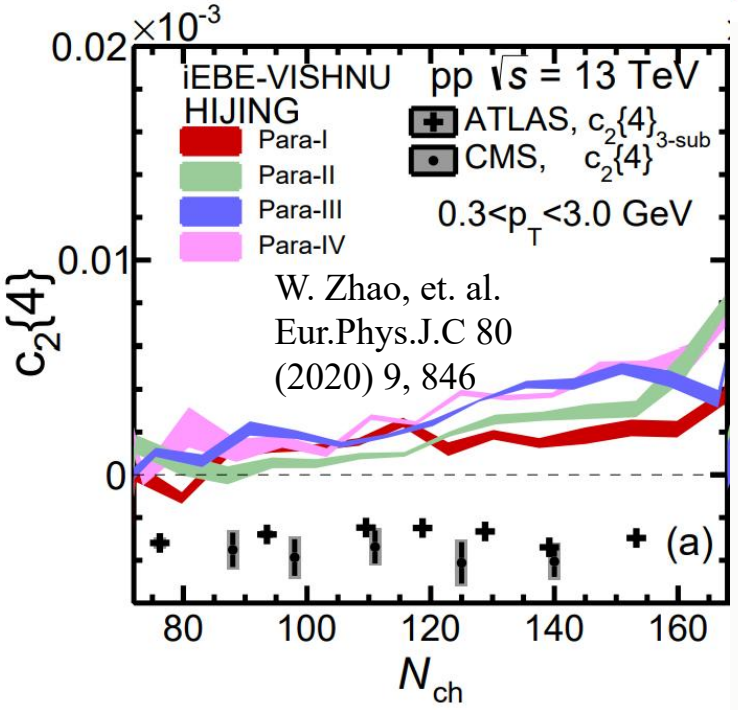

- Experimental side:
  Non-flow subtrction
  Multiplicity fluctuations
  Kinetic acceptance
  …

- Theoretical side:
  Subnuclonic structure
  Early stage dynamics
  Hybrid approach
  …

Hydro partially works and debet remains

Validaty of Hydrodynamics

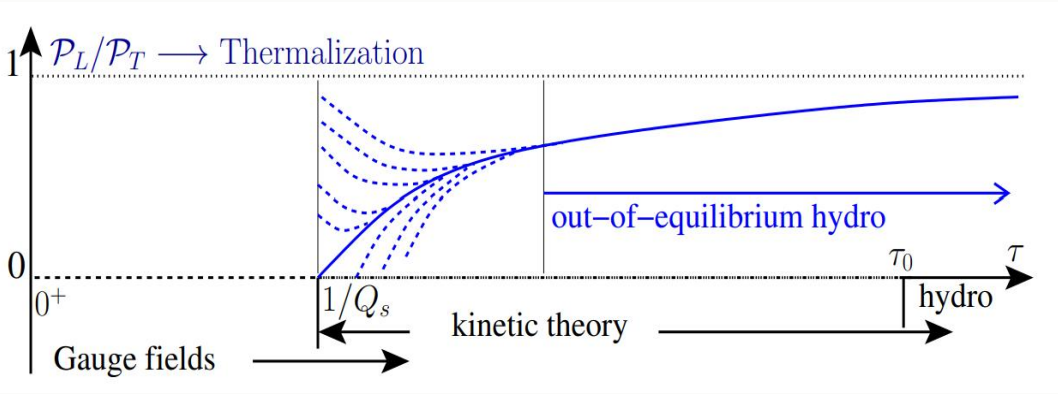

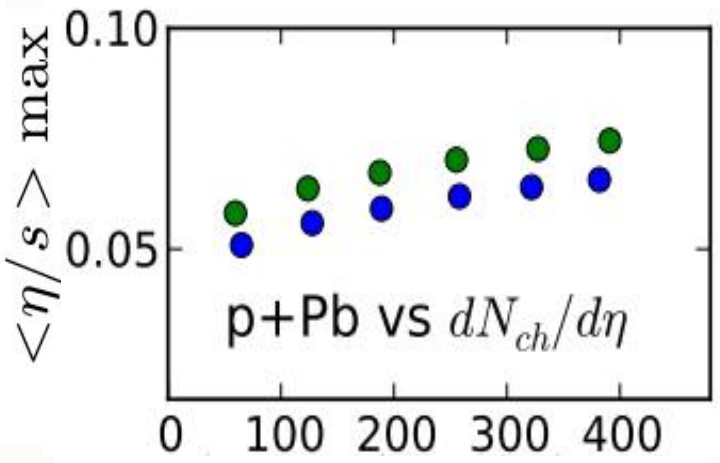

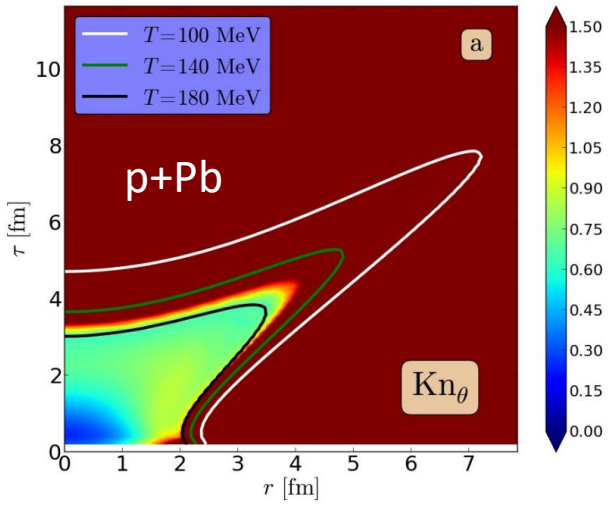

H. Niemi, et. al. arXiv: 1404.7327

- Large Deviations from Equilibrium

Initial anisotropic expansion

Small system size

Large shear viscous correction

...

- Extending the Applicability of Hydro

Attractor behavior

Resummed hydrodynamics

...

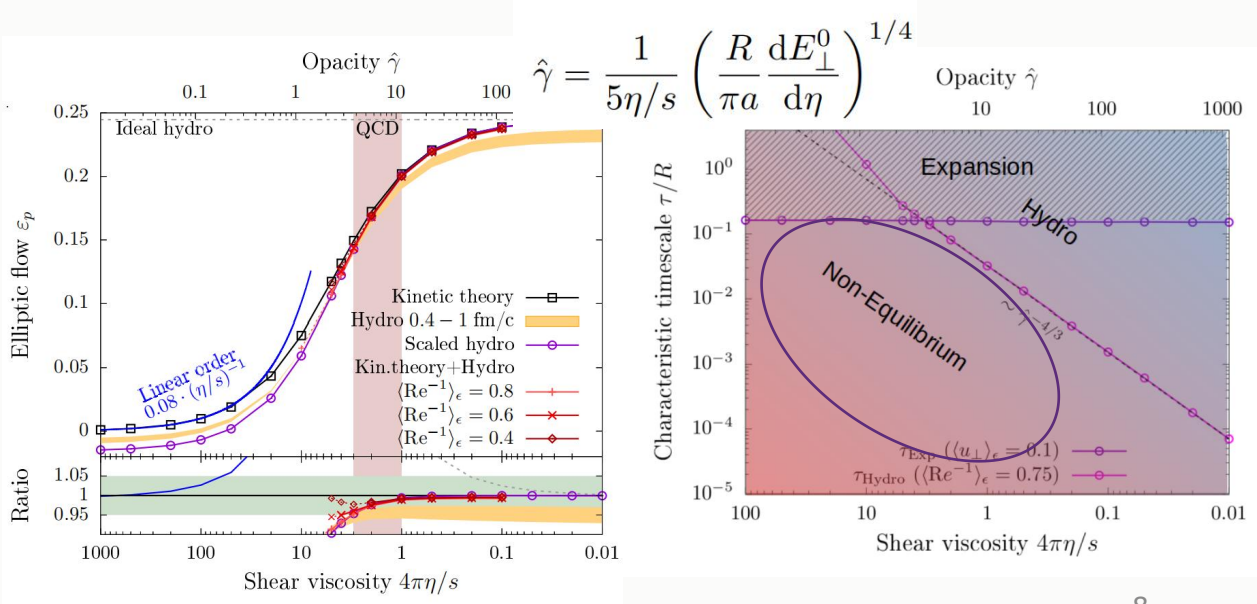

V. E. Ambrus, et. al. Phys.Rev.Lett. 130 (2023) 15, 152301

Viscous Anisotropic Hydrodynamics

- Redecomposition of $T^{\mu\nu}$:

$$T^{\mu\nu} = \mathcal{E}u^\mu u^\nu + \mathcal{P}_L z^\mu z^\nu - \mathcal{P}_\perp \Xi^{\mu\nu} + 2W_{\perp z}^{(\mu} z^{\nu)} + \pi_\perp^{\mu\nu},$$

Pressure Anisotropy

Residual Shear Stress

- Redecomposition of viscous term

$$\pi^{\mu\nu} = \frac{1}{3}(\mathcal{P}_L - \mathcal{P}_T)(2z^\mu z^\nu + \Xi^{\mu\nu}) + 2W_{\perp z}^{(\mu} z^{\nu)} + \pi_\perp^{\mu\nu}$$

$$\Pi = \frac{1}{3}(\mathcal{P}_L + 2\mathcal{P}_T) - \mathcal{P}_{\rm eq}$$

Viscous Anisotropic Hydrodynamics

- Redecomposition of $T^{\mu\nu}$:

$$T^{\mu\nu} = \mathcal{E}u^\mu u^\nu + \mathcal{P}_L z^\mu z^\nu - \mathcal{P}_\perp \Xi^{\mu\nu} + 2W_{\perp z}^{(\mu} z^{\nu)} + \pi_\perp^{\mu\nu},$$

Pressure Anisotropy

Residual Shear Stress

- Redecomposition of viscous term

$$\pi^{\mu\nu} = \frac{1}{3}(\mathcal{P}_L - \mathcal{P}_T)(2z^\mu z^\nu + \Xi^{\mu\nu}) + 2W_{\perp z}^{(\mu} z^{\nu)} + \pi_\perp^{\mu\nu}$$

$$\Pi = \frac{1}{3}(\mathcal{P}_L + 2\mathcal{P}_T) - \mathcal{P}_{\rm eq}$$

- Anisotropic particle distribution:

$$f_a(x,p) = f_{\rm eq}\left(\frac{\sqrt{\Omega_{\mu\nu}p^\mu p^\nu}}{\Lambda(x)}\right).$$

$$\Omega_{\mu\nu}p^\mu p^\nu = m^2 + \frac{p_{\perp,\rm LRF}^2}{\alpha_\perp^2} + \frac{p_{z,\rm LRF}^2}{\alpha_L^2}.$$

$(\Lambda, \alpha_L, \alpha_\perp)$ determined from the generalized Landau matching condition.

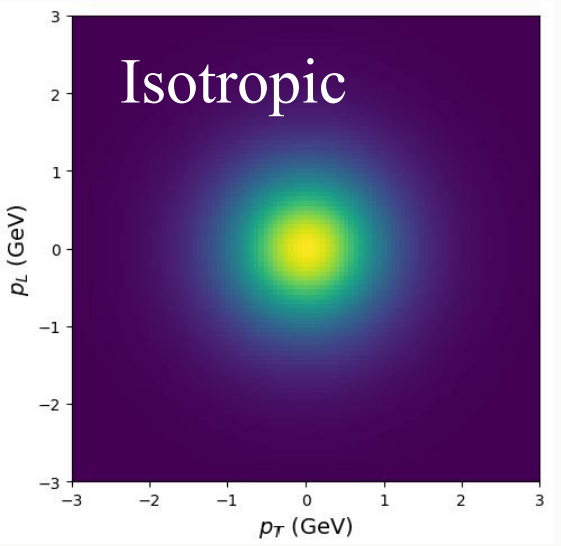

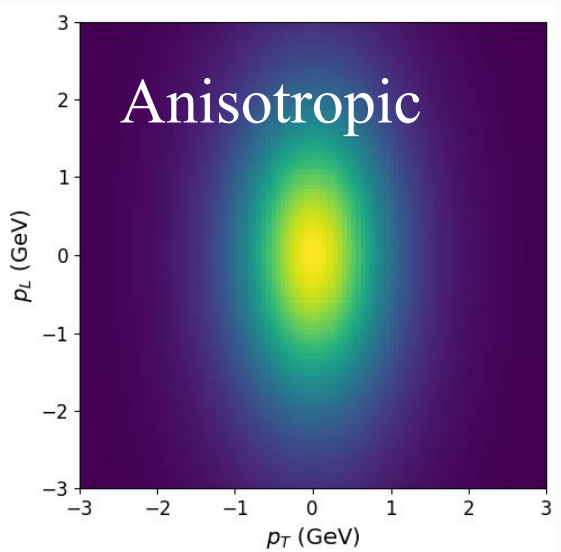

Viscous Anisotropic Hydrodynamics

- Redecomposition of $T^{\mu\nu}$:

$$T^{\mu\nu} = \mathcal{E}u^\mu u^\nu + \mathcal{P}_L z^\mu z^\nu - \mathcal{P}_\perp \Xi^{\mu\nu} + 2W_{\perp z}^{(\mu} z^{\nu)} + \pi_\perp^{\mu\nu},$$

Pressure Anisotropy

Residual Shear Stress

- Resummation over different orders

$$\begin{aligned}
\bar{\zeta}_z^L &= -c_s^2(\mathcal{E}+\mathcal{P}_L) - \frac{4\eta}{3\tau_\pi} - \frac{\zeta}{\tau_\Pi} - \delta_{\Pi\Pi}(\bar{\mathcal{P}}-\mathcal{P}_{\rm eq}) - \frac{2}{3}\delta_{\pi\pi}(\mathcal{P}_L-\mathcal{P}_\perp) + \cdots \\
\bar{\zeta}_\perp^L &= -c_s^2(\mathcal{E}+\mathcal{P}_\perp) + \frac{2\eta}{3\tau_\pi} - \frac{\zeta}{\tau_\Pi} - \delta_{\Pi\Pi}(\bar{\mathcal{P}}-\mathcal{P}_{\rm eq}) - \frac{2}{3}\delta_{\pi\pi}(\mathcal{P}_L-\mathcal{P}_\perp) + \cdots \\
\bar{\zeta}_z^\perp &= -c_s^2(\mathcal{E}+\mathcal{P}_L) - \frac{4\eta}{3\tau_\pi} - \frac{\zeta}{\tau_\Pi} - \delta_{\Pi\Pi}(\bar{\mathcal{P}}-\mathcal{P}_{\rm eq}) + \frac{1}{3}\delta_{\pi\pi}(\mathcal{P}_L-\mathcal{P}_\perp) + \cdots \\
\bar{\zeta}_\perp^\perp &= -c_s^2(\mathcal{E}+\mathcal{P}_\perp) + \frac{2\eta}{3\tau_\pi} - \frac{\zeta}{\tau_\Pi} - \delta_{\Pi\Pi}(\bar{\mathcal{P}}-\mathcal{P}_{\rm eq}) + \frac{1}{3}\delta_{\pi\pi}(\mathcal{P}_L-\mathcal{P}_\perp) + \cdots \\
&\cdots \quad \cdots
\end{aligned}$$

Isotropic transport coefficients

Anisotropic transport coefficients

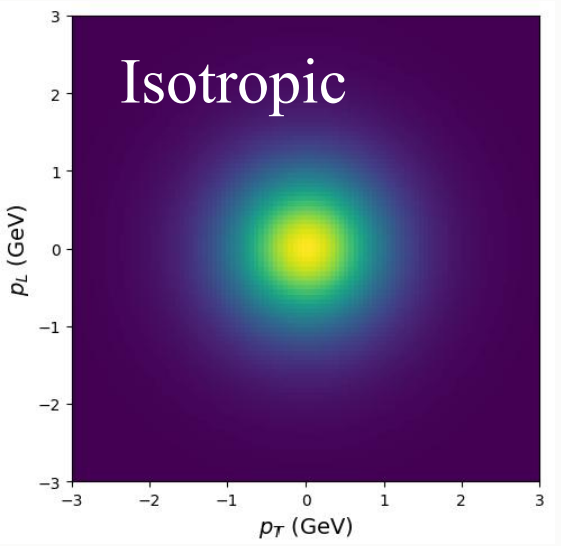

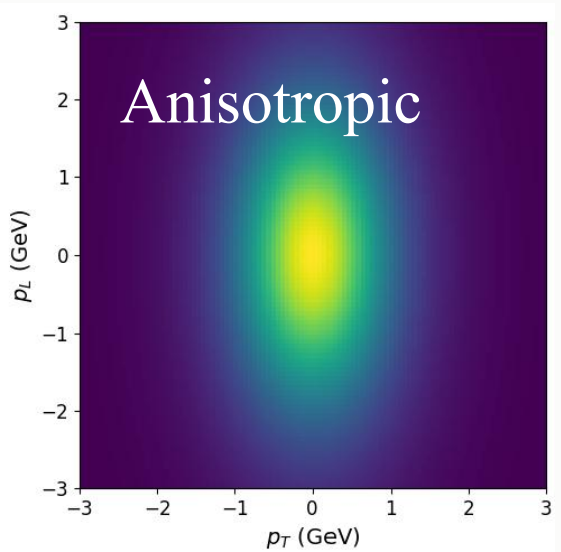

Model Framework

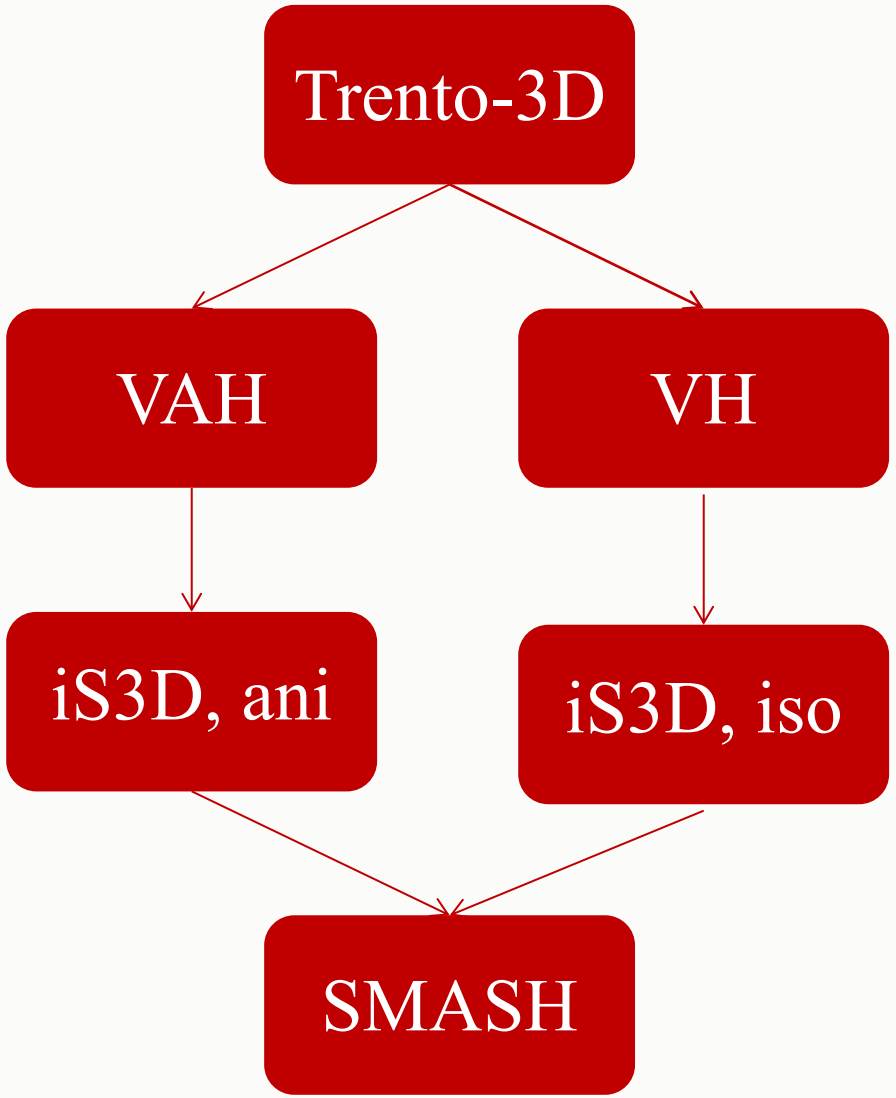

- Initial energy deposition

$$\mathcal{E}_{\rm tot} = \mathcal{E}_{\rm fb} + \mathcal{E}_{\rm frag,A} + \mathcal{E}_{\rm frag,B}$$

- Hydro evolution

$$T^{\mu\nu} \sim (\mathcal{E}, u^\mu, \mathcal{P}, \pi^{\mu\nu}, \Pi)$$

$$T^{\mu\nu} \sim (\mathcal{E}, u^\mu, \mathcal{P}_L, \mathcal{P}_T, W^\mu_{\perp z}, \pi^{\mu\nu}_\perp)$$

- Particle Sampling

$$E\frac{{\rm d}N_i}{{\rm d}^3p} = \frac{g_i}{(2\pi^3)}\int_\Sigma {\rm d}^3\sigma_\mu(x) p^\mu f_i(x;p),$$

- Hadronic afterburner

$$p^\mu \partial_\mu f_i(x,p) = C_i[f]$$

Simultaneous Description for pp & pPb collisions

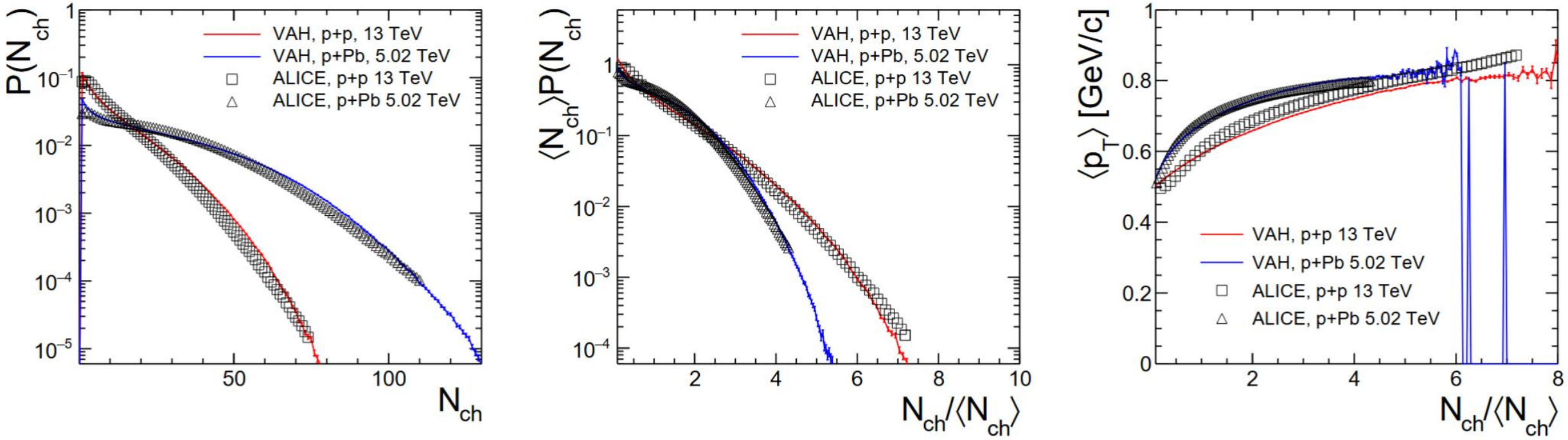

Same initial configuration (nucleon width, subnucleonic fluc, entropy fluctuation)

Same relaxation time (controlled by η/s and ζ/s) and transport coefficients

Same freeze-out temperature

Different τ_0 count for non-hydro contribution in p+p ← early stage dynamics affect $\langle p_T \rangle$

Good description for both the two systems

Zhao, Y. Peng, U. Heinz, H. Song. arXiv:2509.03841 & Paper in preparation

Collectivity from two particle correlations

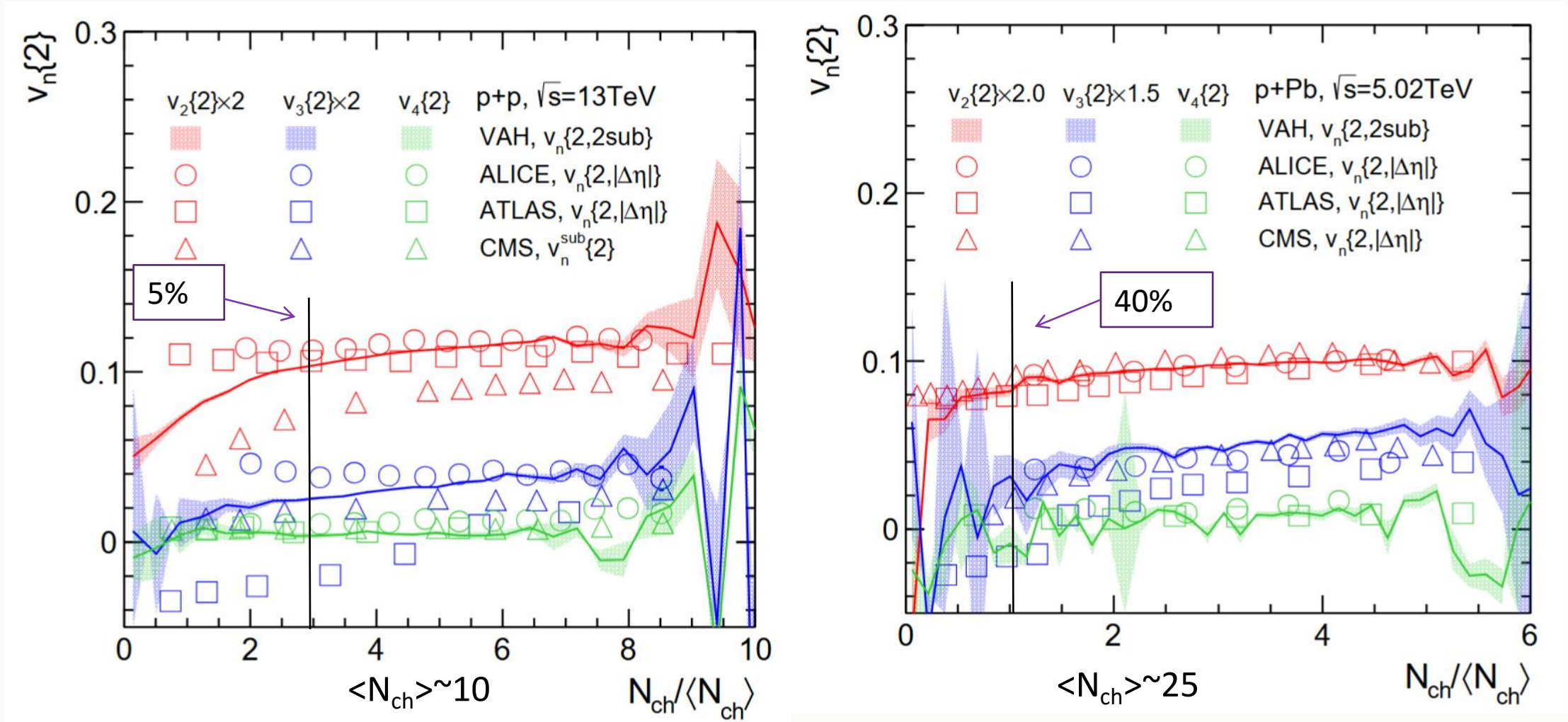

Good description for two particle correlation up to <N_{ch}> ~ 20

v_2/v_3 ratio ~ microscopic details of the system

Zhao, Y. Peng, U. Heinz, H. Song. arXiv:2509.03841 & Paper in preparation

Collectivity from four particle cumulants

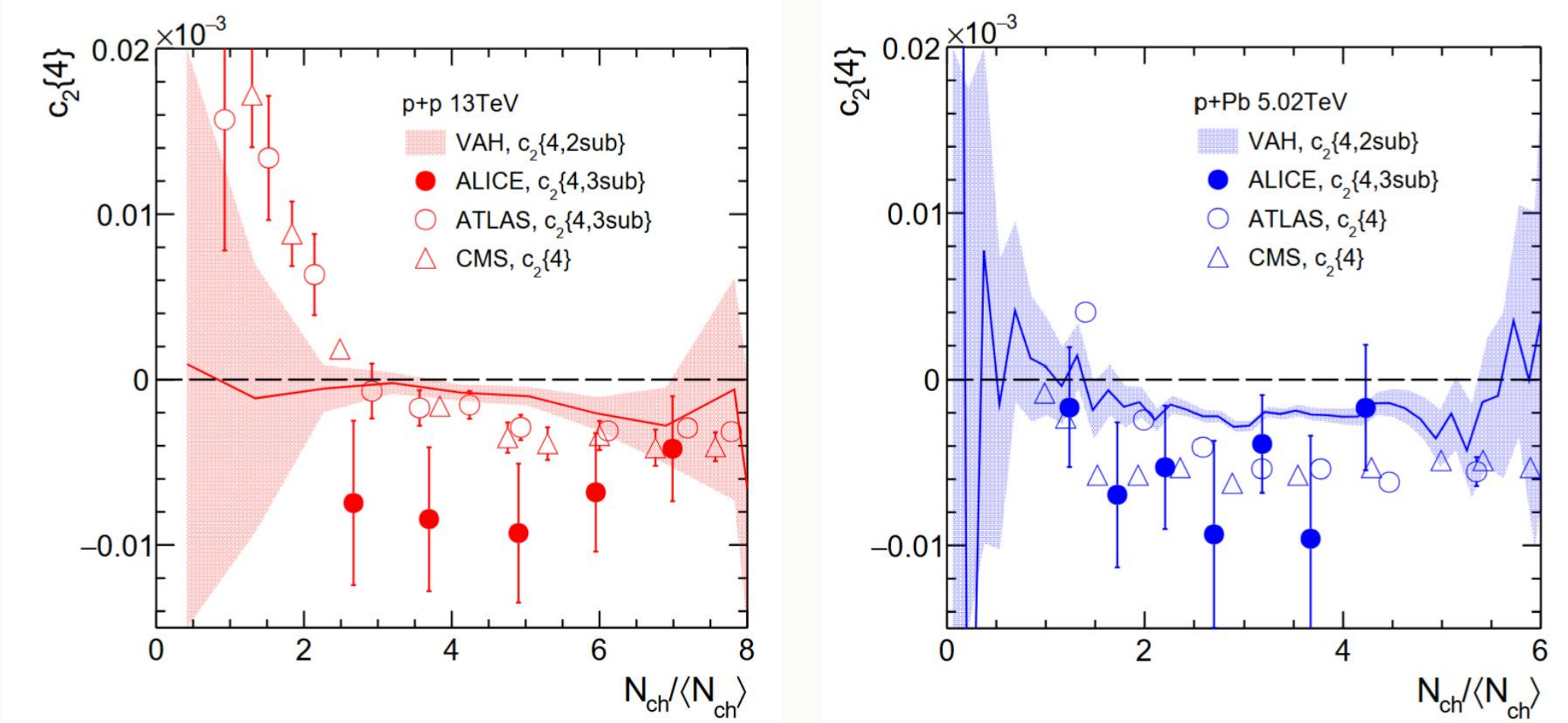

The $c_2\{4\}$ signs in two collision systems are well reproduced.

Quantitatively smaller flow magnitude than experimens.

→Initial stage correlation & non-flow effects should be included in the future work.

Zhao, Y. Peng, U. Heinz, H. Song. arXiv:2509.03841 & Paper in preparation

VAH v.s. VH

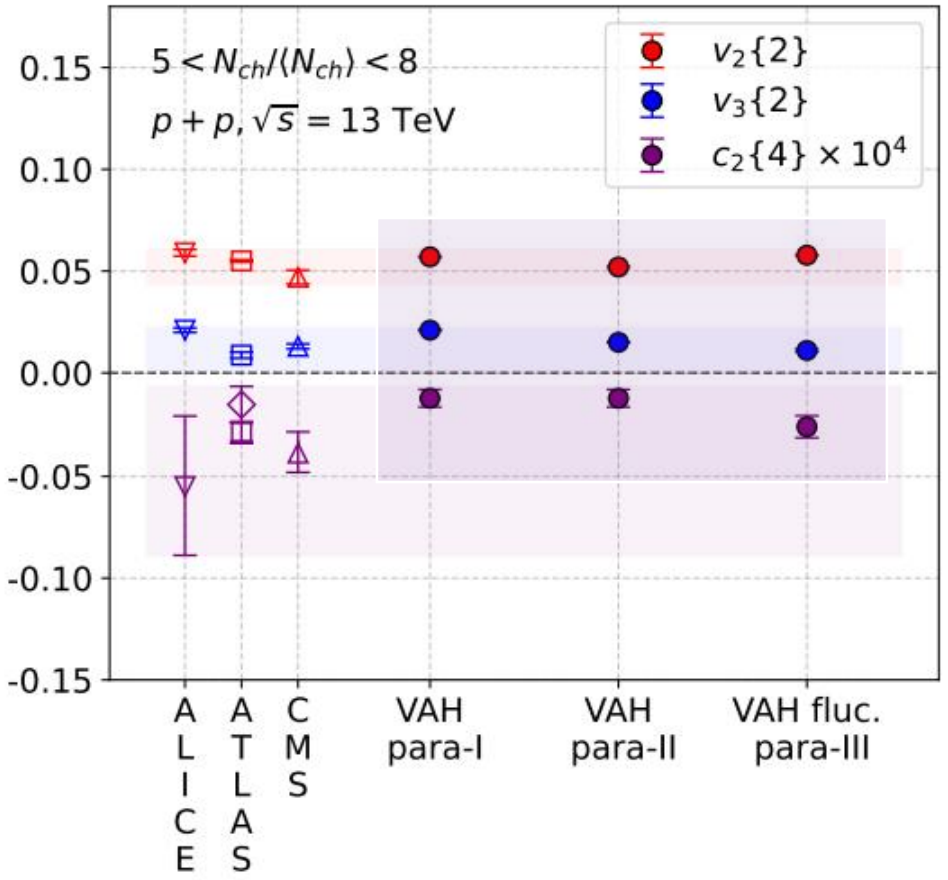

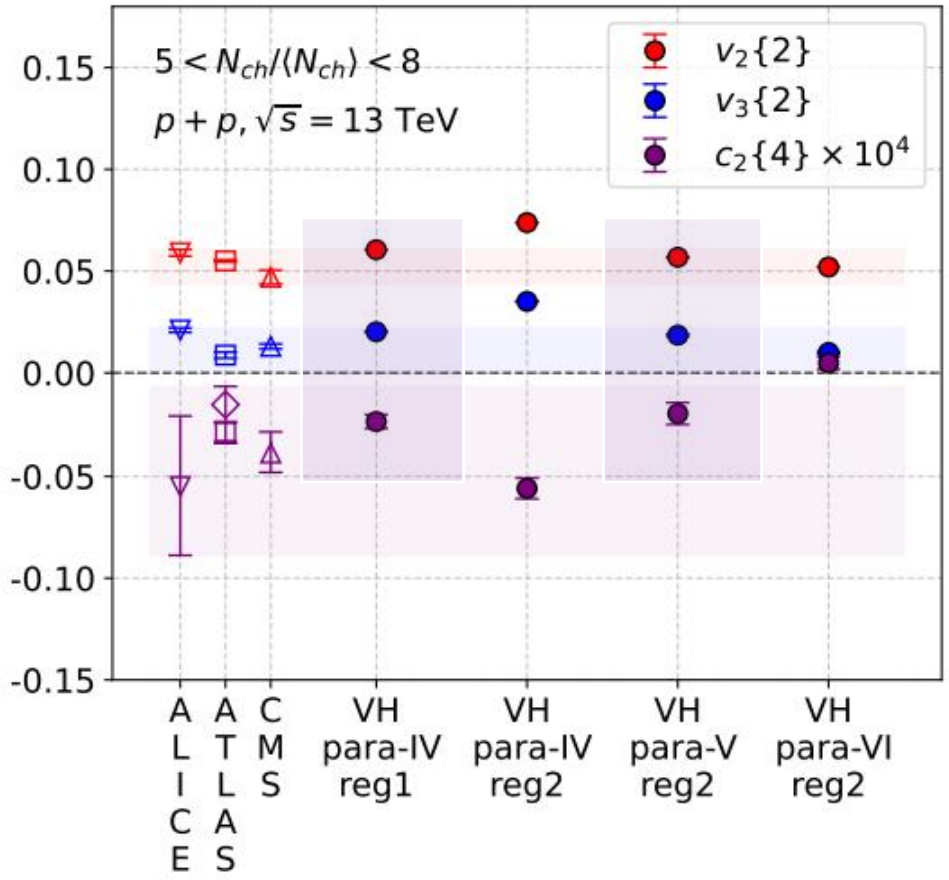

Zhao, Y. Peng, U. Heinz, H. Song. arXiv:2509.03841

VAH v.s. VH

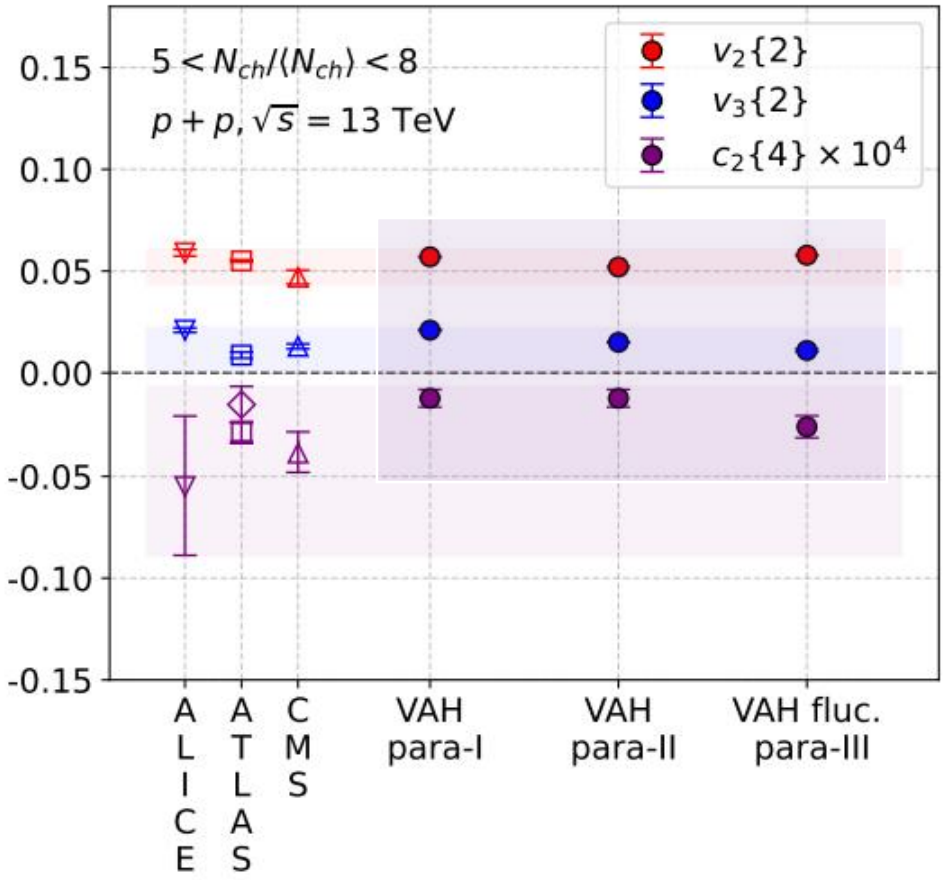

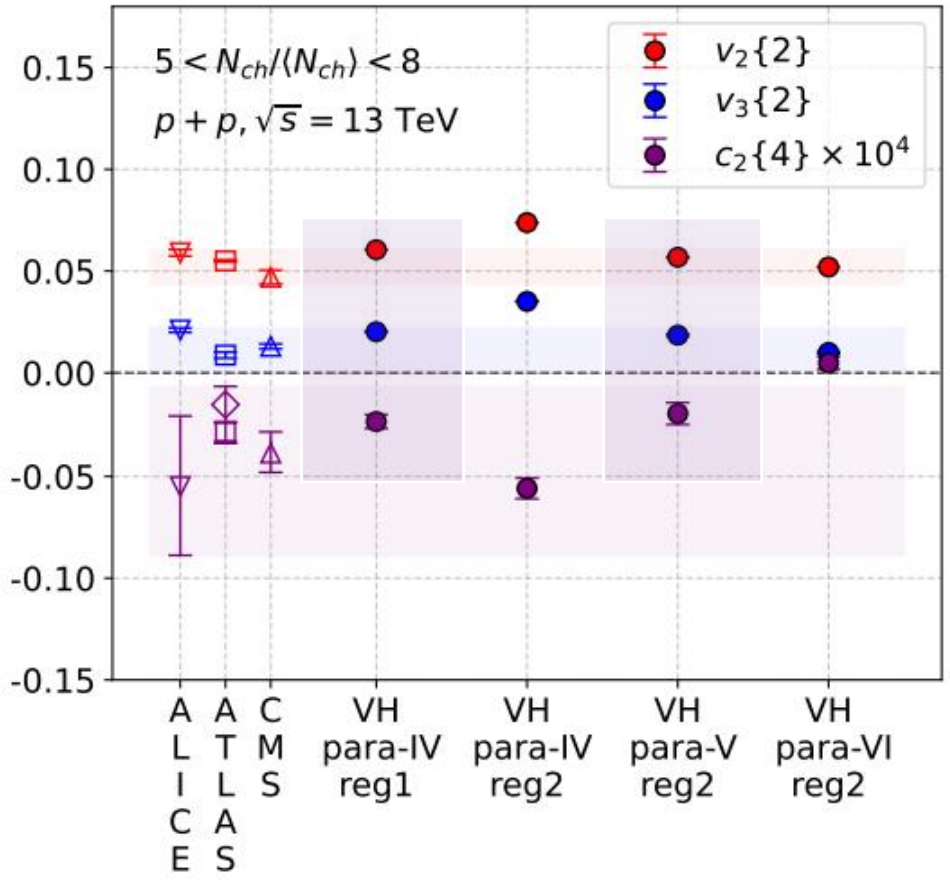

Phenomenologically valid ? Theoretically consistent? Numerically correct?

Zhao, Y. Peng, U. Heinz, H. Song. arXiv:2509.03841

Isotropization in p+p Collisions

<P_L/P_T>, VAH, pp 13TeV

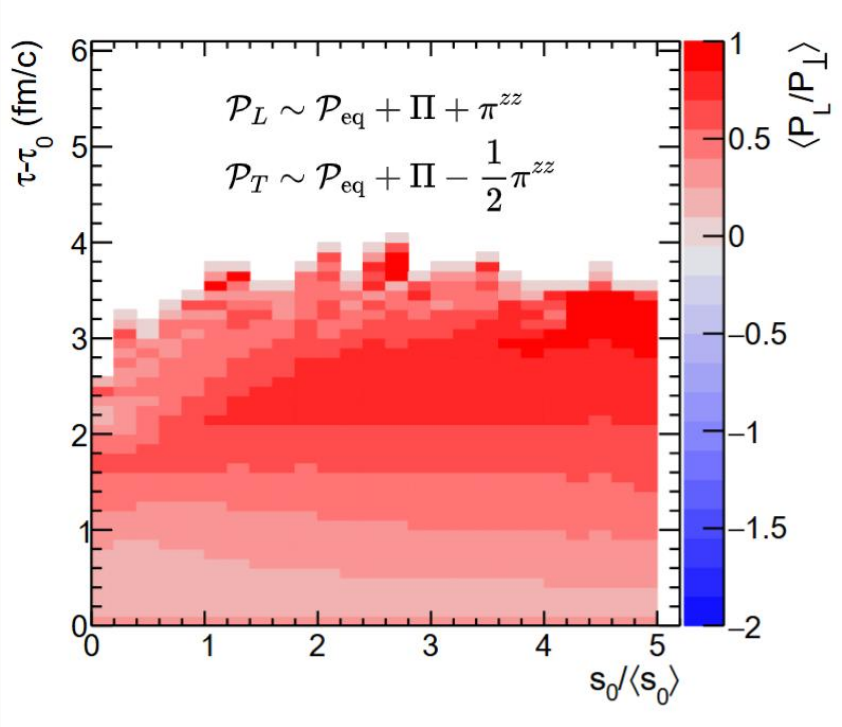

Low dN/dη → High dN/dη

VAH extends reliable description to low-multiplicity systems.
Anisotropic evolution well captured by VAH

Zhao, Y. Peng, U. Heinz, H. Song. arXiv:2509.03841 & Paper in preparation

Isotropization in p+p Collisions

<P_L/P_T>, VAH, pp 13TeV

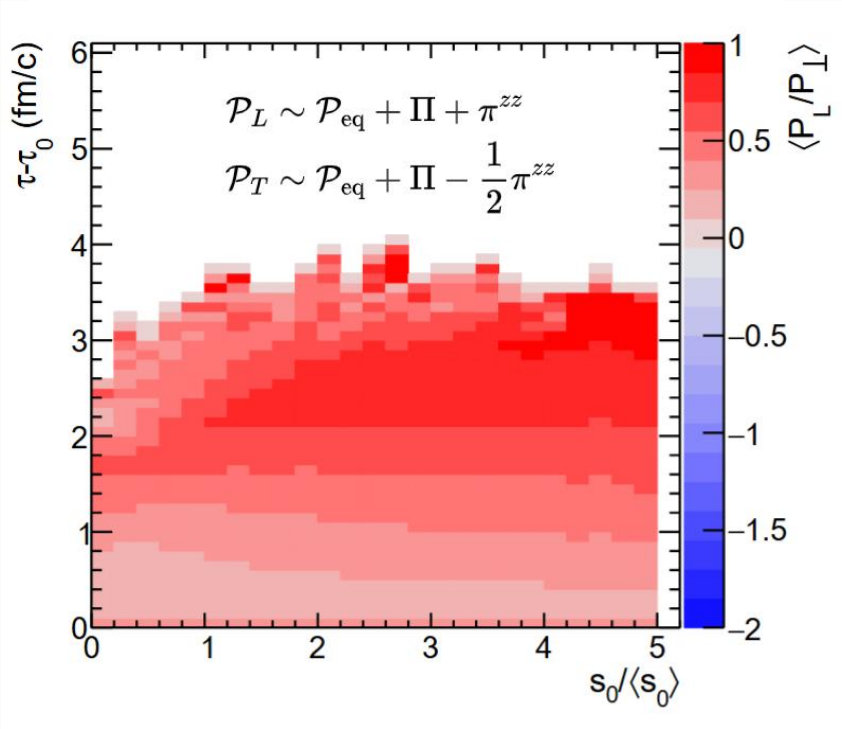

Low dN/dη → High dN/dη

<P_L/P_T>, VH, pp 13TeV

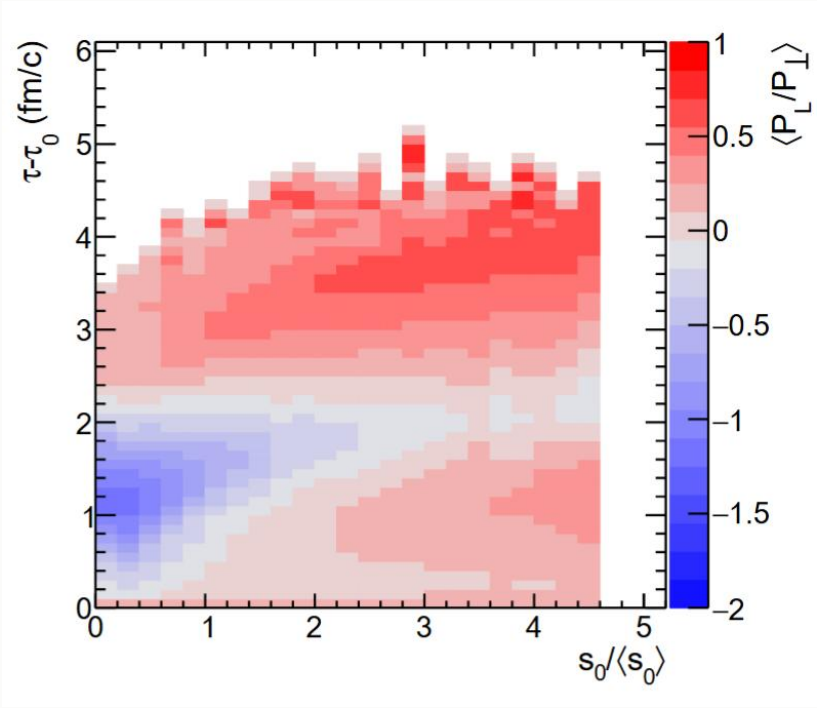

Low dN/dη → High dN/dη

VAH extends reliable description to low-multiplicity systems.
Anisotropic evolution well captured by VAH but not by VH.

Zhao, Y. Peng, U. Heinz, H. Song. arXiv:2509.03841 & Paper in preparation

Isotropization in p+p Collisions

<P_L/P_T>, VAH, pp 13TeV

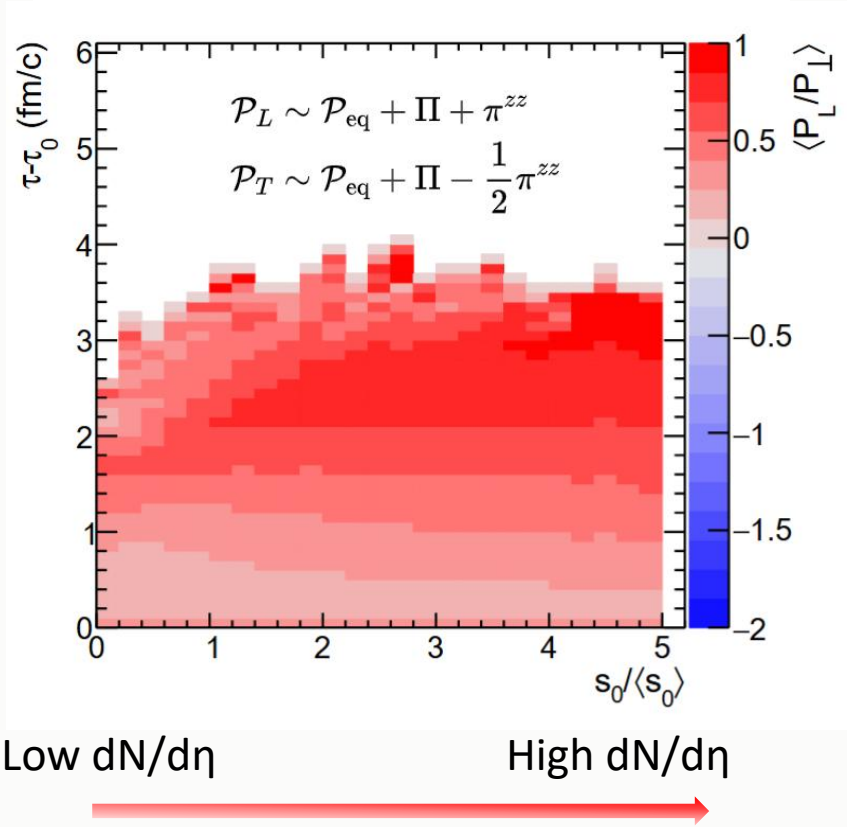

<P_L/P_T>, VH, pp 13TeV

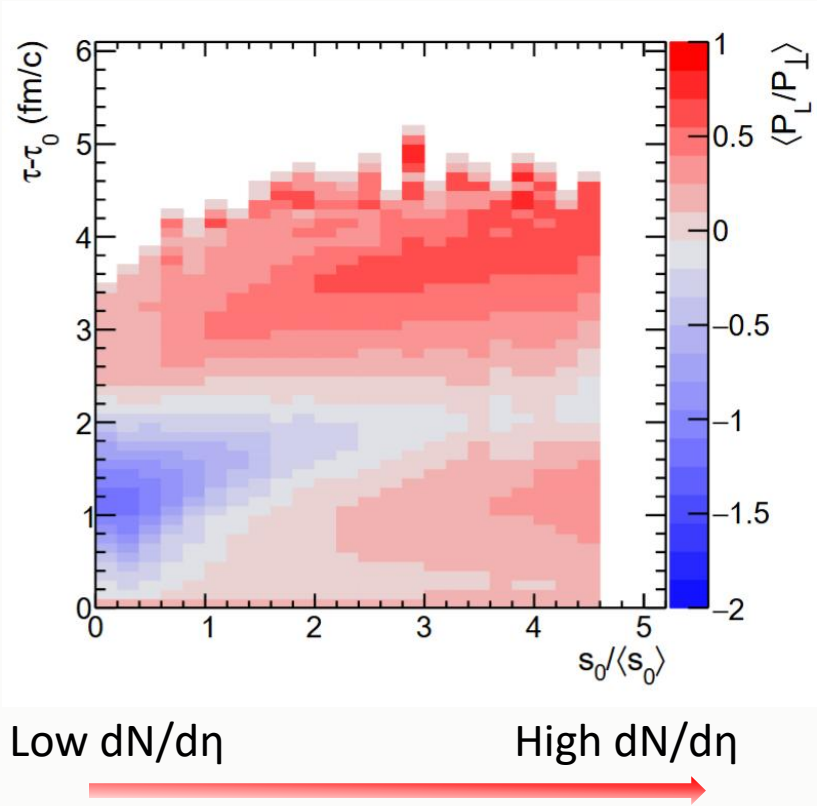

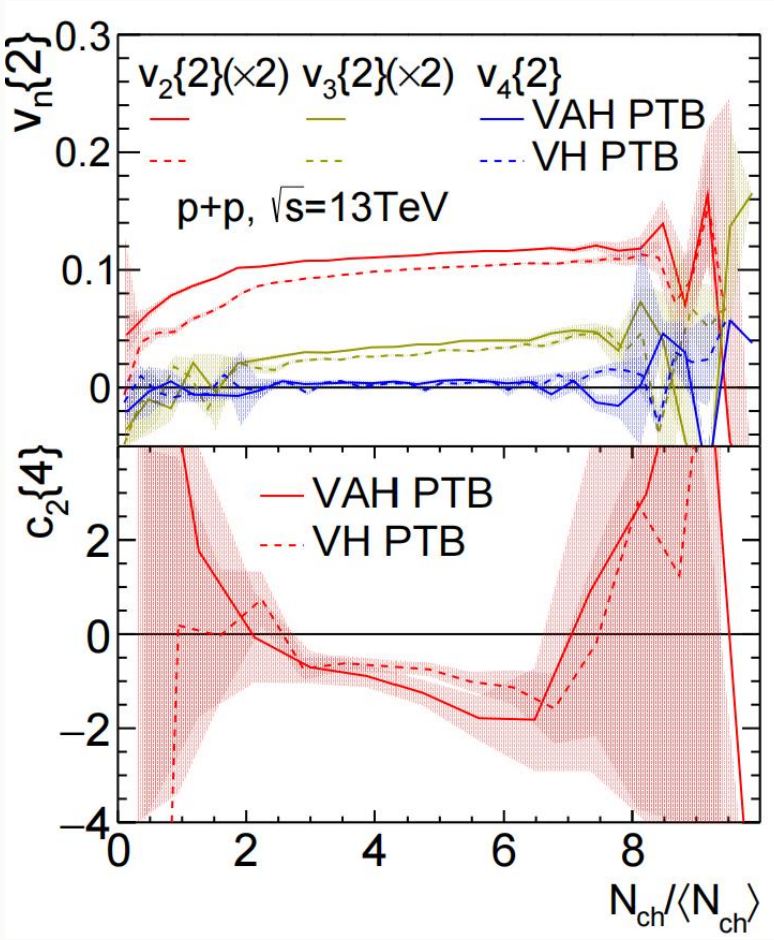

VAH extends reliable description to low-multiplicity systems.
Anisotropic evolution well captured by VAH but not by VH.

Zhao, Y. Peng, U. Heinz, H. Song. arXiv:2509.03841 & Paper in preparation

Isotropization in p+p Collisions

<P_L/P_T>, VAH, pp 13TeV

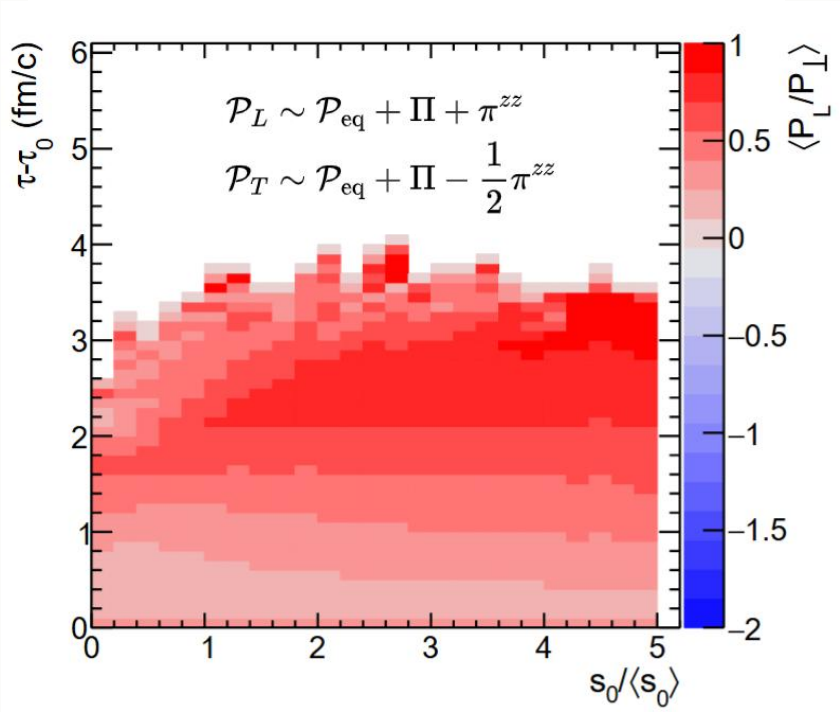

Low dN/dη → High dN/dη

<P_L/P_T>, VH, pp 13TeV

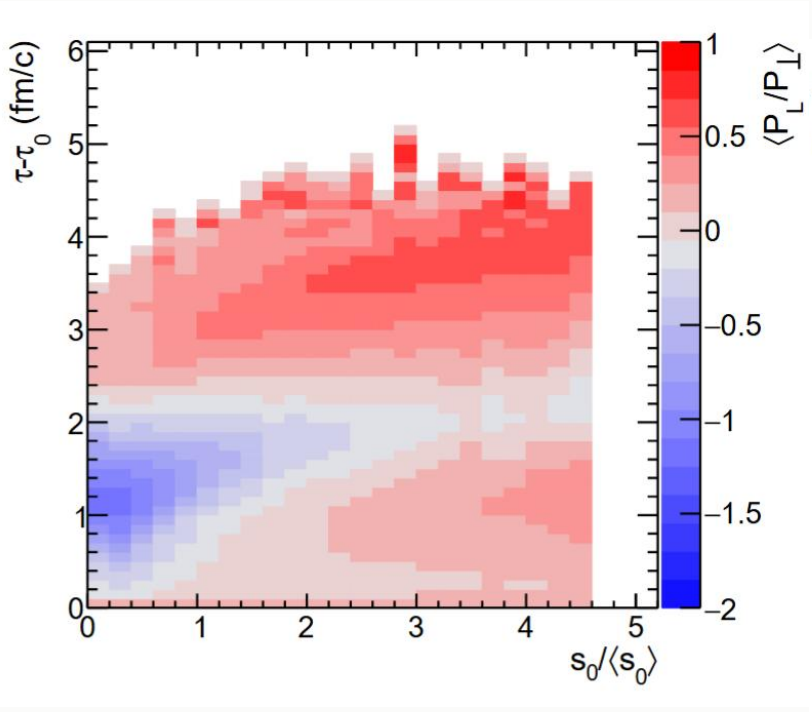

Low dN/dη → High dN/dη

Validity: $Re^{-1} \ll 1$

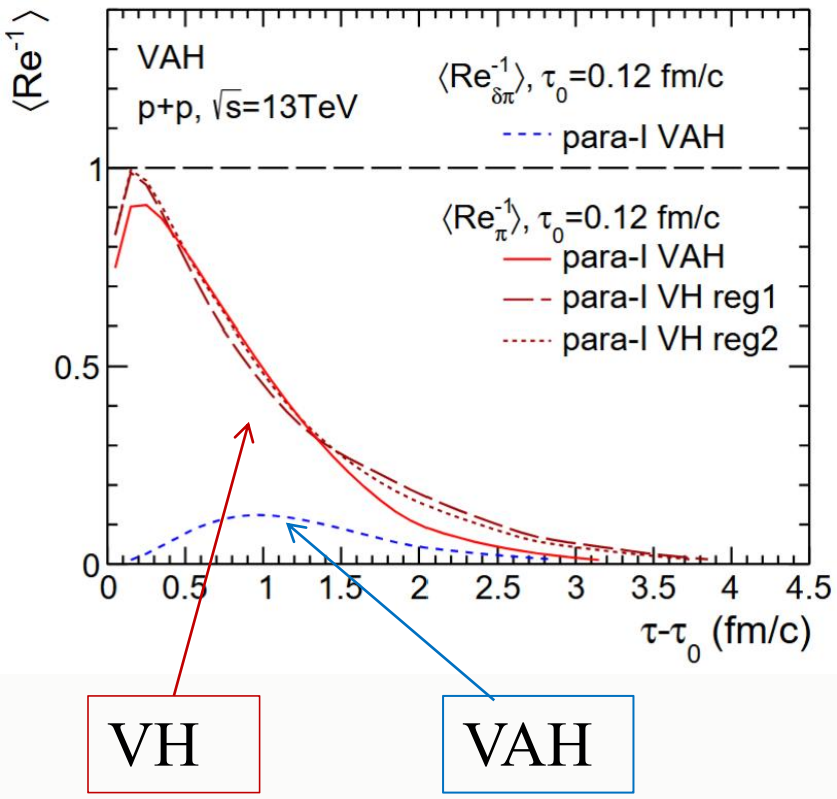

VAH extends reliable description to low-multiplicity systems.
Anisotropic evolution well captured by VAH but not by VH.

Zhao, Y. Peng, U. Heinz, H. Song. arXiv:2509.03841 & Paper in preparation

How the evolution changed?

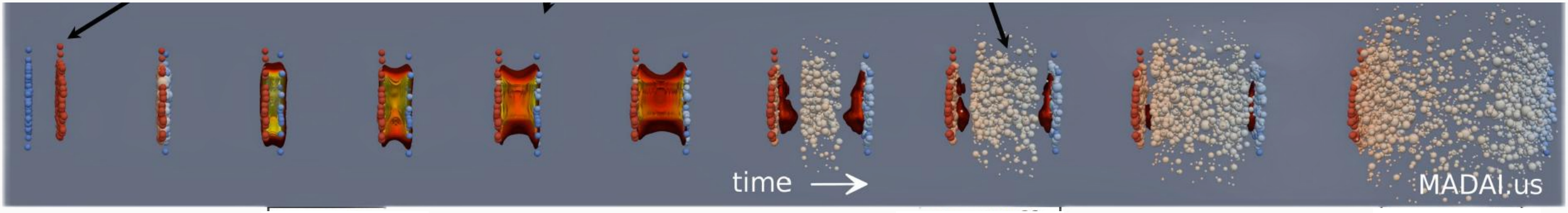

1-2 fm/c

3-4 fm/c

10-20 fm/c

1. Competiable evolution time between pre-equilibrium stage and hydro stage.

How the evolution changed?

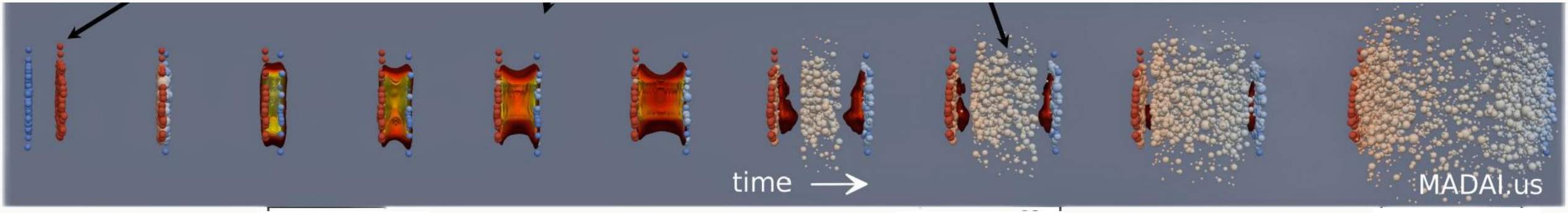

1-2 fm/c

3-4 fm/c

10-20 fm/c

1. Competiable evolution time between pre-equilibrium stage and hydro stage.
2. Uncertainty from pre-eq stage will mimic initial conditions

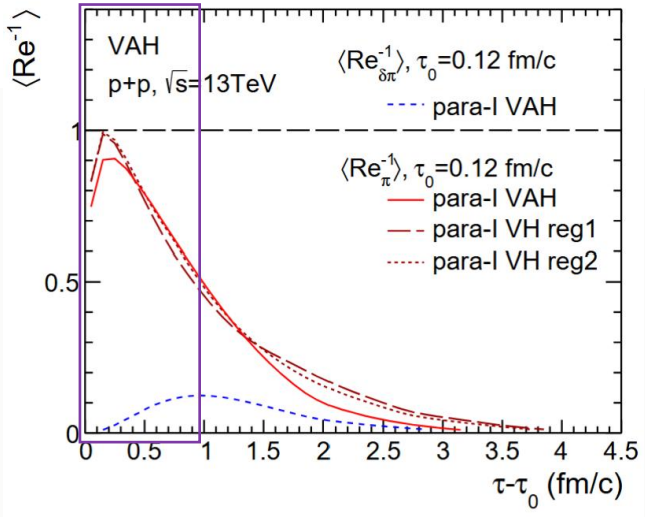

How the evolution changed?

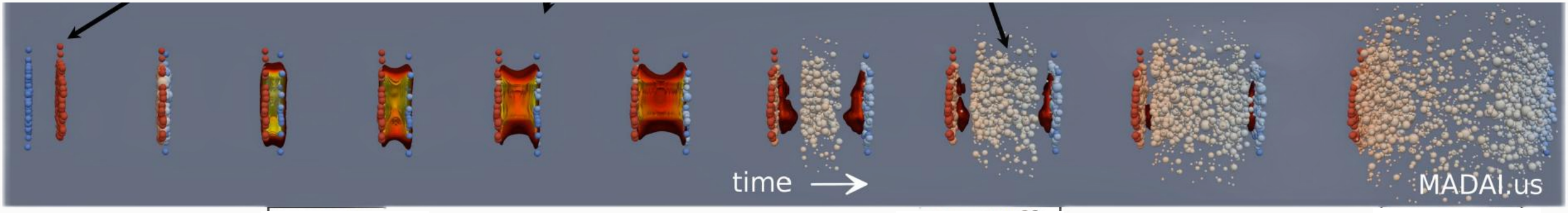

1-2 fm/c

3-4 fm/c

10-20 fm/c

1. Competiable evolution time between pre-equilibrium stage and hydro stage.
2. Uncertainty from pre-eq stage will mimic initial conditions
3. Non-eq state reached in the final stage then affect hadronic phase

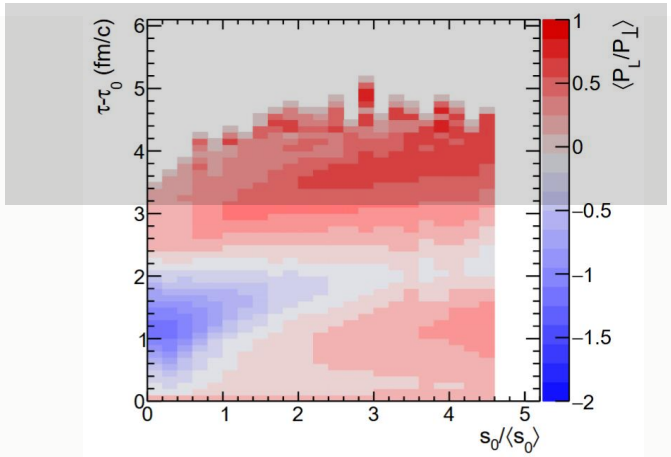

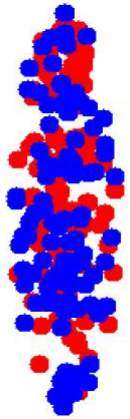

Collision rate
Entropy production
Additional decorrelations
… …

Dispersion relation in VAH

Start from the VAH equations (conformal, drop δf):

$$u^\mu \partial_\mu \Psi(x) = F(\Psi(x)) \qquad \Psi(x) = (\mathcal{E}, \mathcal{P}_L, u^\mu)^T$$

With the linear response,

$$A\tilde{\Psi}(p) = 0, \qquad P(\omega, k^2, \theta, \alpha_L) \sim \det A \sim \sum_{n=0}^{4} F_n(\alpha_L, k^2, \theta)\omega^n$$

Critical points are determined by:

$$P(\omega, k^2, \theta, \alpha_L) = 0, \qquad \partial_\omega P(\omega, k^2, \theta, \alpha_L) = 0$$

Sound mode: 2
Shear mode: 1
Gapped mode: 1

To determine $k_c(\alpha_L, \theta)$:

$$Q(k^2, \theta, \alpha_L) \equiv \mathrm{Disc}_\omega P(\omega, k^2, \theta, \alpha_L) = 0$$

$\tan\theta = k_T/k_z$

Zhao, et. al. Paper in preparation

Case I: Isotropic Perturbation Limit (Conformal)

Location of critical point:

$$\tilde{k}^2_{D\gamma} = \frac{27}{4\delta\Gamma}, \qquad \tilde{k}_{\pm\gamma} = \mp\frac{9ic_s}{3c_s^2 - \delta\Gamma},$$

P_L/P_T decrease, $k_x=k_y=k_z$

For realistic collision systems:

> Dominate by shear & gap collisions

> Anisotropic expansion increase convergent radius

System → extremely anisotropic

> Sound based collision dominate.

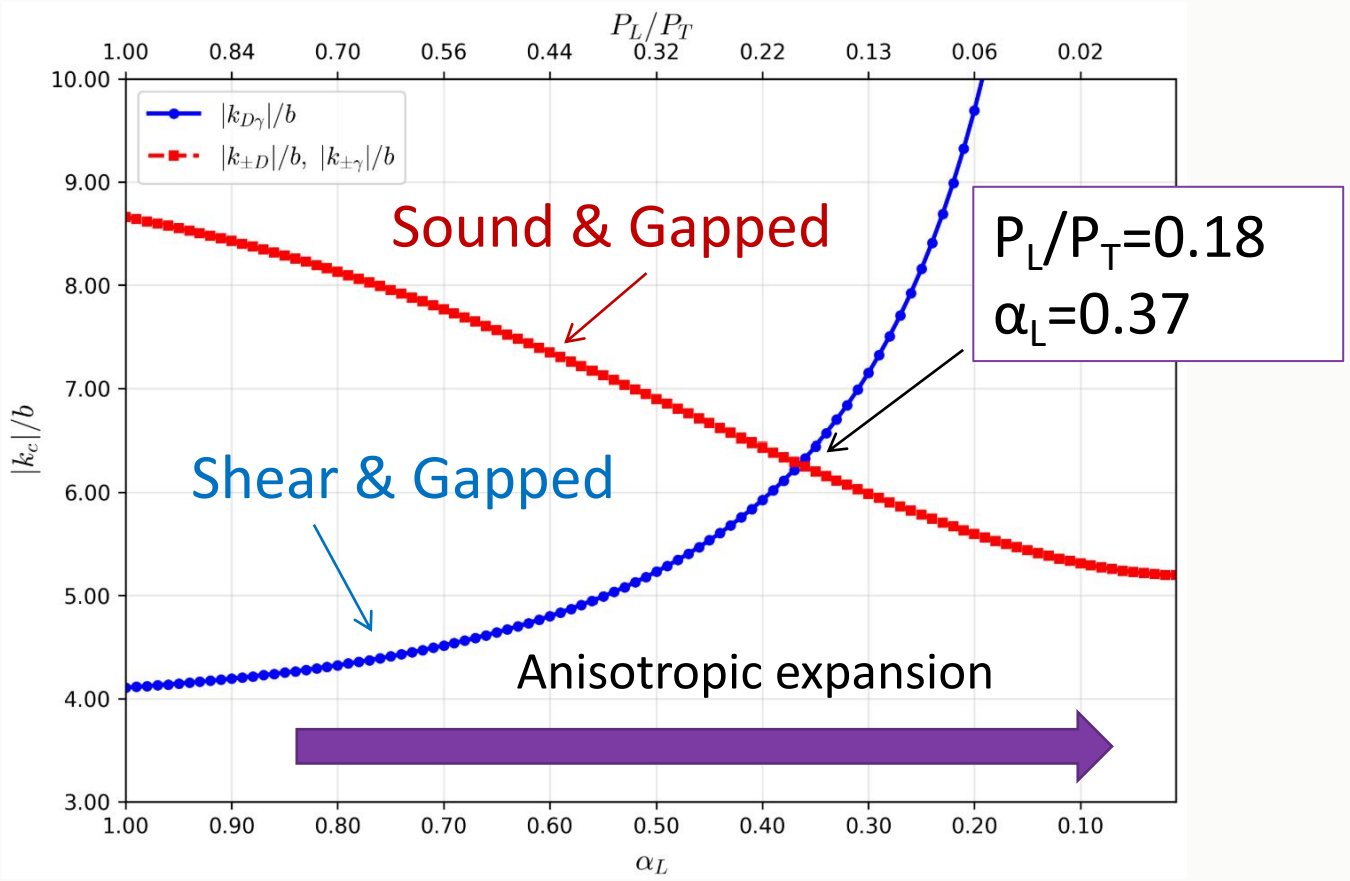

Zhao, et. al. Paper in preparation

Case II: General Case (Conformal)

θ dependence:

Critical point → Critical line

(Three collision cases)

polar angle affect the large-k behavior

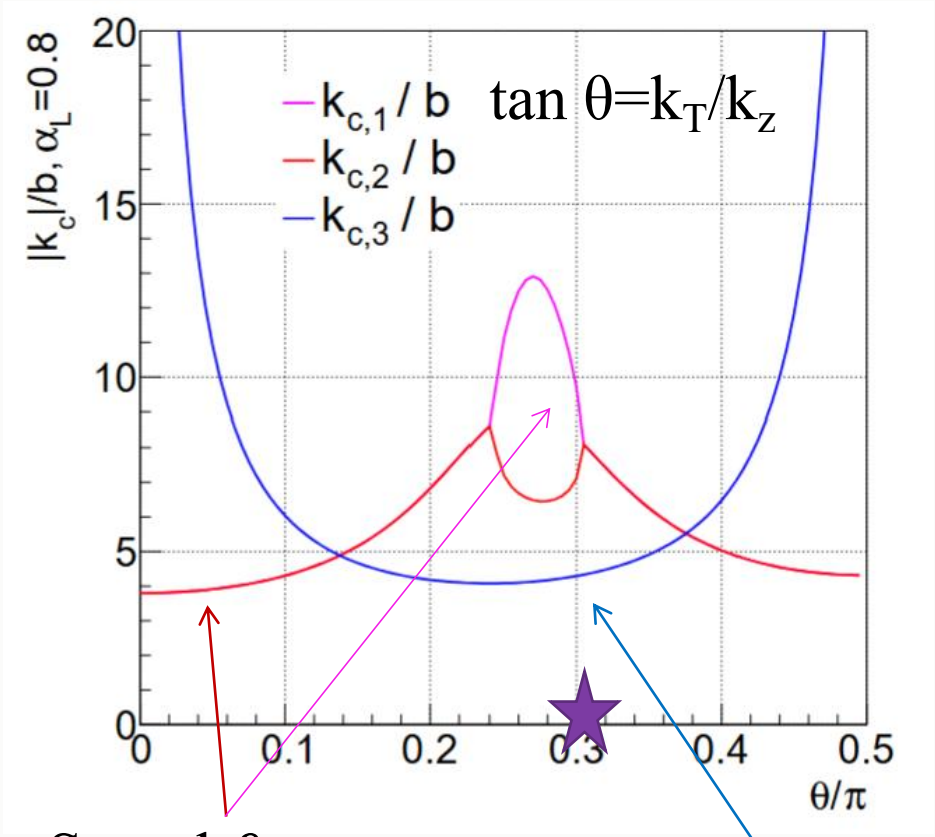

Sound & gapped mode collision (*2)

Shear & gapped mode collision (*1)

Zhao, et. al. Paper in preparation

Case II: General Case (Conformal)

θ dependence:

Critical point → Critical line

(Three collision cases)

polar angle affect the large-k behavior

With proper choice of τ_π

$$\tau_{\pi,3} = f(\alpha_L)\frac{5\eta}{\Lambda s}$$

validity still preserved when $(P_L/P_T)_0 << 1$

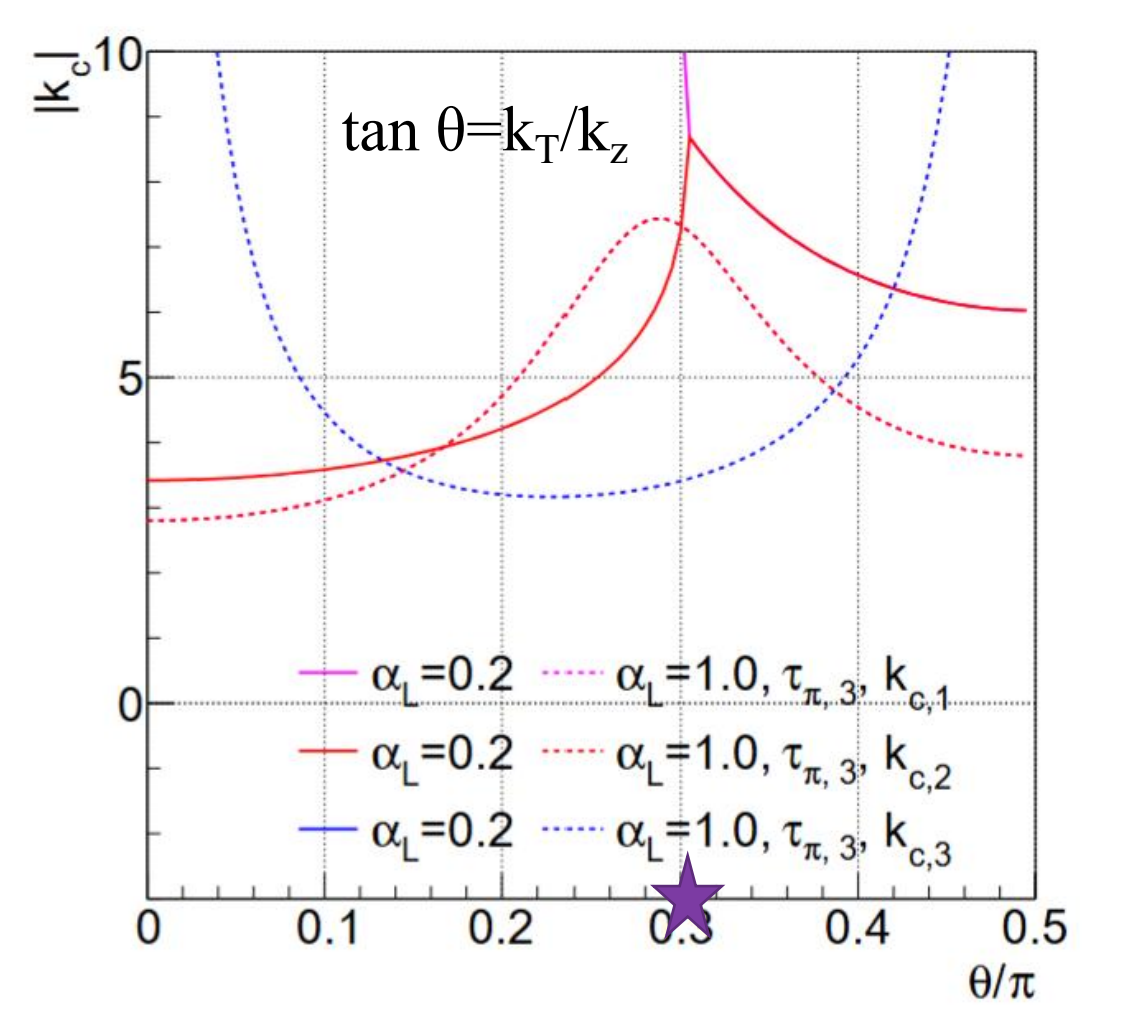

Zhao, et. al. Paper in preparation

Validity of hydrodynamics

VAH:

1. Phenomologically valid
2. P_L/P_T & inverse Reynold number well controlled
3. Convergent radius still large enough in anisotropic expansion

VH:

1. Phenomologically valid?
2. Negative P_L/P_T, large inverse Reynold number
3. Cannot apply to highly anisotropic expanding system.

Mid-rapidity Forward rapidity Ultra-forward

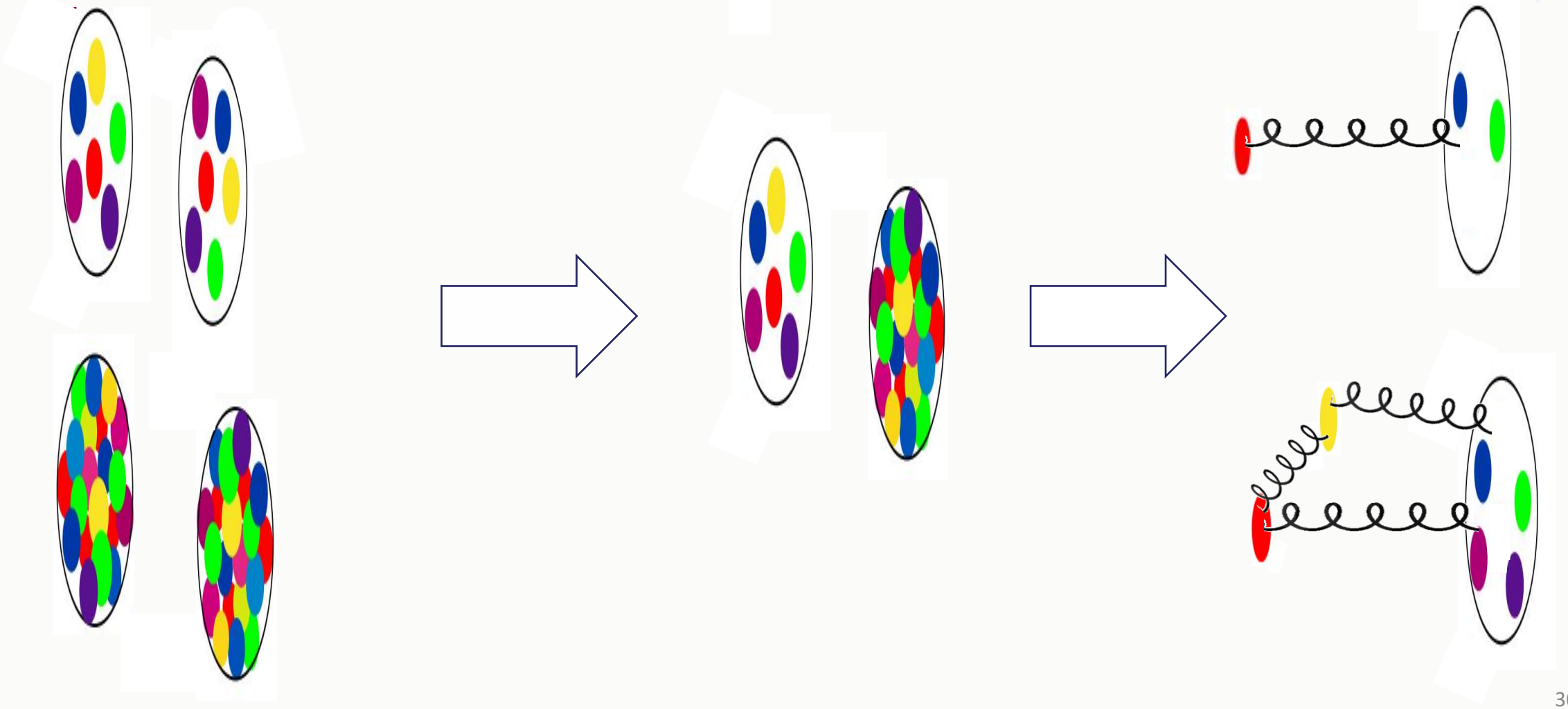

Oppotunities for Constraining PDFs/nPDFs

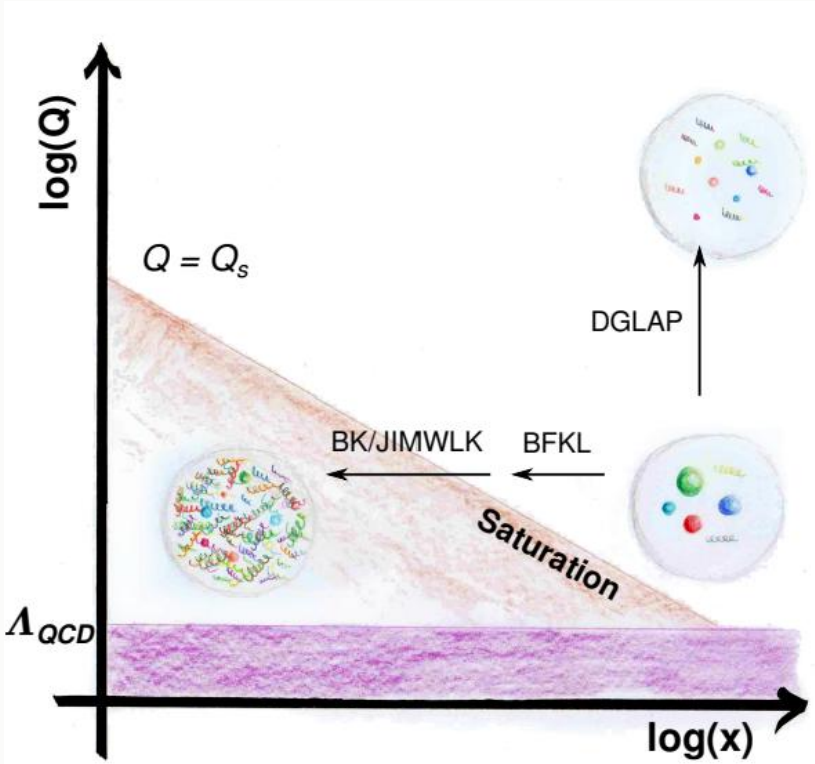

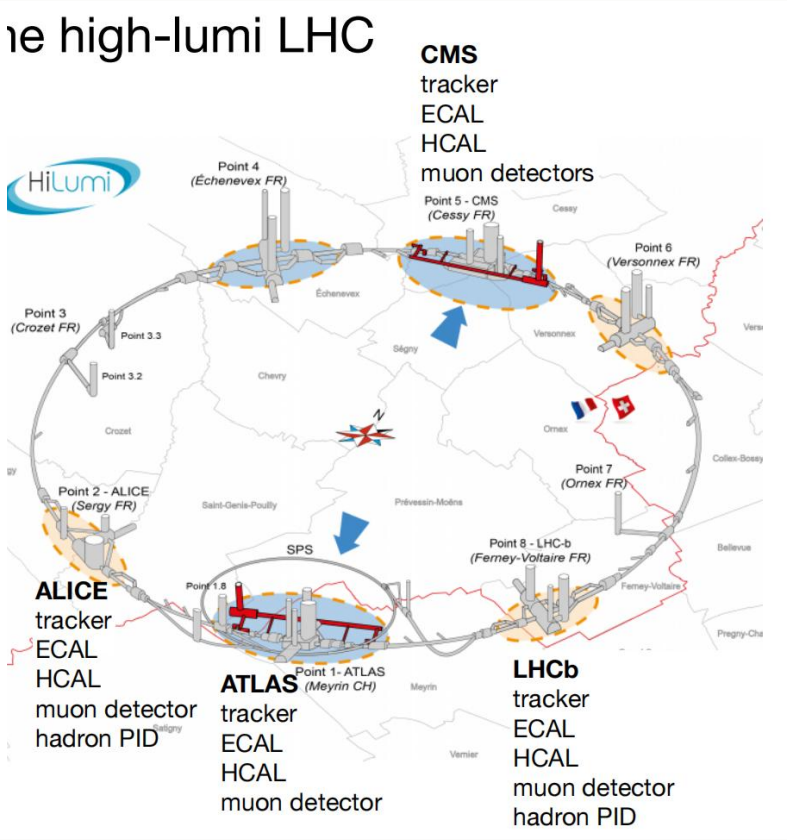

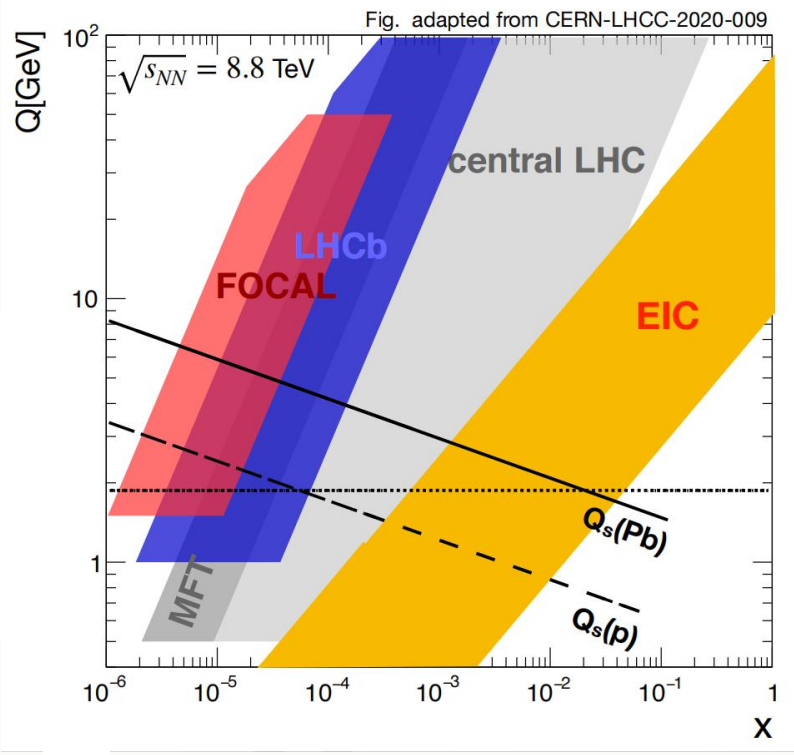

LHCb & Upgraded FoCal detector provides unique chance for probing and constraining small-x physics.

Theoretical development in the last few years

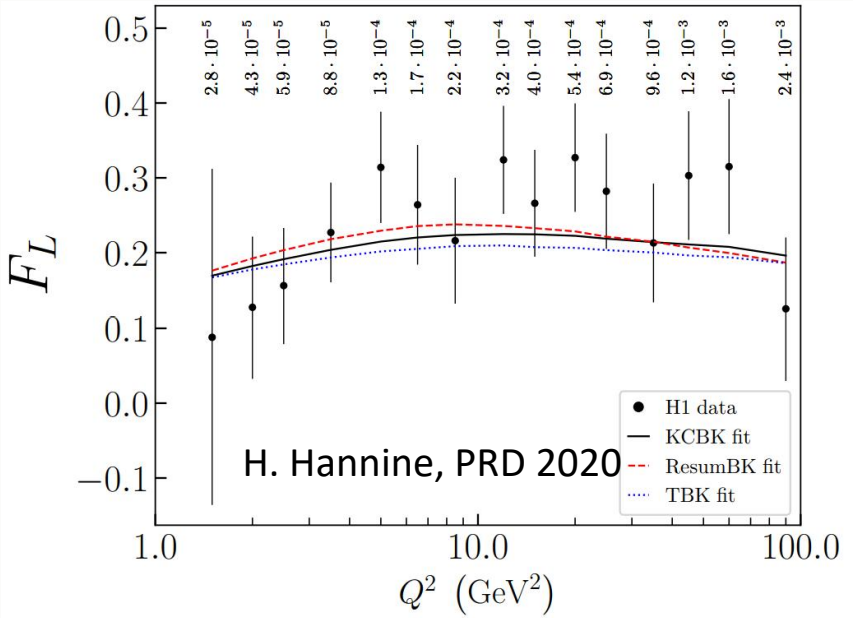

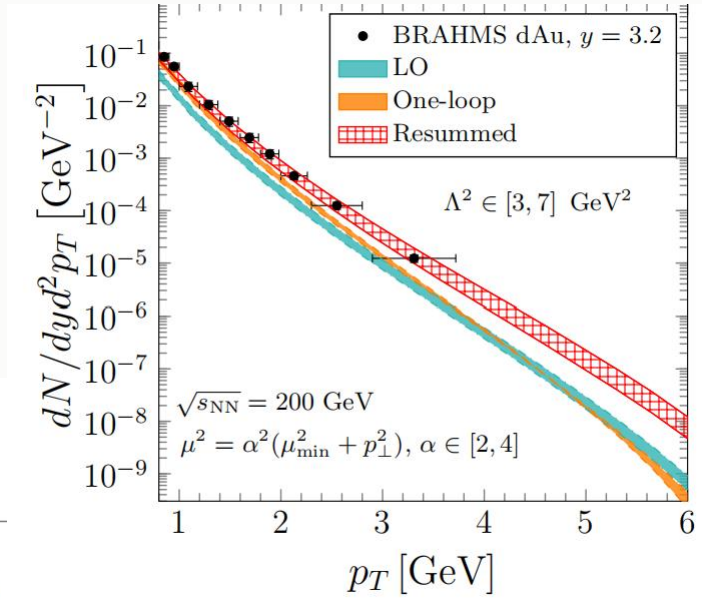

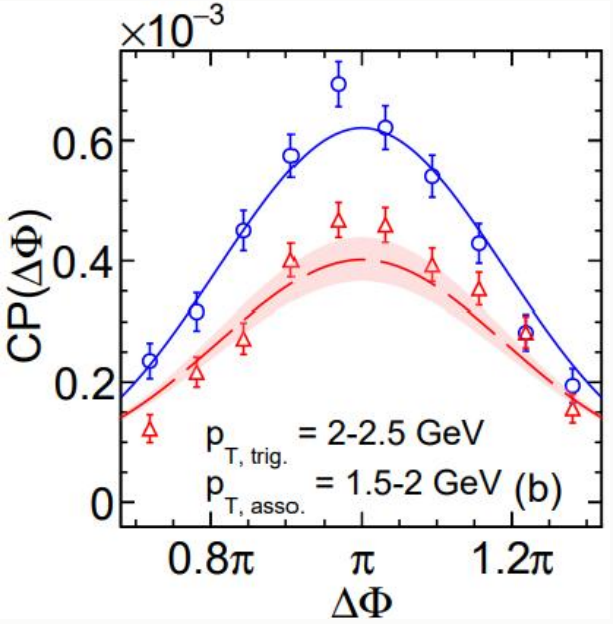

P. Caucal, et. al. arXiv:2512.21466

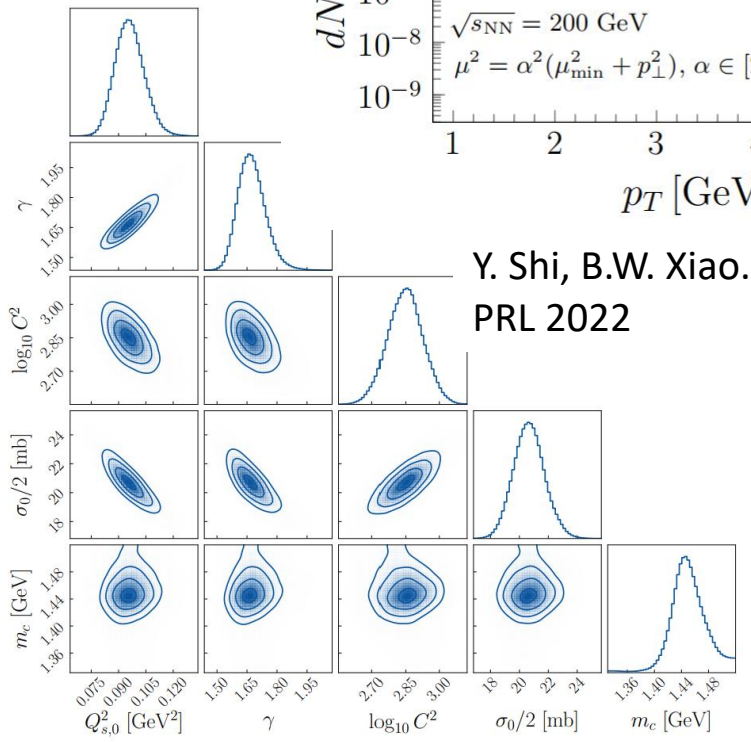

Y. Shi, B.W. Xiao. et. al. PRL 2022

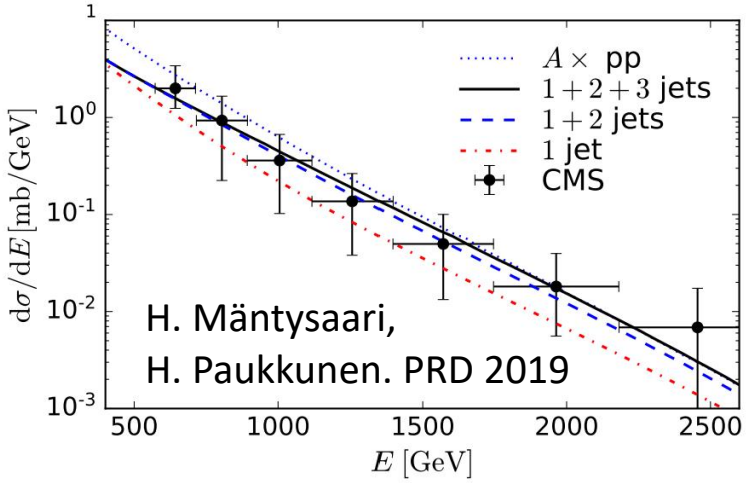

Constring rcBK ICs
Single particle production
Azimuthal angle correlations
Jet production
… …
Lack of consistent treating for
1. e-b-e Fluctuations
2. non-CGC effects

Event generator is essential

H.Mantysaari, et. al. PRD 2025

Model setup

For dilute-dense system:

$$\frac{d\sigma_{DHJ}}{dyd^2p_T} = \frac{K}{(2\pi)^2}\frac{\sigma_0}{2}\sum_{i=q,g} x_1 f_{i/p}(x_1, Q^2) N_i(x_2.p_T)$$

For dense-dense system:

$$\frac{d\sigma_{kT}}{dyd^2p_T} = \frac{K}{2C_F}\frac{1}{p_T^2}\left(\frac{\sigma_0}{2}\right)^2 \int d^2\boldsymbol{k}_T\, \alpha_s(Q_M^2) \times \varphi(x_1, \frac{\boldsymbol{p}_T + \boldsymbol{k}_T}{2})\varphi(x_2, \frac{\boldsymbol{p}_T - \boldsymbol{k}_T}{2}),$$

rcBK ICs and evolution

$$N_F(r, x_0) = 1 - \exp\left[-\frac{(r^2Q_{s0}^2)^\gamma}{4}\ln\left(\frac{1}{\Lambda r} + e_c \cdot e\right)\right]$$

rcBK ICs	γ	Q_{s0}^2 (GeV^2)	Λ_{QCD} (GeV)	e
MV	1	0.200	0.241	2.718
MV$^\gamma$	1.101	0.157	0.241	2.718
MV^e	1	0.060	0.241	18.9

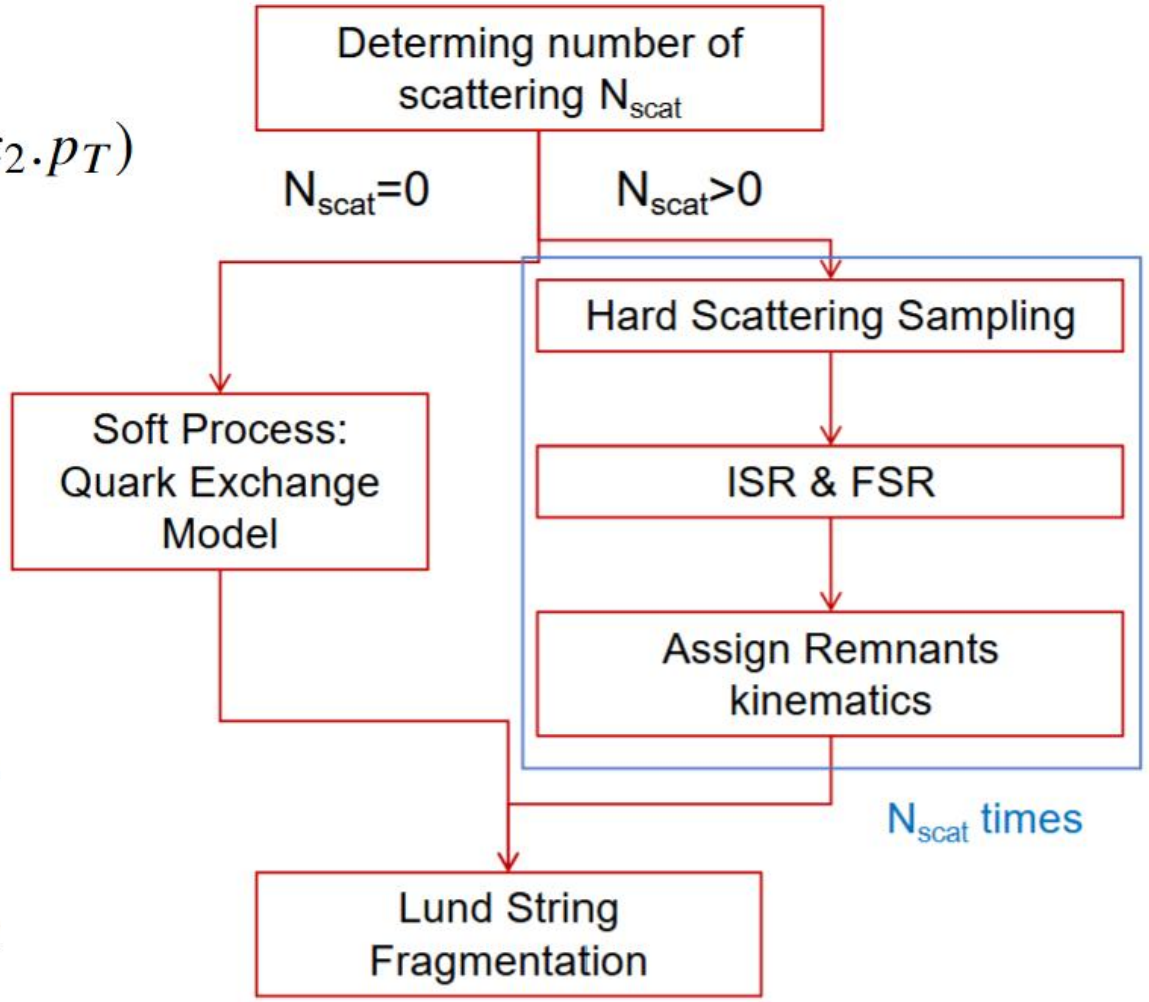

W. Deng, H. Fujii, T. Hirano, K. Itakura, Y. Nara, Phys.Rev.D 91 (2015) 1, 014006
Zhao, H. Fujii, T. Hirano, K. Itakura, Y. Nara, paper in preparation

Calibrate the Soft Parts

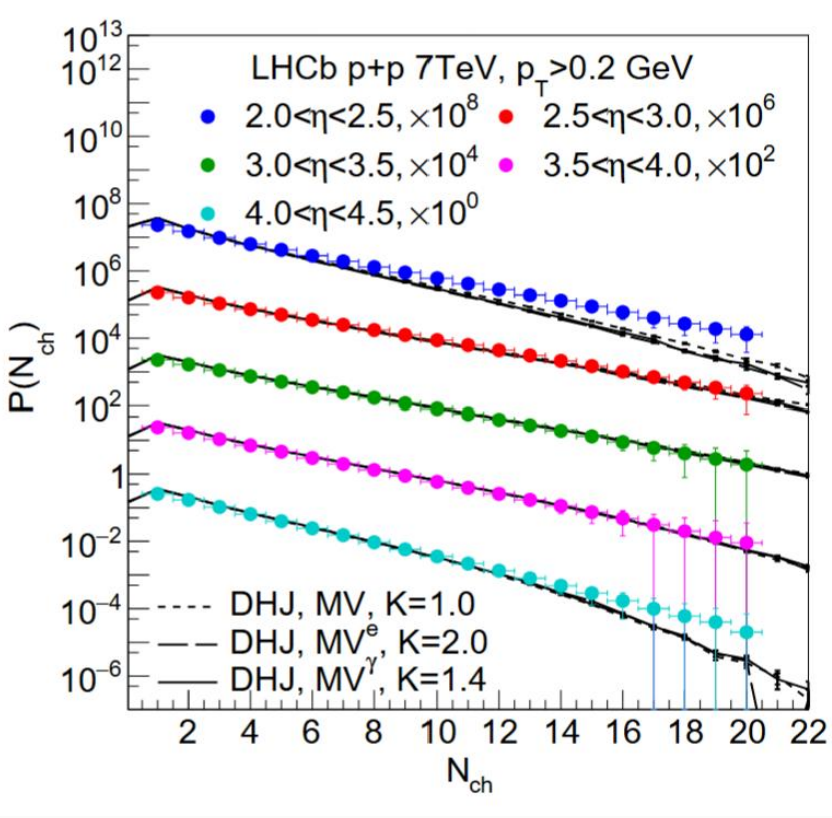

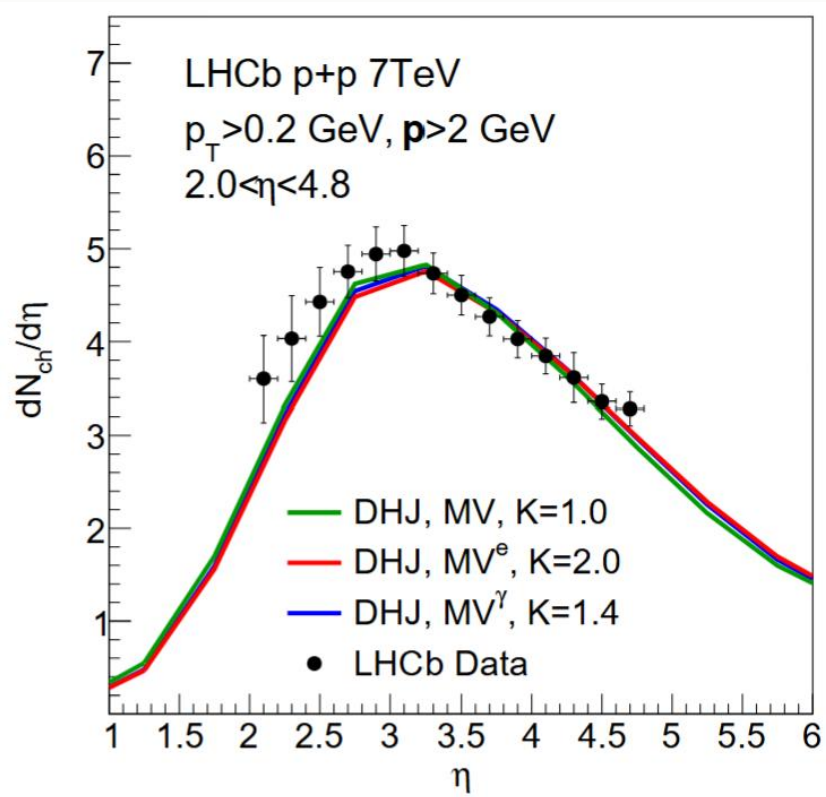

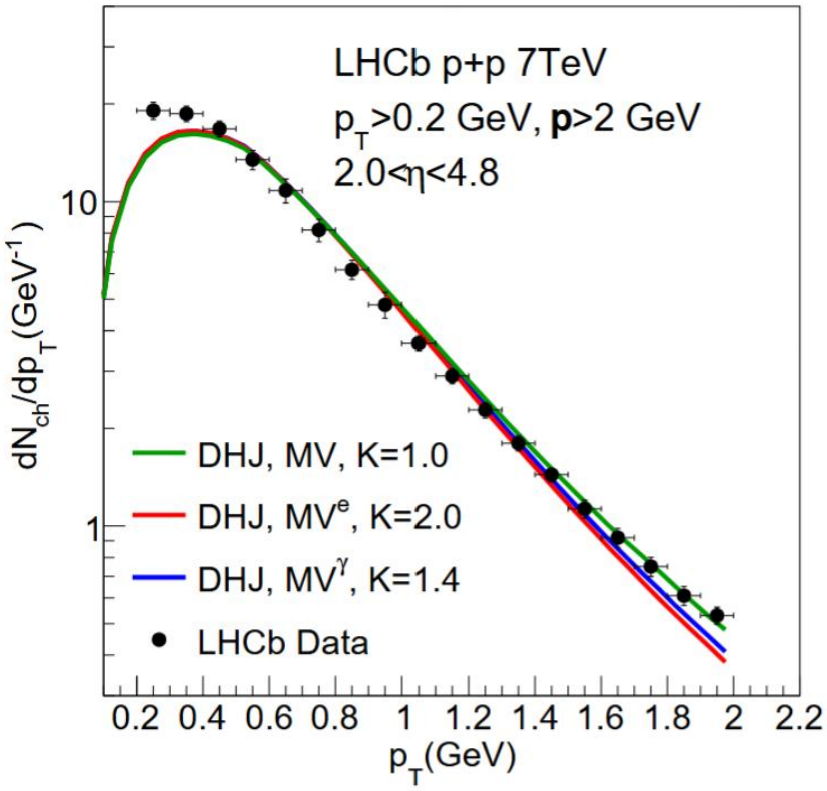

Good description for the existing soft part physics.

W. Deng, H. Fujii, T. Hirano, K. Itakura, Y. Nara, Phys.Rev.D 91 (2015) 1, 014006
Zhao, H. Fujii, T. Hirano, K. Itakura, Y. Nara, paper in preparation

p_T Spectra in RHIC and LHC

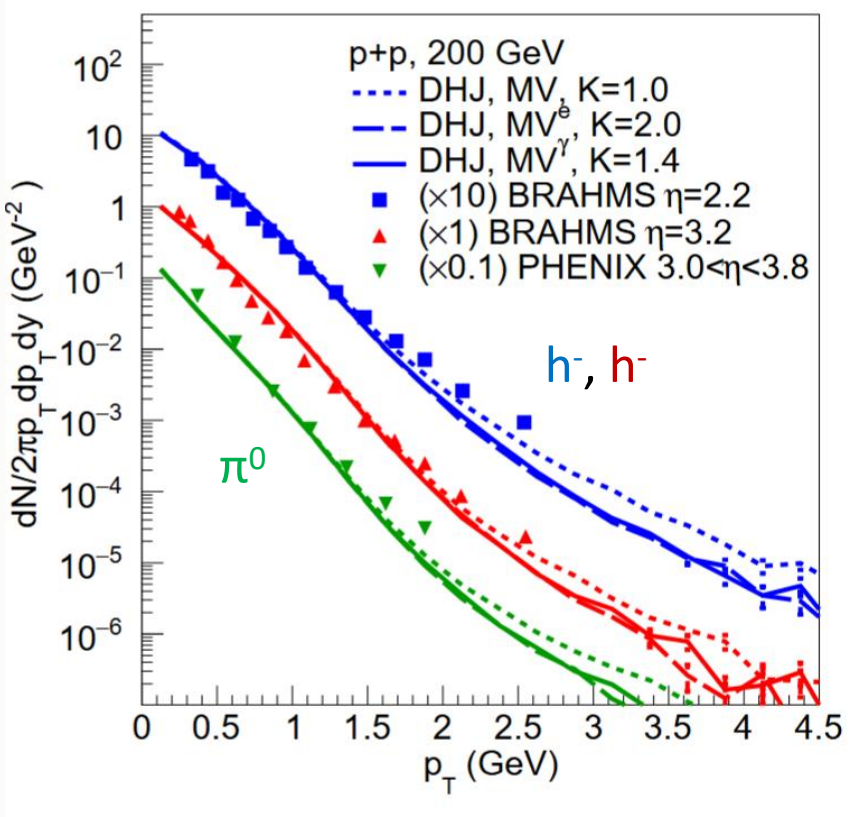

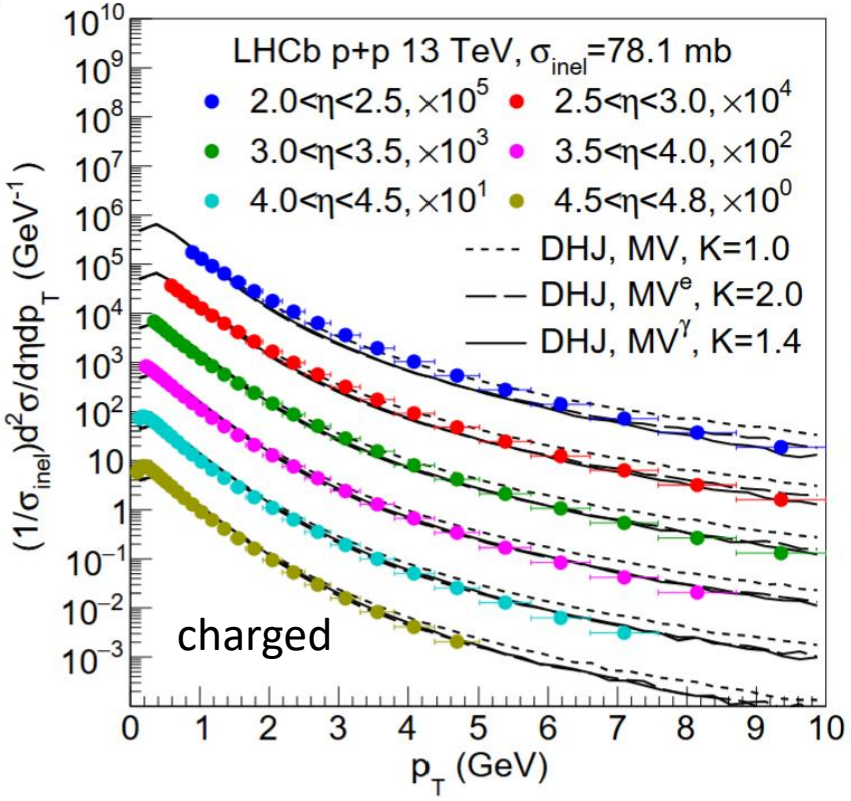

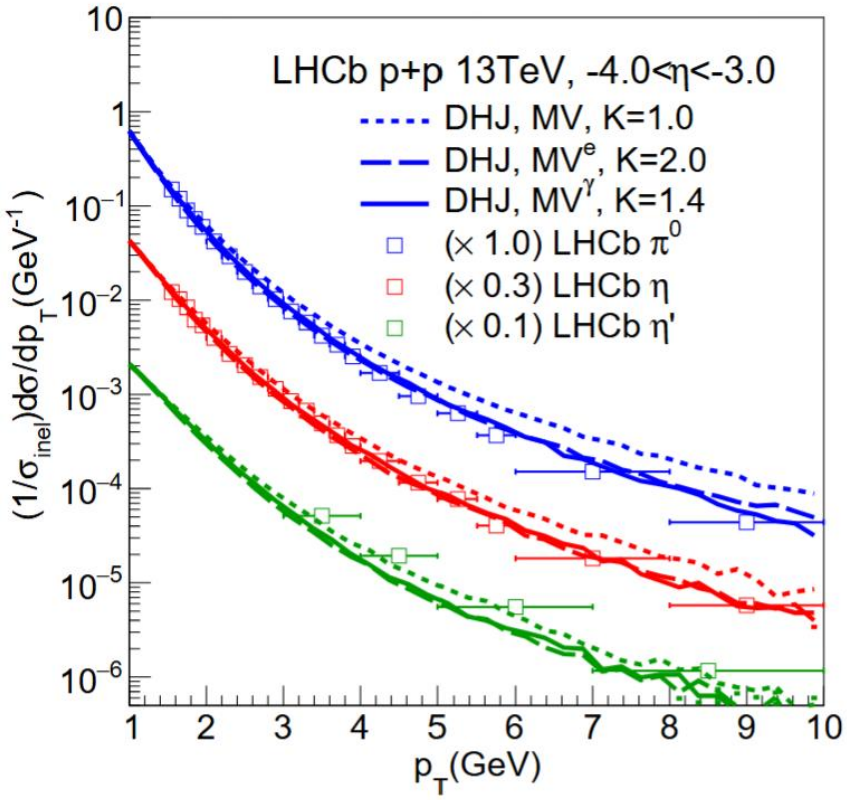

RHIC forward

LHC forward

LHC forward

Correctly reproduce the asymptotical behavior with MV$^\gamma$ initial condition.
Hard to distinguish MV$^\gamma$ and MV^e initial condition, except in high p_T region.

W. Deng, H. Fujii, T. Hirano, K. Itakura, Y. Nara, Phys.Rev.D 91 (2015) 1, 014006
Zhao, H. Fujii, T. Hirano, K. Itakura, Y. Nara, paper in preparation

Dense-Dense v.s. Dilute-Dense Framework

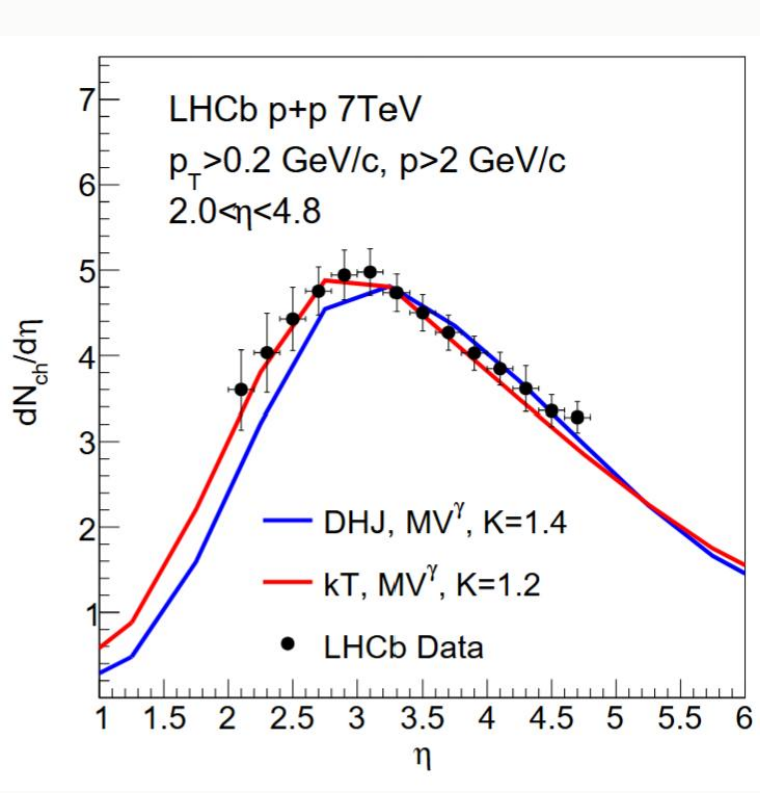

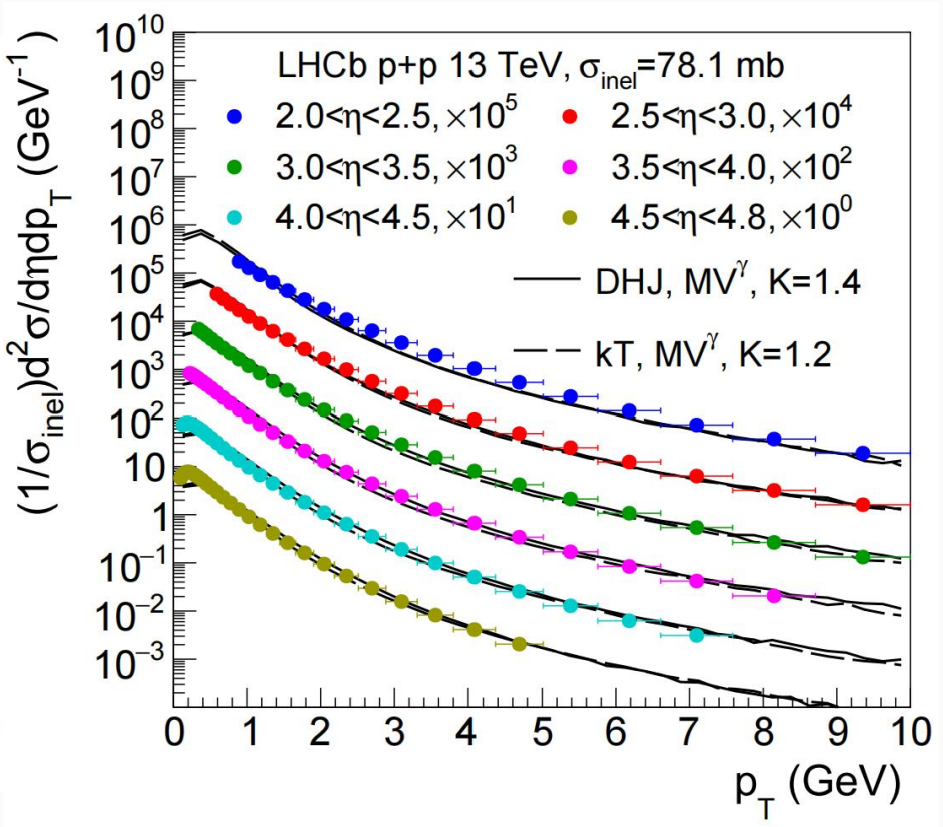

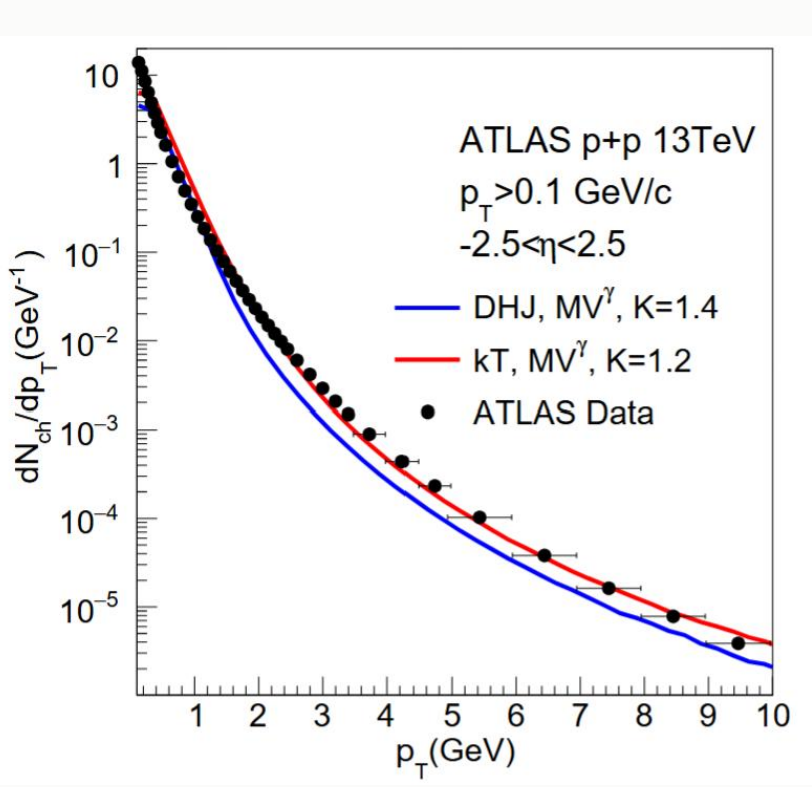

With fixed normalization K, k_T factorization can have better description power than DHJ in the mid-rapidity.

<u>p+p @ mid-rapidity dense enough? More investigation needed</u>

W. Deng, H. Fujii, T. Hirano, K. Itakura, Y. Nara, Phys.Rev.D 91 (2015) 1, 014006

Zhao, H. Fujii, T. Hirano, K. Itakura, Y. Nara, paper in preparation

Conclusion

- Heavy-ion collision @ mid-rapidity

Well known dynamics, Quantitative constrain on nuclear structure

Fruitful calibration on nuclear shape, nucleon correlations and shape fluctuations.

- Towards smaller collision system

Validity of hydrodynamics questionable

Pre-equilibrium stage may be significant

With VAH framework: well description for smallest collision system, large convergent radius when $(P_L/P_T)_0 << 1$

- Towards forward rapidity

Uncertainty from pre-eq stage: Existence of CGC medium?

More info may be obtained from beam remnant

Conclusion & Outlook

- Heavy-ion collision @ mid-rapidity

Well known dynamics, Quantitative constrain on nuclear structure

Fruitful calibration on nuclear shape, nucleon correlations and shape fluctuations.

- Towards smaller collision system → **Extension to light-ion**

Validity of hydrodynamics questionable

Pre-equilibrium stage may be significant

With VAH framework: well description for smallest collision system, large convergent radius when $(P_L/P_T)_0 << 1$

- Towards forward rapidity → **Extension to p+A, light-ion and heavy-ion**

Uncertainty from pre-eq stage: Existence of CGC medium?

More info may be obtained from beam remnant

More on collectivity: Flow Correlations

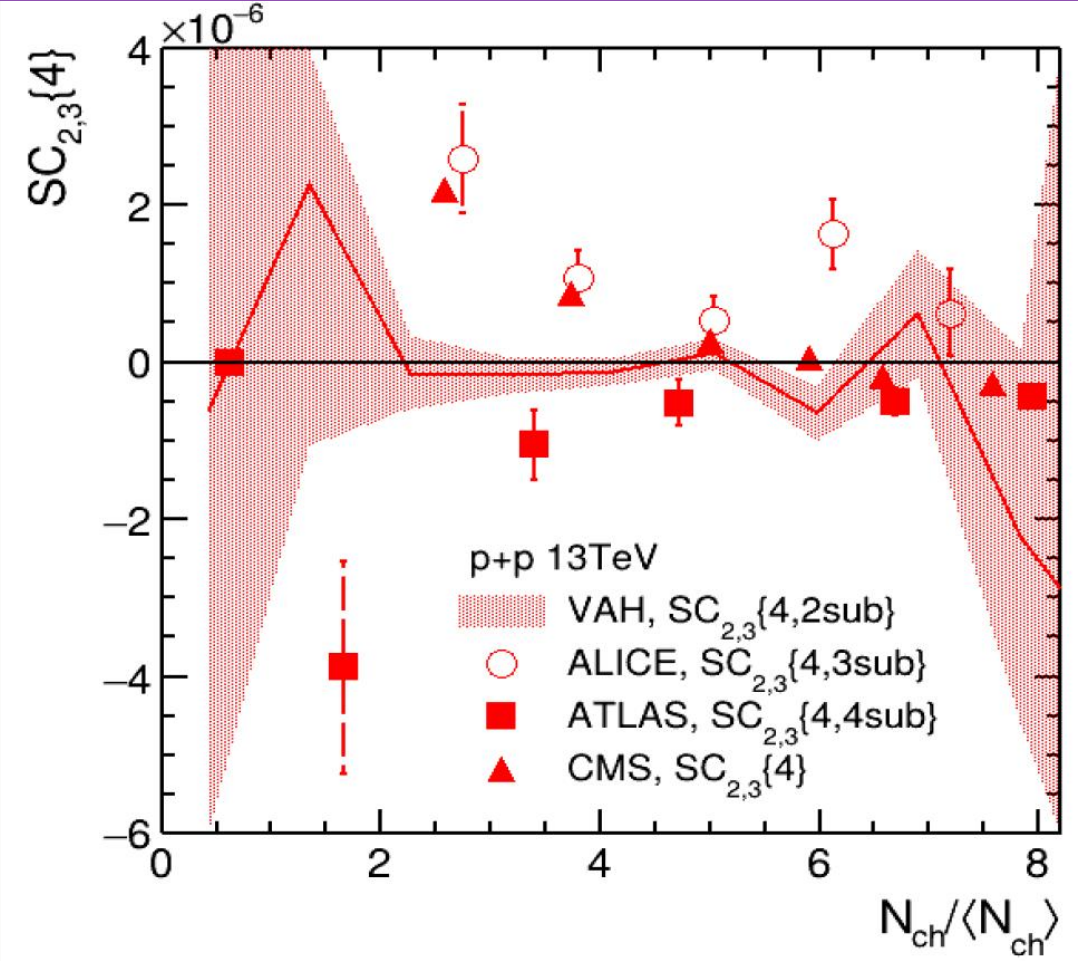

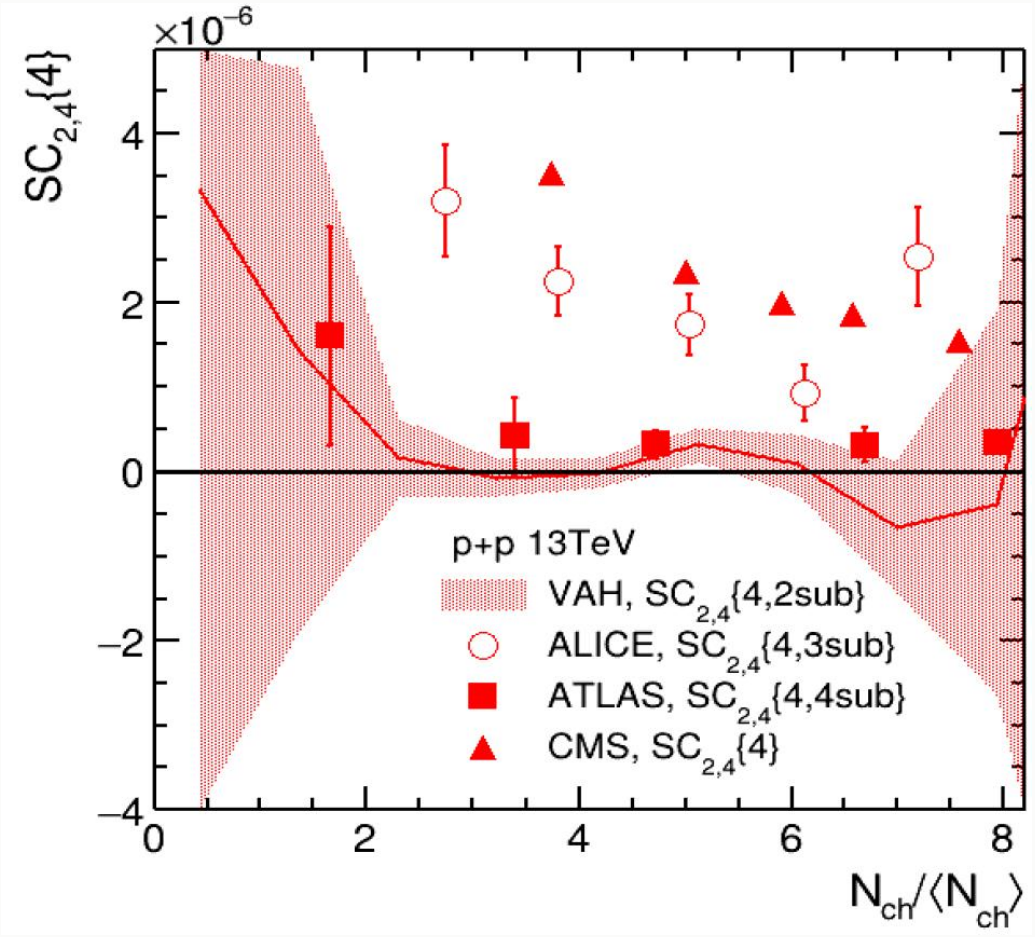

For p+p:

Consistent with zero with large error-bar.

Discripancy arise from experimental side.

More on collectivity: Flow Correlations

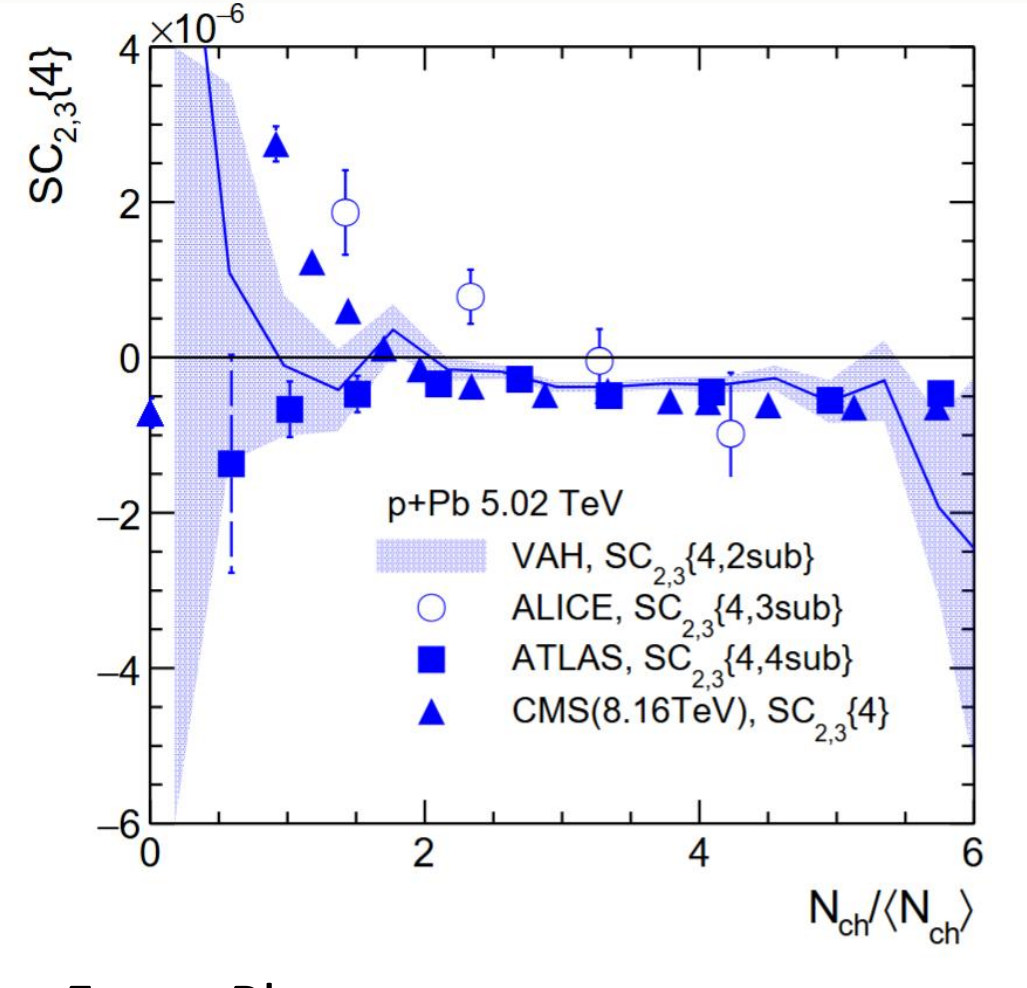

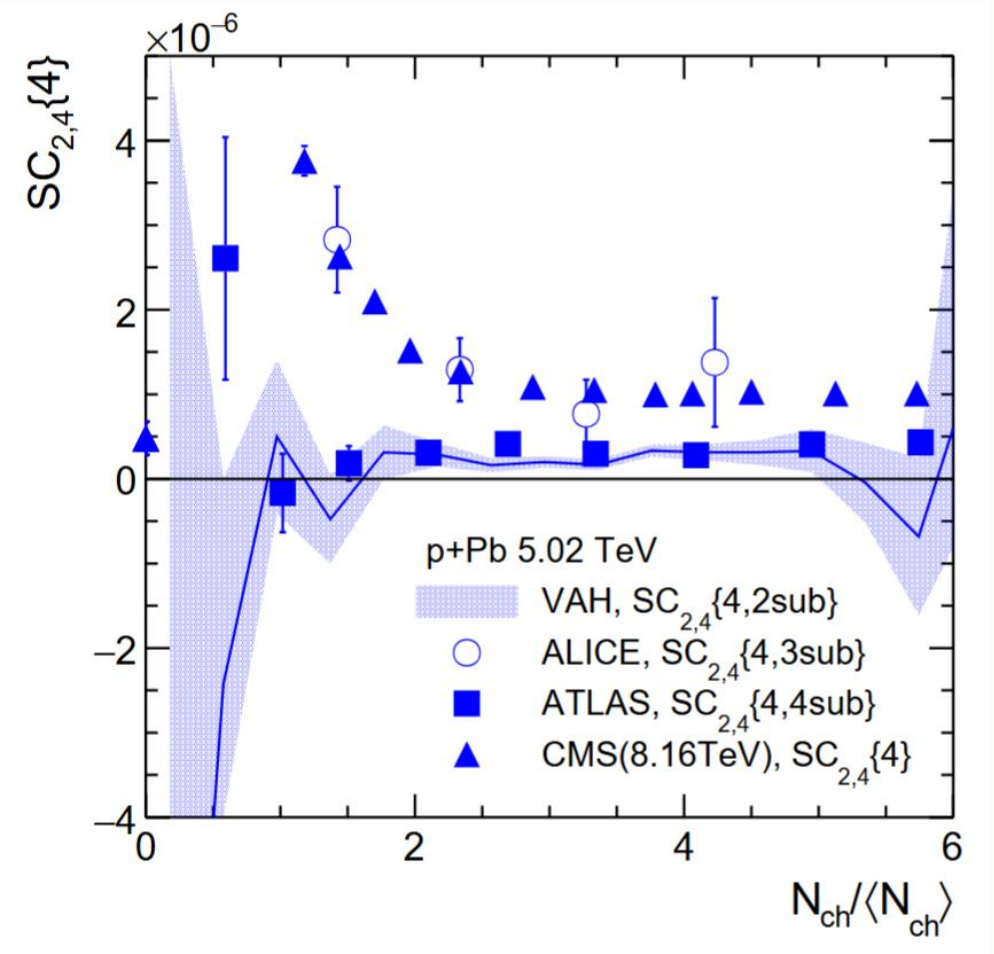

For p+Pb:

Correct sign produced in high multiplicity

Consistent with ATLAS & CMS predictions

Zhao, Y. Peng, U. Heinz, H. Song. Paper in preparation

Collectivity in Small Collision Systems?

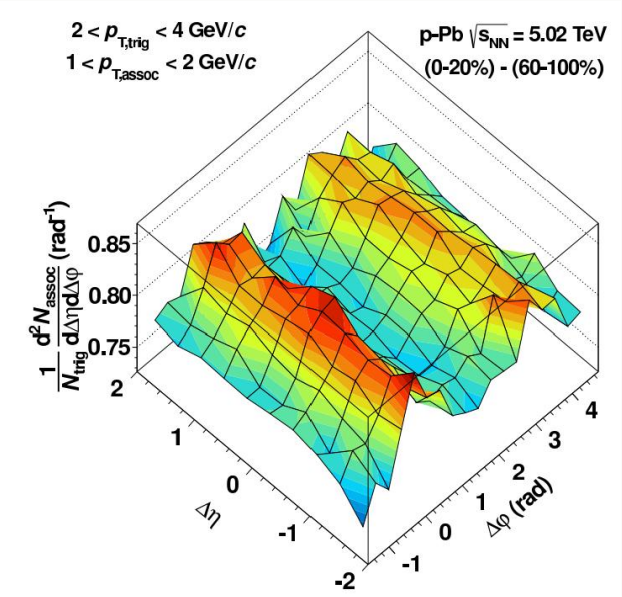

ALICE, Phys.Lett. B719 (2013) 29-41

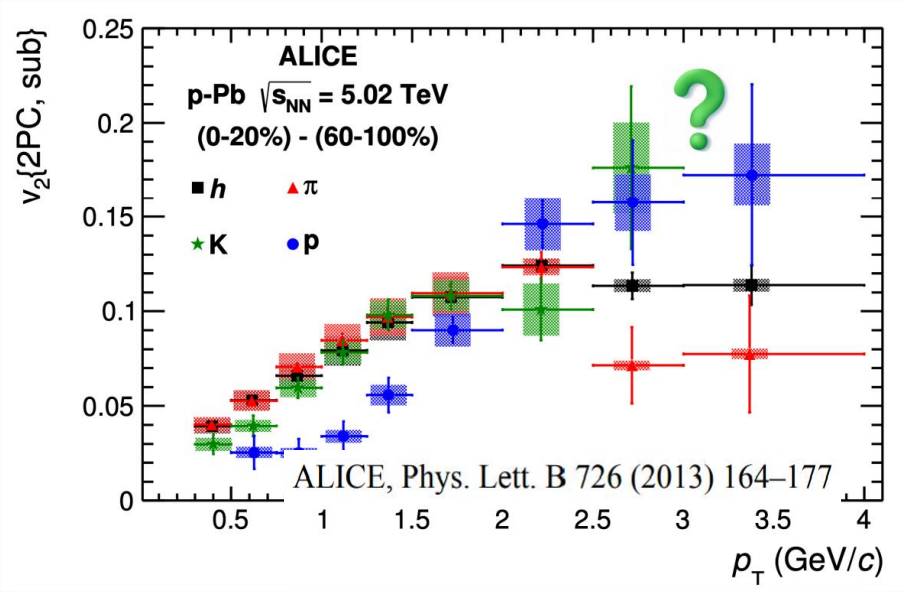

ALICE, Phys. Lett. B 726 (2013) 164–177

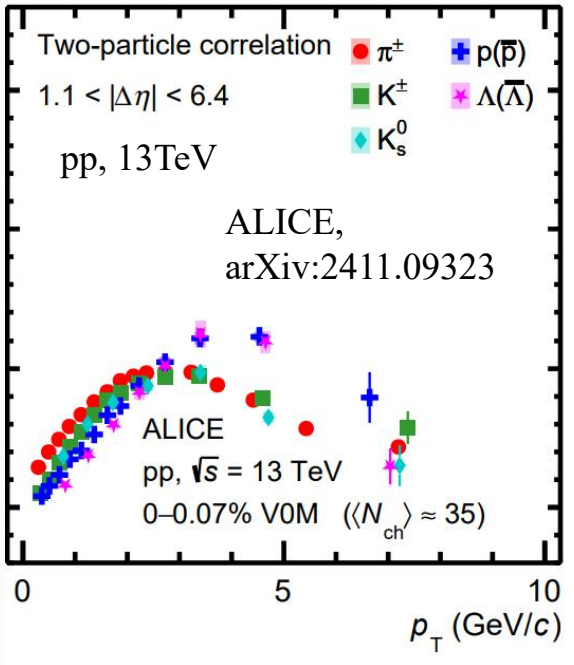

ALICE, Nature Phys. 13 (2017) 535-539

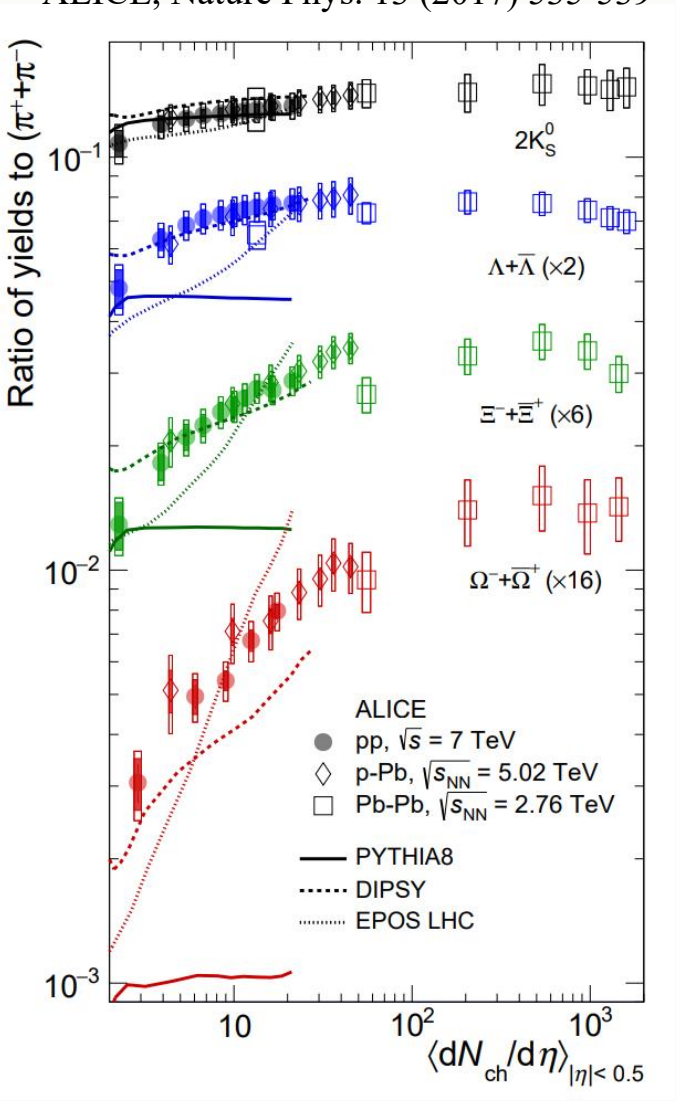

Origin of 'Collectivity'?

- Hydrodynamic response
- Gluon saturation
- Escape mechanism
- Multi parton interaction
- ...

$$\tau_{\pi,1} = \frac{5\eta}{Ts}, \quad \tau_{\pi,2} = \frac{5\eta}{\Lambda s}, \quad \tau_{\pi,3} = f(\alpha_L)\frac{5\eta}{\Lambda s}$$

$$\tau_\pi^{\mathrm{VAH}} = \eta/\beta_\pi^{\mathrm{VAH}}$$

$$\beta_\pi^{\mathrm{VAH}} \equiv \tilde{I}_{32}/\Lambda$$

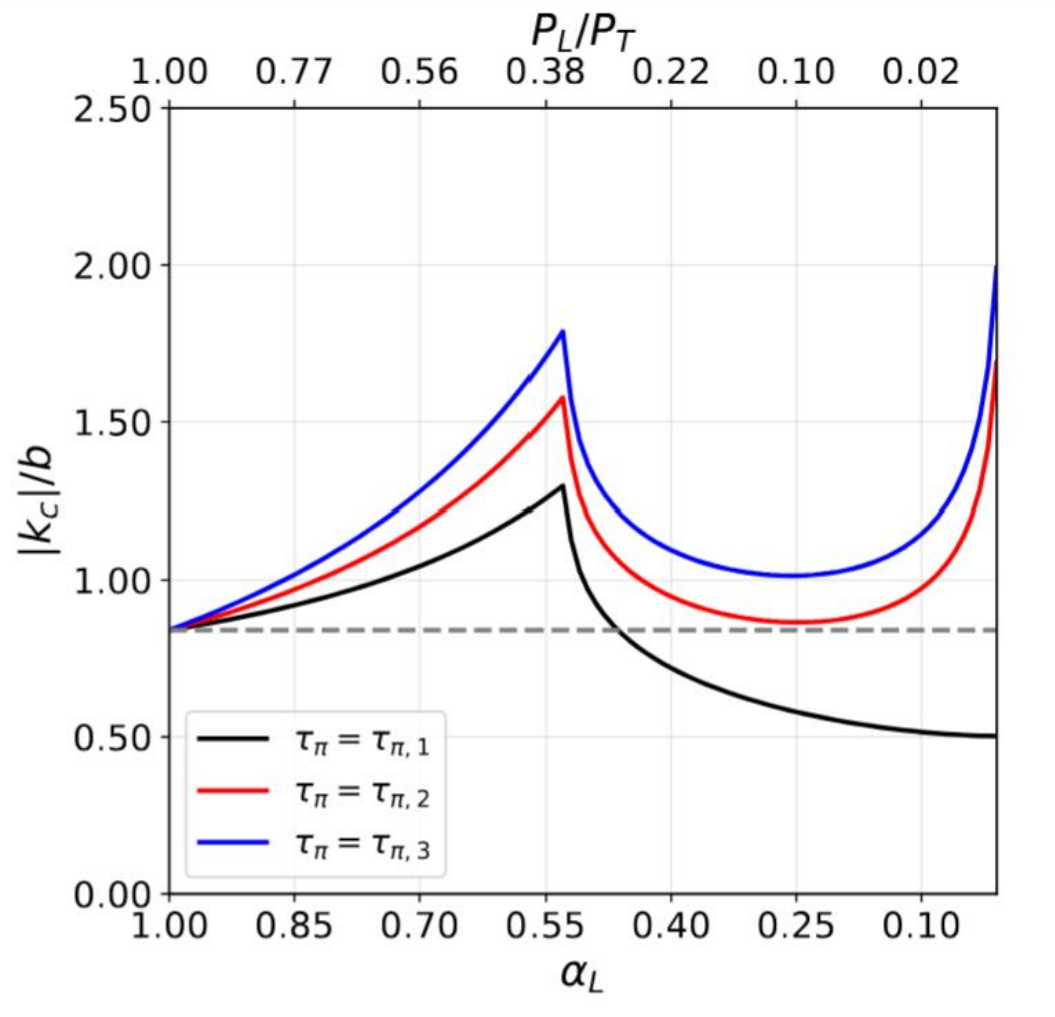

Case II: Anisotropic Perturbation

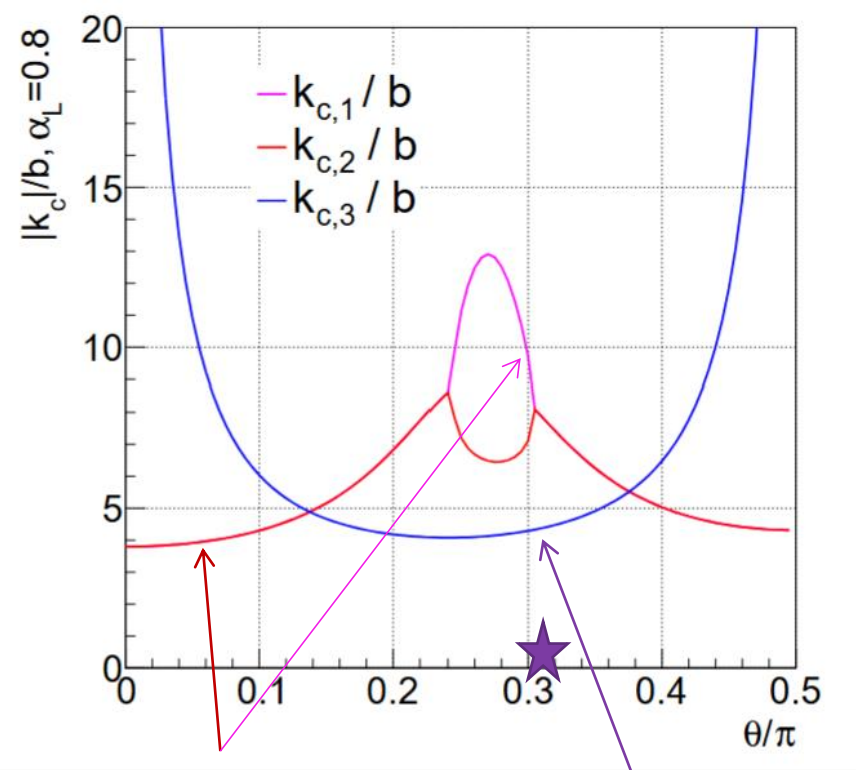

Sound & gapped mode collision (*2)

Shear & gapped mode collision (*1)

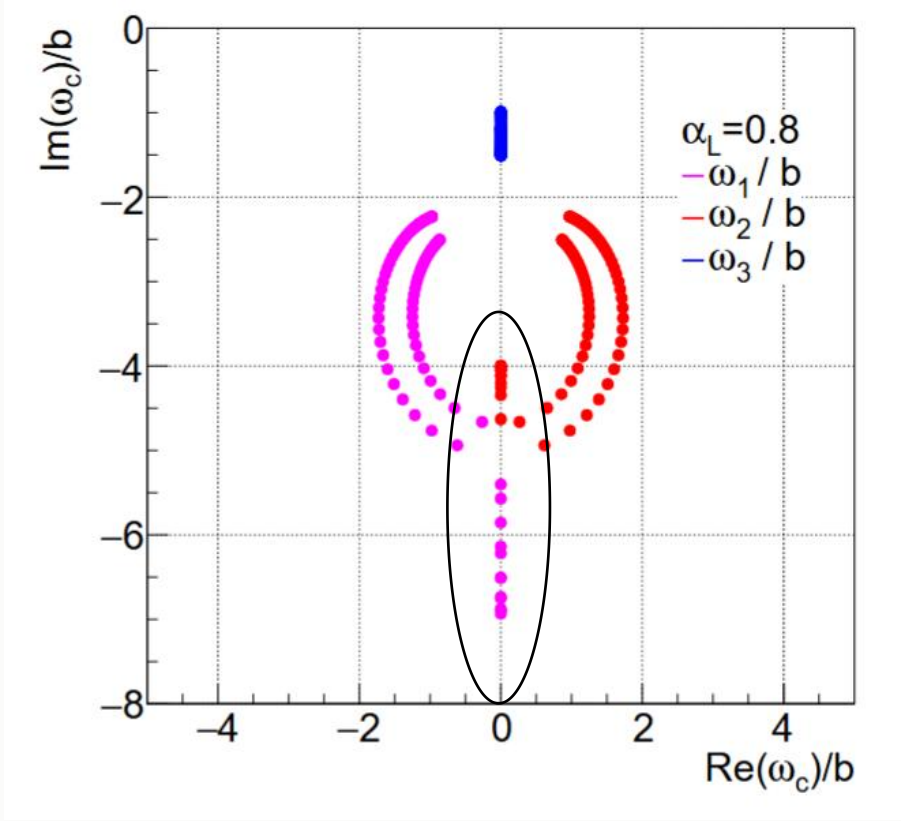

Well controlled large-k behavior

Zhao, et. al. Paper in preparation

Case II: Anisotropic Perturbation

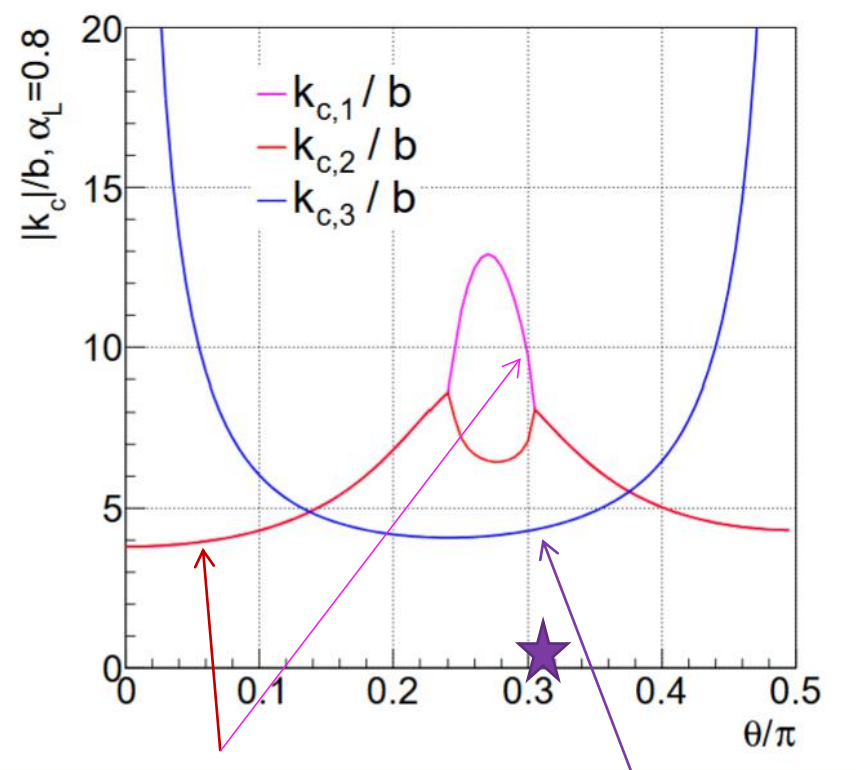

Sound & gapped mode collision (*2)

Shear & gapped mode collision (*1)

Zhao, et. al. Paper in preparation

Case II: Anisotropic Perturbation

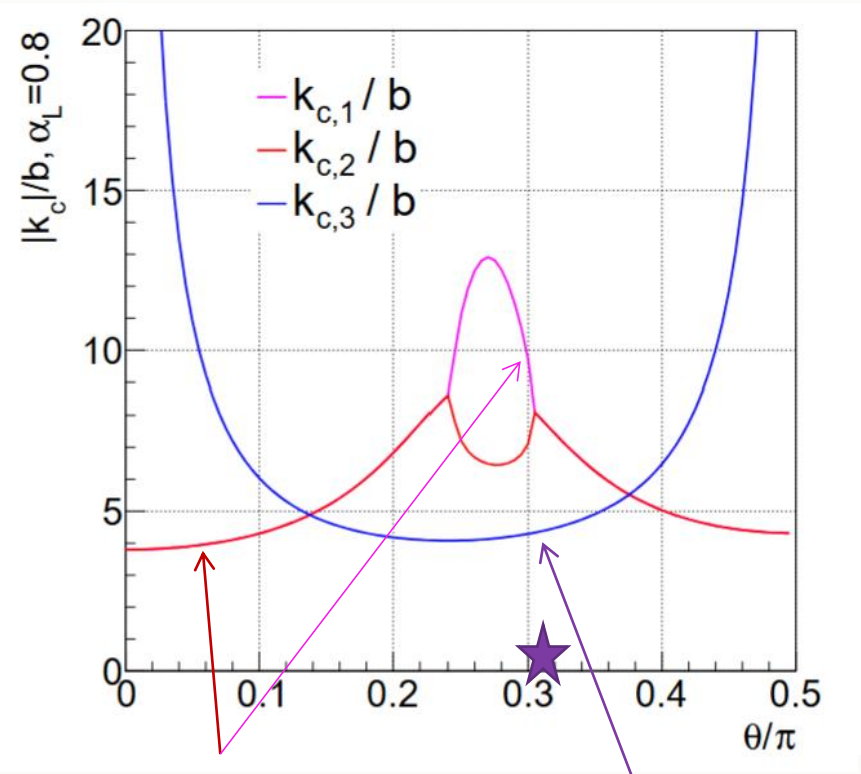

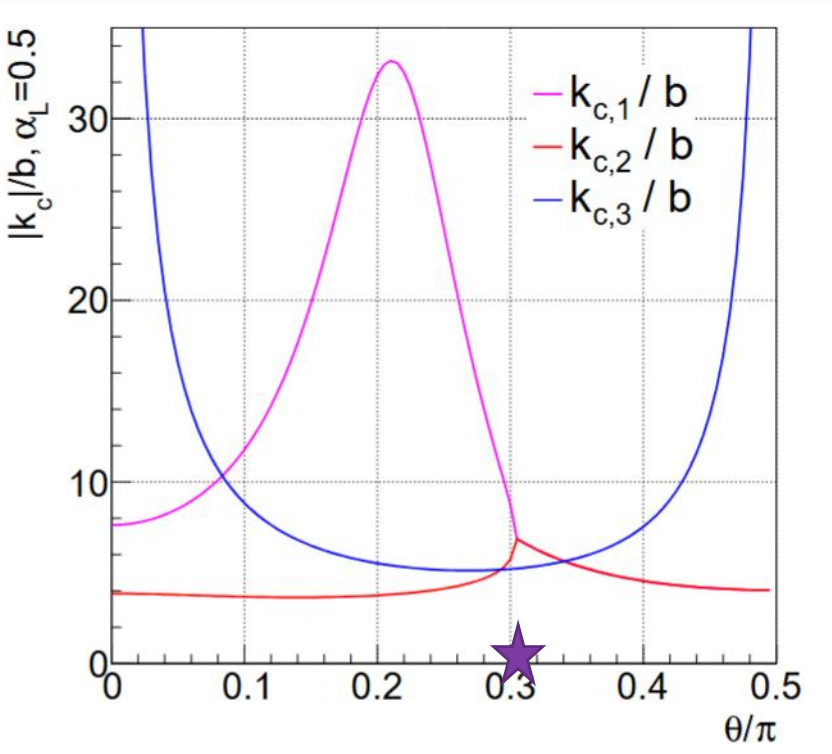

Sound & gapped mode collision (*2)

Shear & gapped mode collision (*1)

Mode splitting: shift from the propagating & damping coupling to well separation.

Zhao, et. al. Paper in preparation

Case II: Anisotropic Perturbation

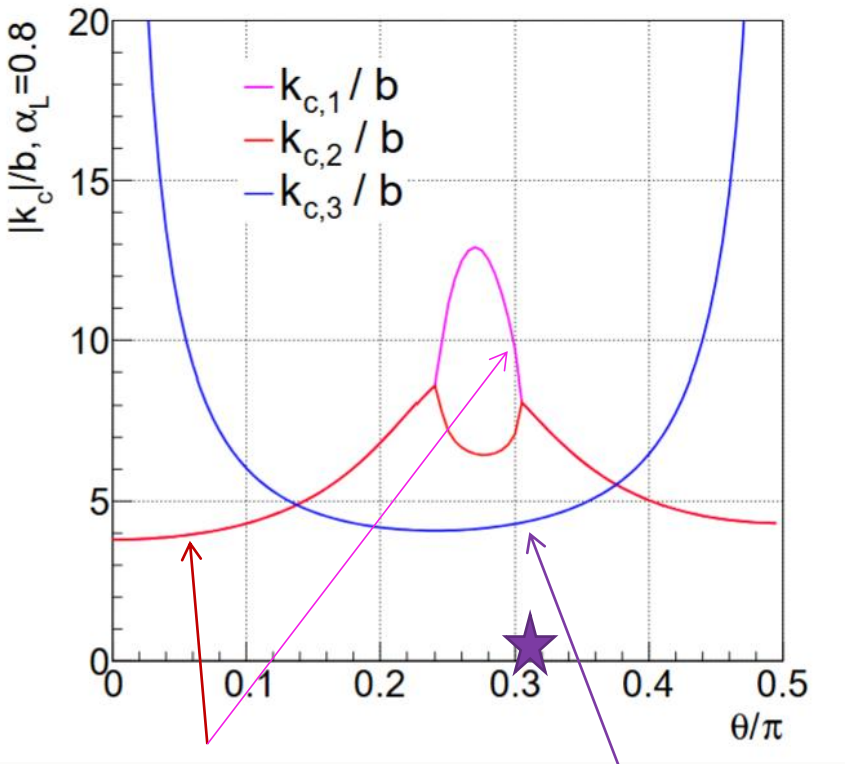

Sound & gapped mode collision (*2)

Shear & gapped mode collision (*1)

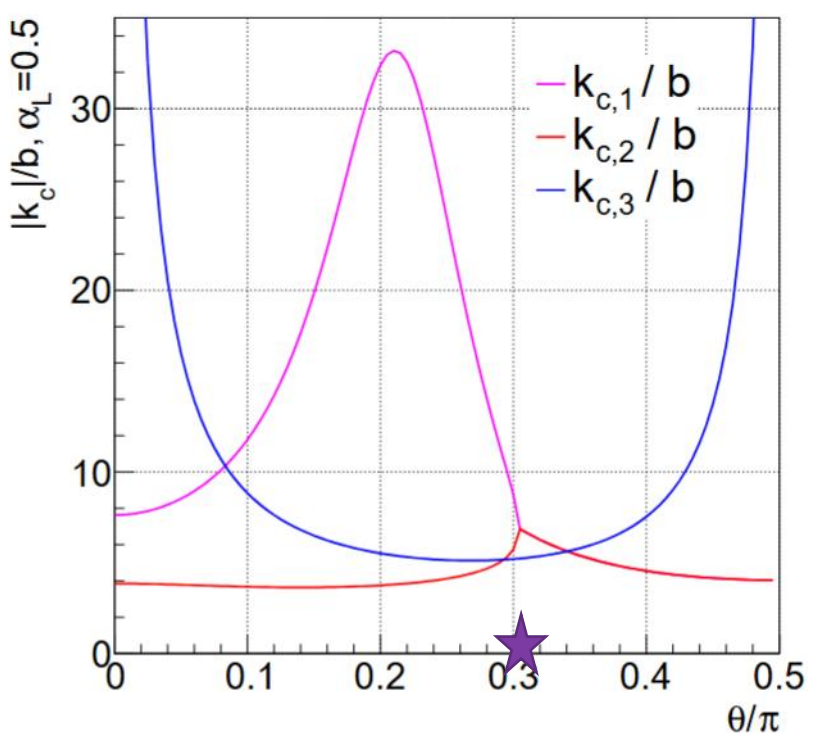

Mode splitting: shift from the propagating & damping coupling to well separation.

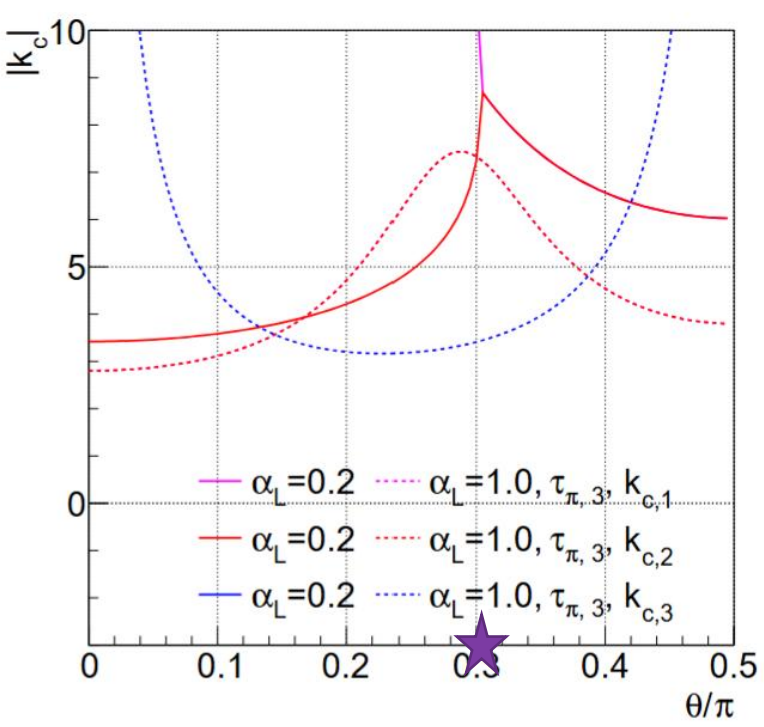

With proper choice of τ_π, validity still preserved when $(P_L/P_T)_0 << 1$

Zhao, et. al. Paper in preparation

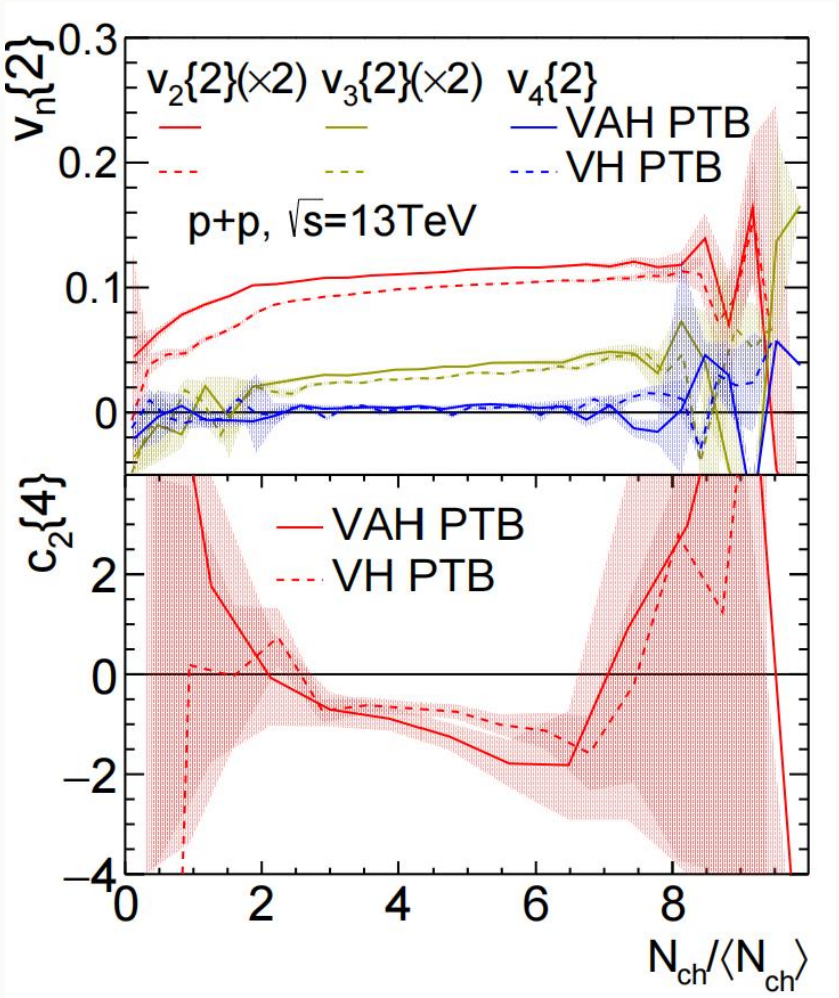
$v_n\{2\}$
$v_2\{2\}(\times2)$ $v_3\{2\}(\times2)$ $v_4\{2\}$
VAH PTB
VH PTB
p+p, $\sqrt{s}$=13TeV
$c_2\{4\}$
VAH PTB
VH PTB
$N_{ch}/\langle N_{ch}\rangle$

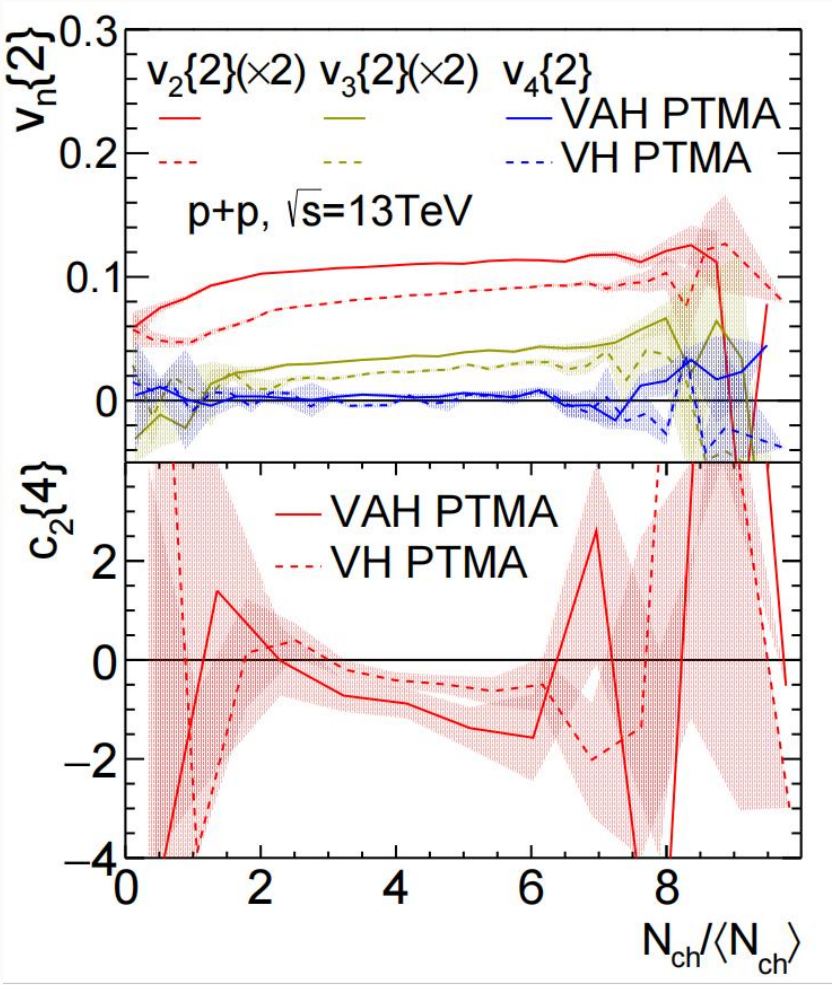
$v_n\{2\}$
$v_2\{2\}(\times2)$ $v_3\{2\}(\times2)$ $v_4\{2\}$
VAH PTMA
VH PTMA
p+p, $\sqrt{s}$=13TeV
$c_2\{4\}$
VAH PTMA
VH PTMA
$N_{ch}/\langle N_{ch}\rangle$

Isotropization: Heavy-Ion, Light-Ion, p+p

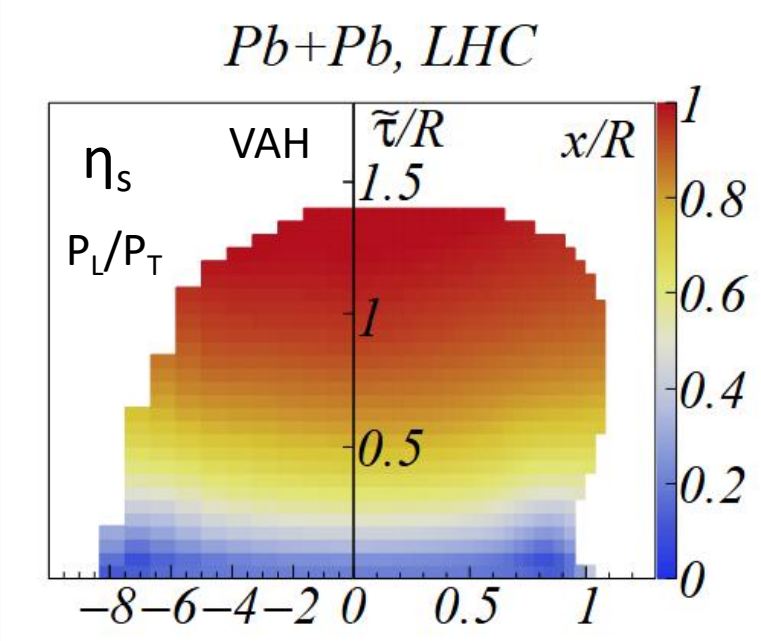

Heavy-ion collisions: Fast thermalization, Near-isotropization.

Zhao, Y. Peng, U. Heinz, H. Song. Paper in preparation.

Isotropization: Heavy-Ion, Light-Ion, p+p

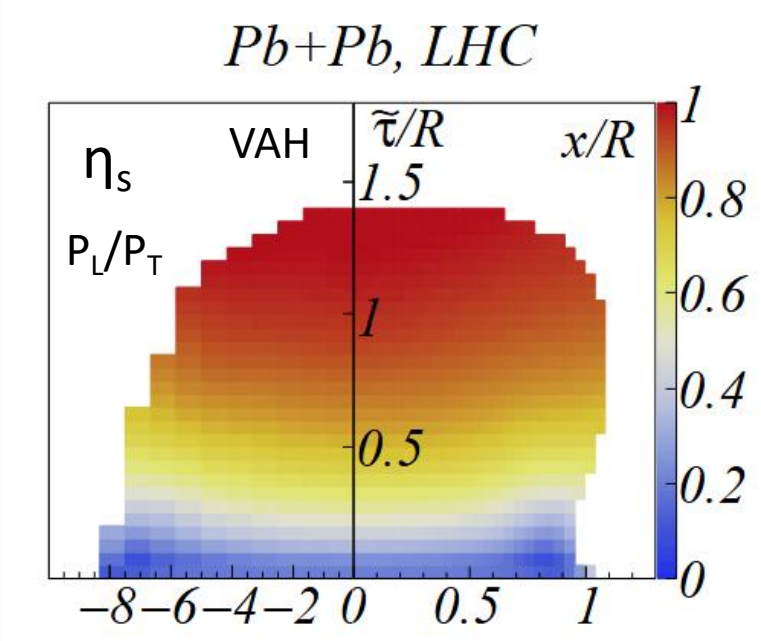

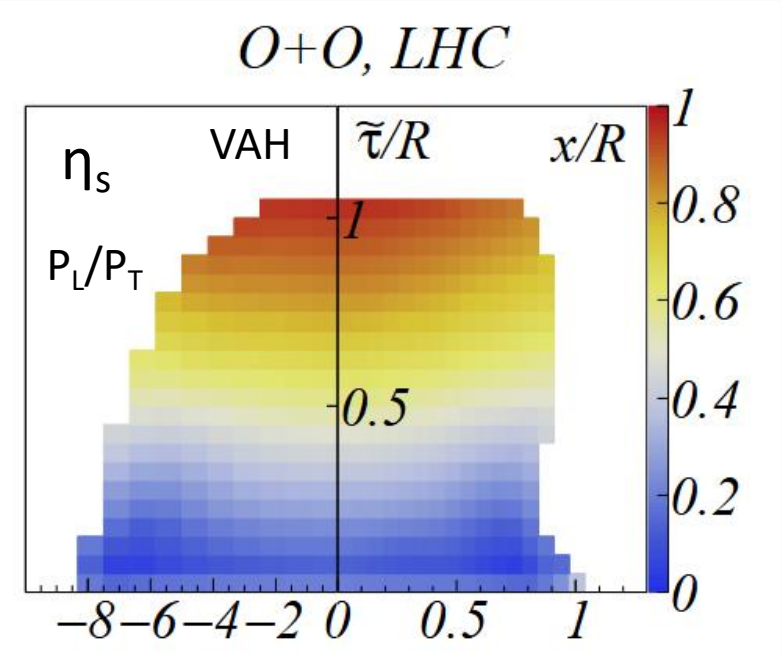

Heavy-ion collisions: Fast thermalization, Near-isotropization.

O+O collisions: Critical case.

Zhao, Y. Peng, U. Heinz, H. Song. Paper in preparation.

Isotropization: Heavy-Ion, Light-Ion, p+p

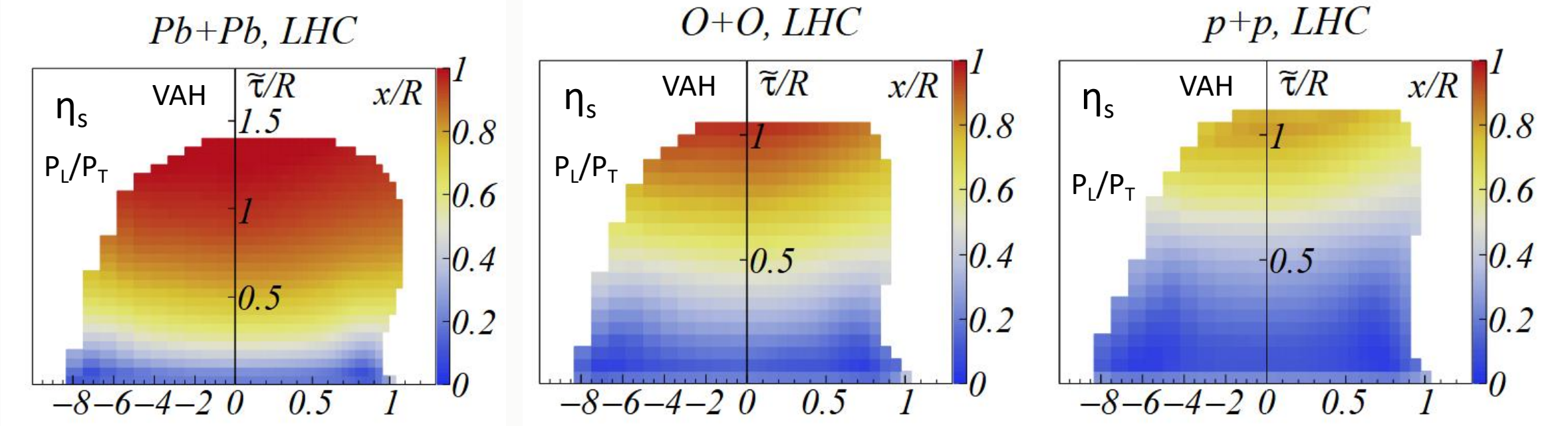

Heavy-ion collisions: Fast thermalization, Near-isotropization.

O+O collisions: Critical case.

p+p collisions: Remain anisotropic.

Zhao, Y. Peng, U. Heinz, H. Song. Paper in preparation.

Attractor behavior of VAH

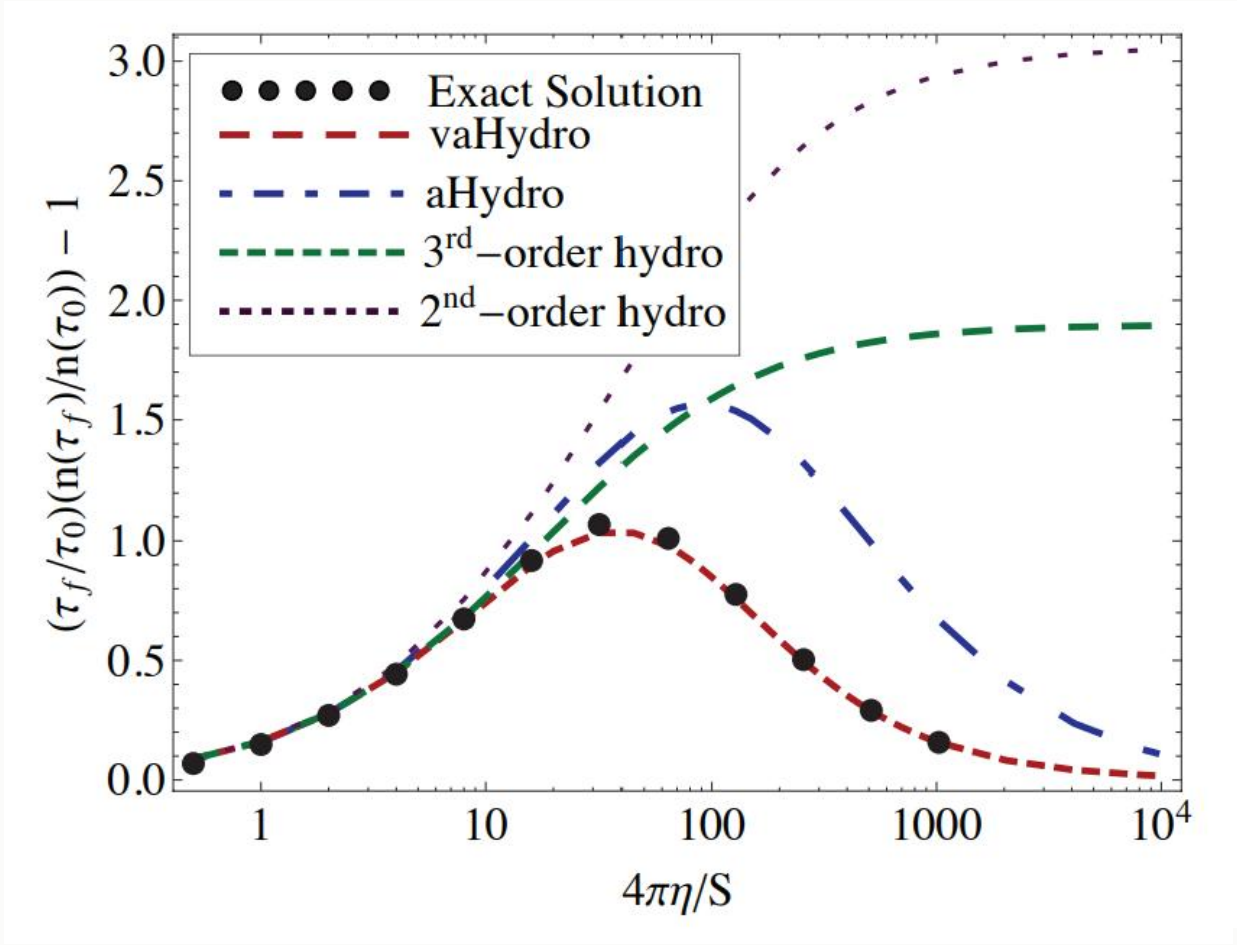

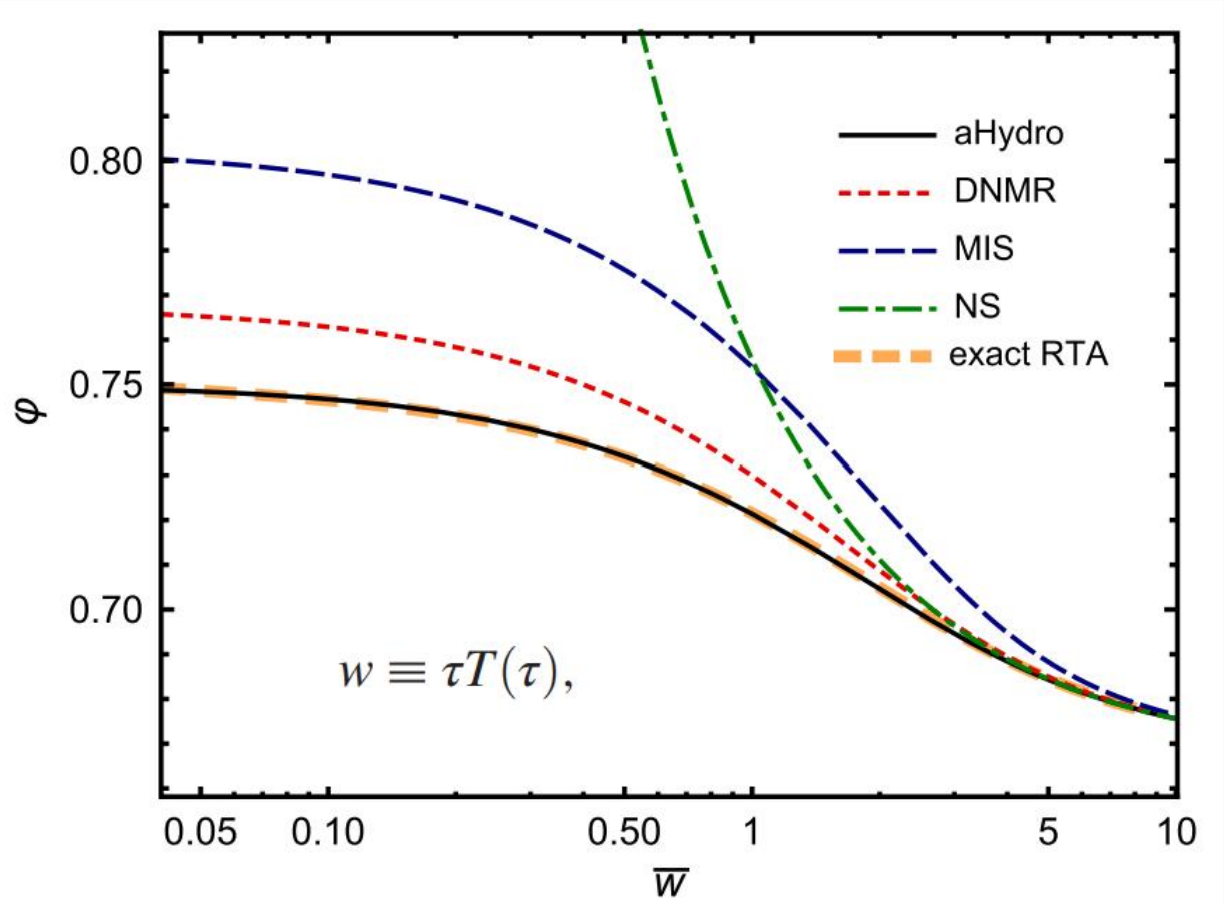

Particle production & Attractor solution perfectly match the Boltzmann solution

D. Bazow, U. W. Heinz, M. Strickland, Phys.Rev.C 90 (2014) 5, 054910
M. Strickland, J. Noronha, G. Denicol. Phys.Rev.D 97 (2018) 3, 036020

Solutions

$$\omega_\pm = \pm c_s k - i\Gamma k^2 + \mathcal{O}(k^3),$$
$$\omega_D = -iDk^2 + \mathcal{O}(k^3),$$
$$\omega_\gamma = -3ib + i\gamma k^2 + \mathcal{O}(k^3)$$

$$\Gamma = \frac{1}{12b}(1-3\chi)\left[c_s^2 + \Gamma_z^L \chi + \Gamma_\perp^L (1-\chi)\right],$$
$$D = \frac{1}{2b}(\Gamma_\perp^L - \Gamma_z^L)\chi(1-\chi),$$
$$\gamma = \frac{1}{6b}\left[(c_s^2 + \Gamma_\perp^L)(1-\chi) - 2(c_s^2 + \Gamma_z^L)\chi\right]$$

- Sound mode: $\tilde{\omega}_\pm = \pm c_s \tilde{k}$
- Diffusion mode: $\tilde{\omega}_D = -\frac{3i}{2} + \frac{\sqrt{3}i}{6}\sqrt{27 - 4\delta\Gamma\ \tilde{k}^2}$
- Gap mode: $\tilde{\omega}_\gamma = -\frac{3i}{2} - \frac{\sqrt{3}i}{6}\sqrt{27 - 4\delta\Gamma\ \tilde{k}^2}$

Hard Parton Production

rcBK ICs and evolution

$$N_F(r,x_0) = 1 - \exp\left[-\frac{(r^2Q_{s0}^2)^\gamma}{4}\ln\left(\frac{1}{\Lambda r} + e_c \cdot e\right)\right]$$

rcBK ICs	γ	Q_{s0}^2 (GeV^2)	$\Lambda_{\rm QCD}$ (GeV)	e
MV	1	0.200	0.241	2.718
MV$^\gamma$	1.101	0.157	0.241	2.718
MV^e	1	0.060	0.241	18.9

$$\partial_Y S_Y^{(2)}(\boldsymbol{x},\boldsymbol{y}) = \int \mathrm{d}^2\boldsymbol{z}\; K_{\rm rc}(\boldsymbol{x},\boldsymbol{y},\boldsymbol{z})\left[S_Y^{(2)}(\boldsymbol{x},\boldsymbol{z})S_Y^{(2)}(\boldsymbol{z},\boldsymbol{y}) - S_Y^{(2)}(\boldsymbol{x},\boldsymbol{y})\right]$$

For dilute-dense system:

$$\frac{\mathrm{d}\sigma_{\rm DHJ}}{\mathrm{d}y\mathrm{d}^2p_T} = \frac{K}{(2\pi)^2}\frac{\sigma_0}{2}\sum_{i=q,g} x_1 f_{i/p}(x_1,Q^2)N_i(x_2.p_T)$$

For dense-dense system:

$$\frac{\mathrm{d}\sigma_{k_T}}{\mathrm{d}y\mathrm{d}^2p_T} = \frac{K}{2C_F}\frac{1}{p_T^2}\left(\frac{\sigma_0}{2}\right)^2\int \mathrm{d}^2\boldsymbol{k}_T\,\alpha_s(Q_M^2) \times \varphi(x_1,\frac{\boldsymbol{p}_T+\boldsymbol{k}_T}{2})\varphi(x_2,\frac{\boldsymbol{p}_T-\boldsymbol{k}_T}{2}),$$

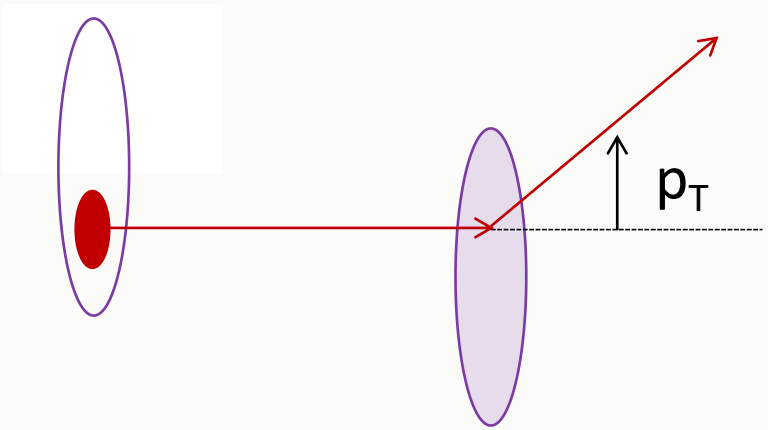

W. Deng, H. Fujii, T. Hirano, K. Itakura, Y. Nara, Phys.Rev.D 91 (2015) 1, 014006
Zhao, H. Fujii, T. Hirano, K. Itakura, Y. Nara, paper in preparation

Radiation Process & Multi-parton Generation

- ISR & FSR share very similar formalism but with reversed process:

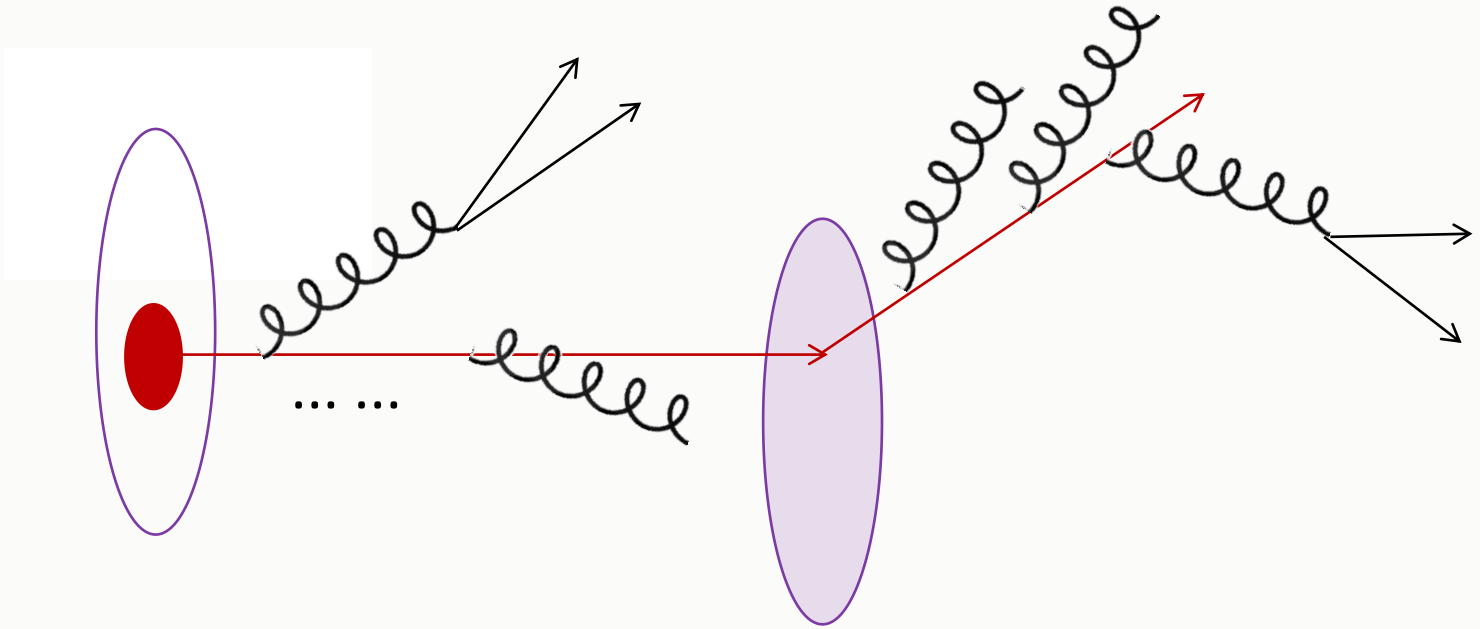

W. Deng, H. Fujii, T. Hirano, K. Itakura, Y. Nara, Phys.Rev.D 91 (2015) 1, 014006
Zhao, H. Fujii, T. Hirano, K. Itakura, Y. Nara, paper in preparation

Radiation Process & Multi-parton Generation

- ISR & FSR share very similar formalism but with reversed process:
- Multiple independent hard scatterings

# of hard scattering ~

$$P(n) = \frac{\Gamma(k+n)}{\Gamma(k)\Gamma(n+1)} \frac{\langle n \rangle^n k^k}{(\langle n \rangle + k)^{n+k}}$$

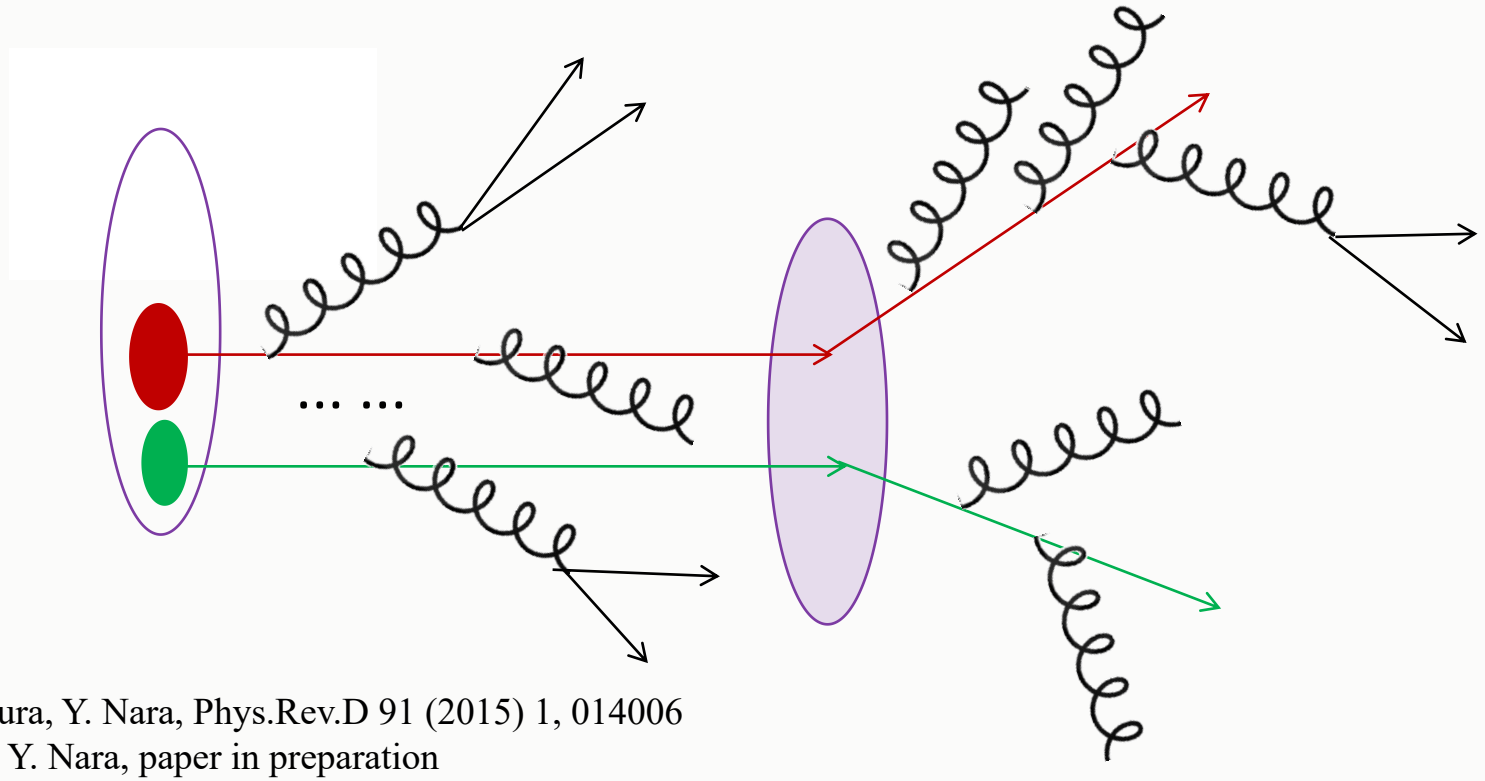

W. Deng, H. Fujii, T. Hirano, K. Itakura, Y. Nara, Phys.Rev.D 91 (2015) 1, 014006
Zhao, H. Fujii, T. Hirano, K. Itakura, Y. Nara, paper in preparation

Fragmentation and Remnants

- Remnants are connected to the produced partons

$$\chi \propto \frac{(1-\chi)^k}{(\chi^2 + c_{\min}^2)^{b_\chi/2}}$$

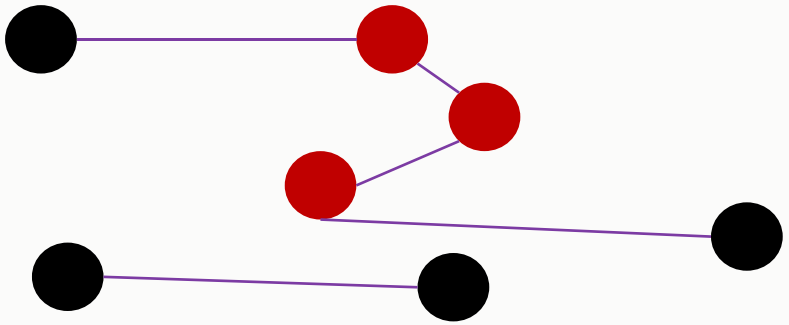

W. Deng, H. Fujii, T. Hirano, K. Itakura, Y. Nara, Phys.Rev.D 91 (2015) 1, 014006
Zhao, H. Fujii, T. Hirano, K. Itakura, Y. Nara, paper in preparation

Fragmentation and Remnants

- Remnants are connected to the produced partons

$$\chi \propto \frac{(1-\chi)^k}{(\chi^2 + c^2_{\min})^{b_\chi/2}}$$

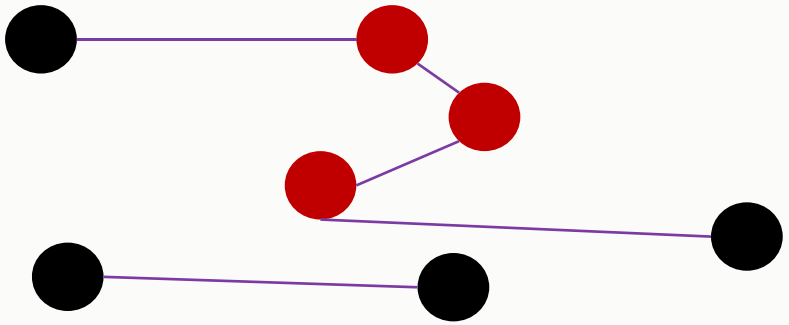

- Fragmentation is performed by Lund-String framework:

  Each partons are connected via color strings

  Lund string fragmentation will introduce additional pT modification:

$$f(z, p_T) \sim \frac{(1-z)^a}{z} \exp\left(-\frac{bm_T^2}{z}\right) \exp\left(-\frac{p_T^2}{\sigma^2}\right)$$

TMD like FFs Gaussian kick

W. Deng, H. Fujii, T. Hirano, K. Itakura, Y. Nara, Phys.Rev.D 91 (2015) 1, 014006
Zhao, H. Fujii, T. Hirano, K. Itakura, Y. Nara, paper in preparation

Light-Ion Collisions

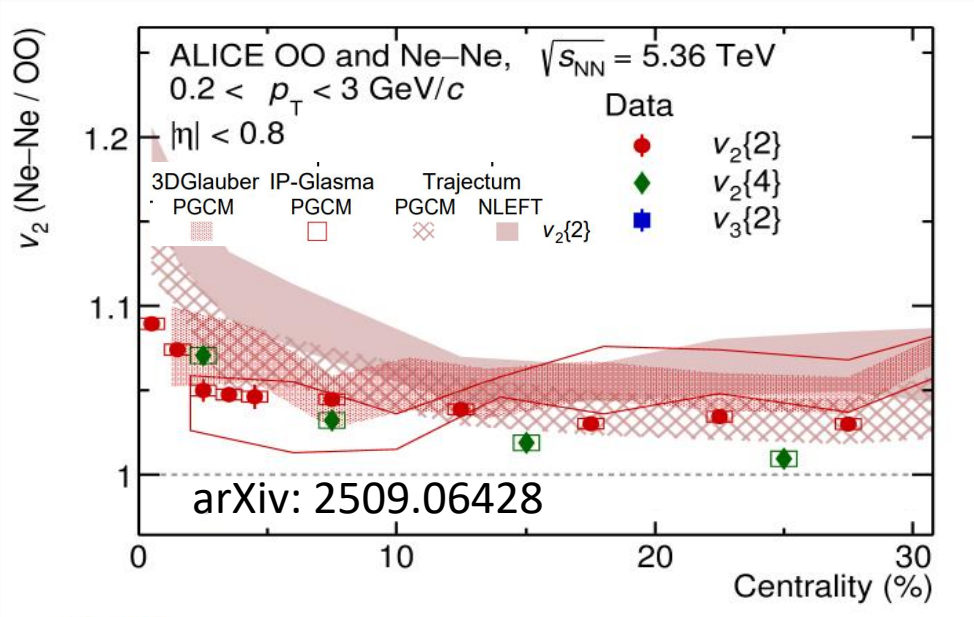

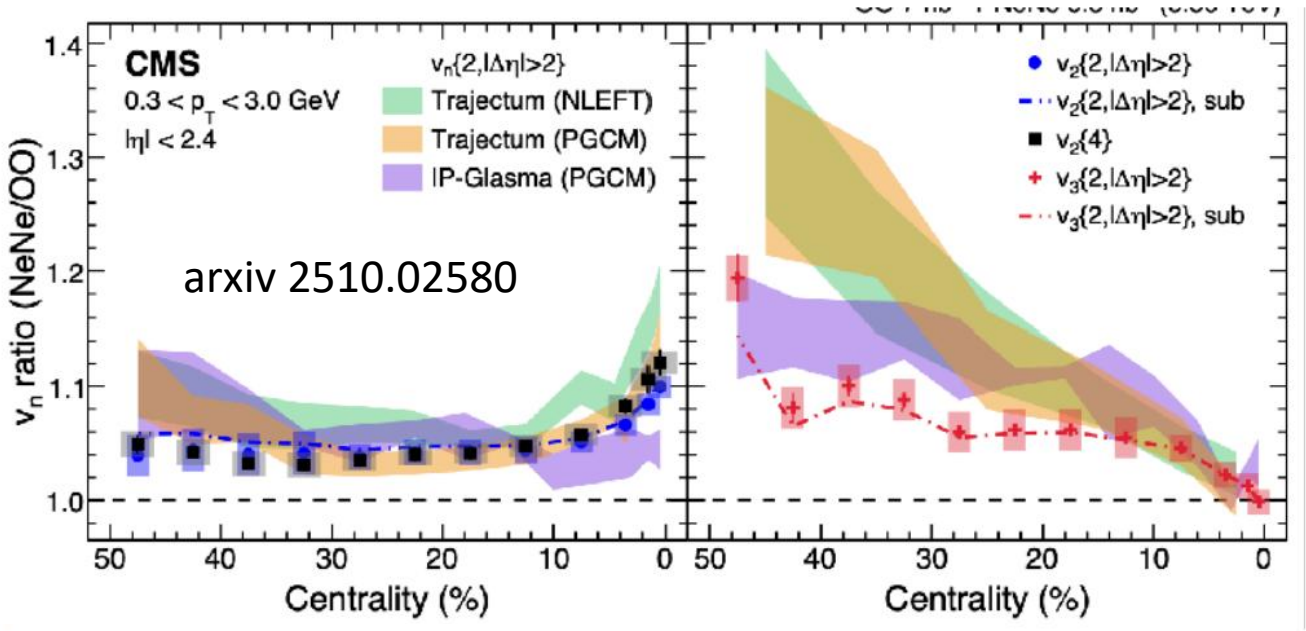

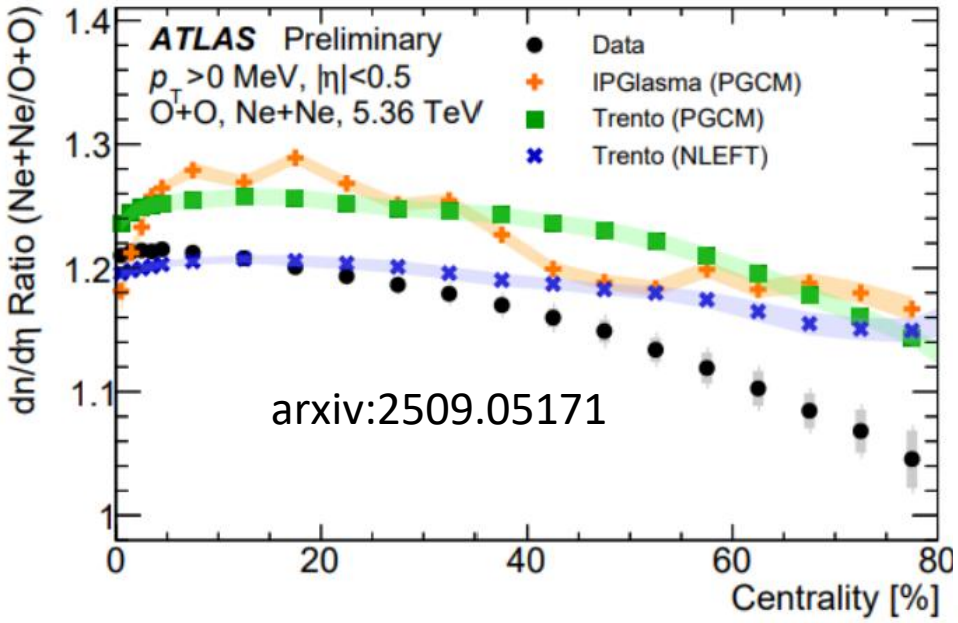

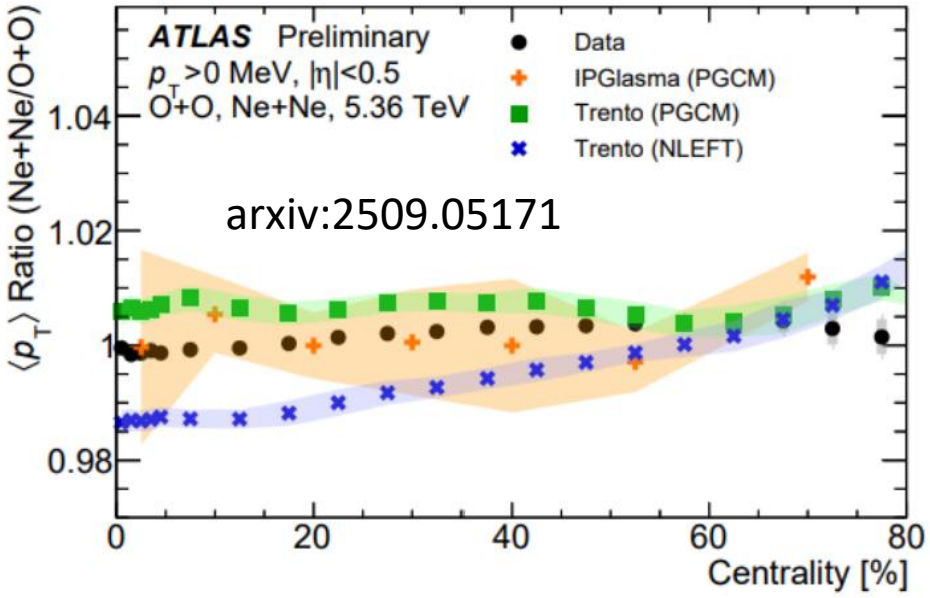

Reasonable description from Hydro + Nucl. Strc.

Improvement for early stage & Exp

$\langle P_L/P_T \rangle$

VH, small-mass, $(P_L/P_T)_0$=0.4, τ0=0.12 fm/c, (η/s)min=0.16

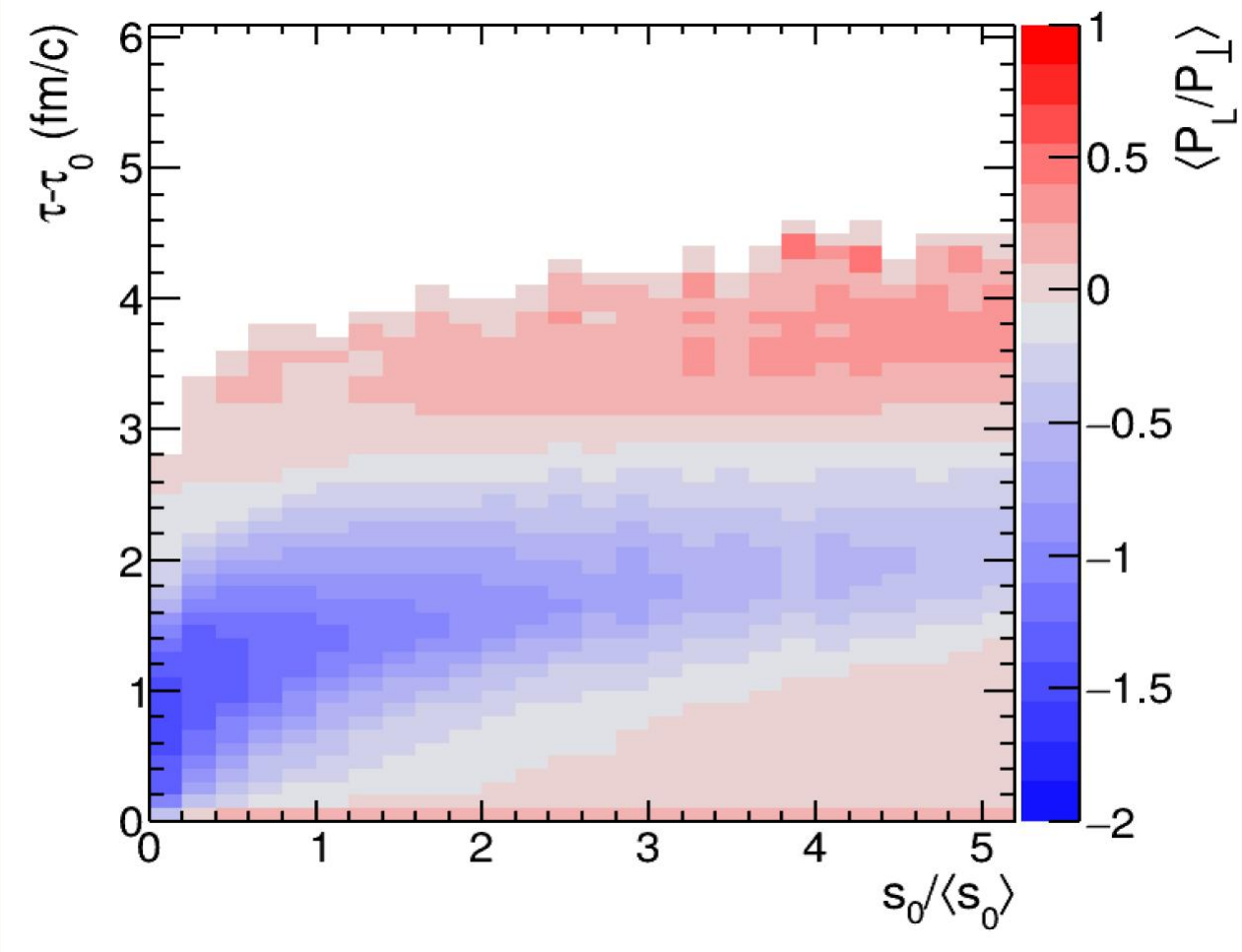

VH, m(T), $(P_L/P_T)_0$=0.4, τ0=0.12 fm/c, (η/s)min=0.16

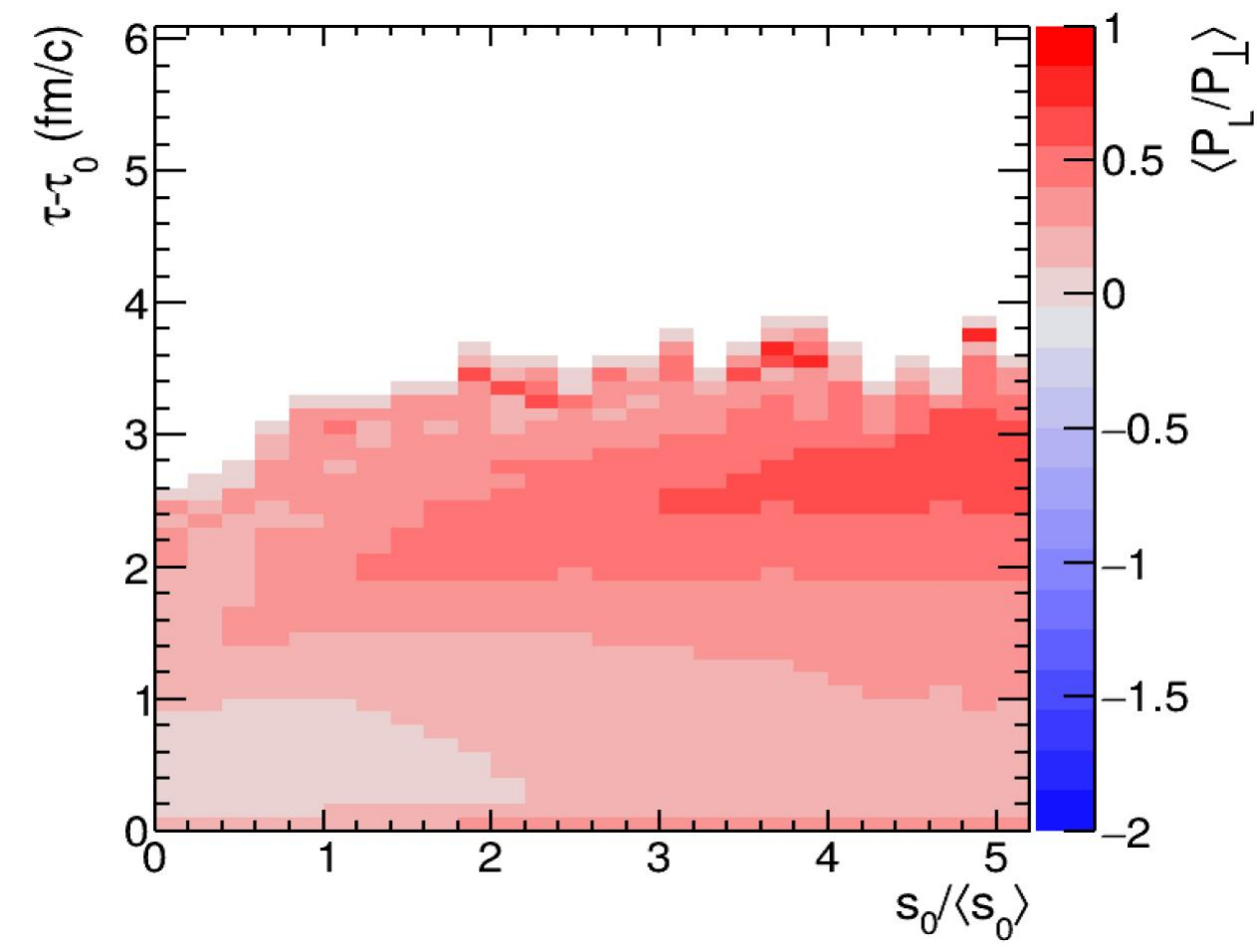

$\langle P_L/P_T \rangle$

VAH, small-mass, $(P_L/P_T)_0$=0.4, τ0=0.12 fm/c, (η/s)min=0.16

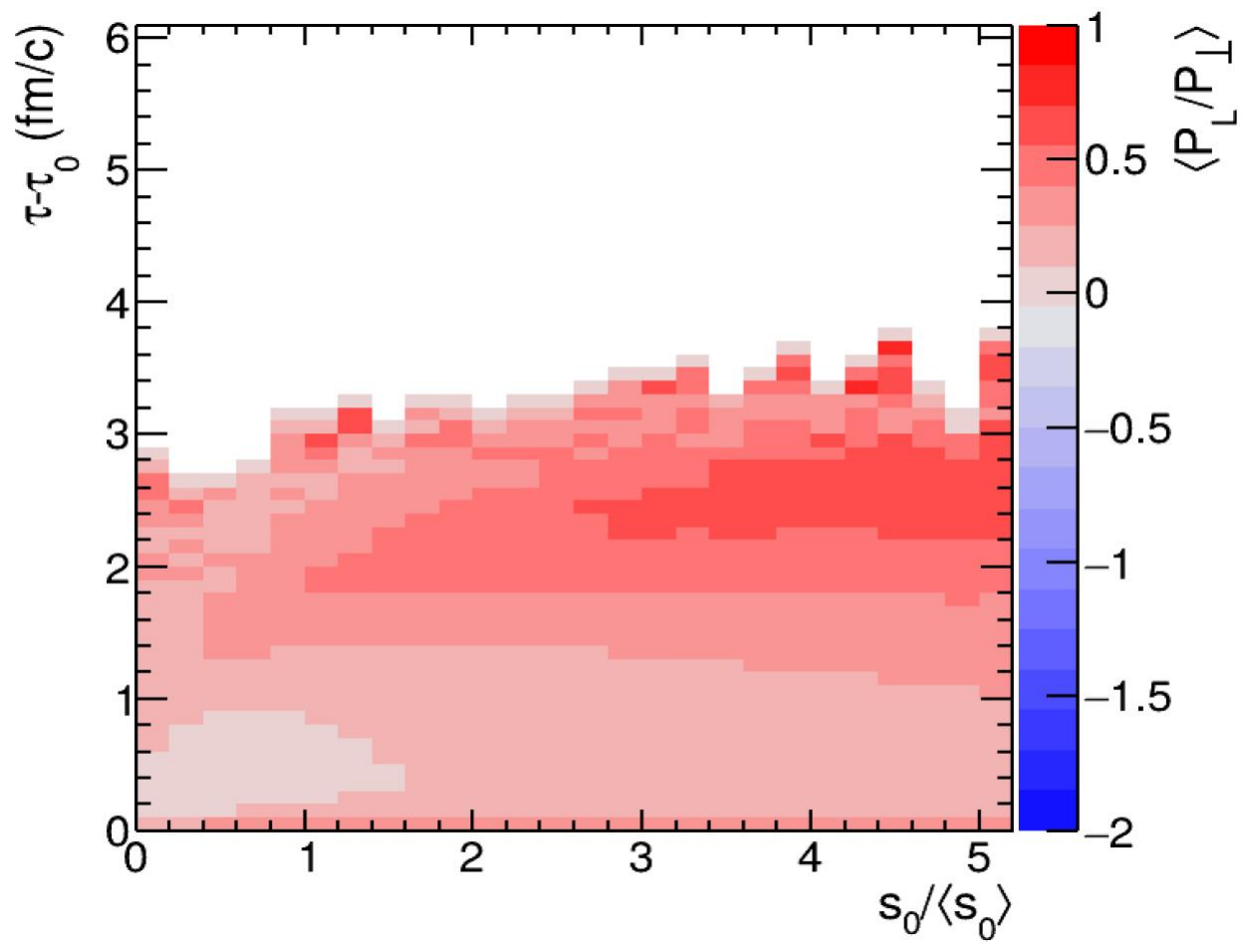

VAH, m(T), $(P_L/P_T)_0$=0.4, τ0=0.12 fm/c, (η/s)min=0.16

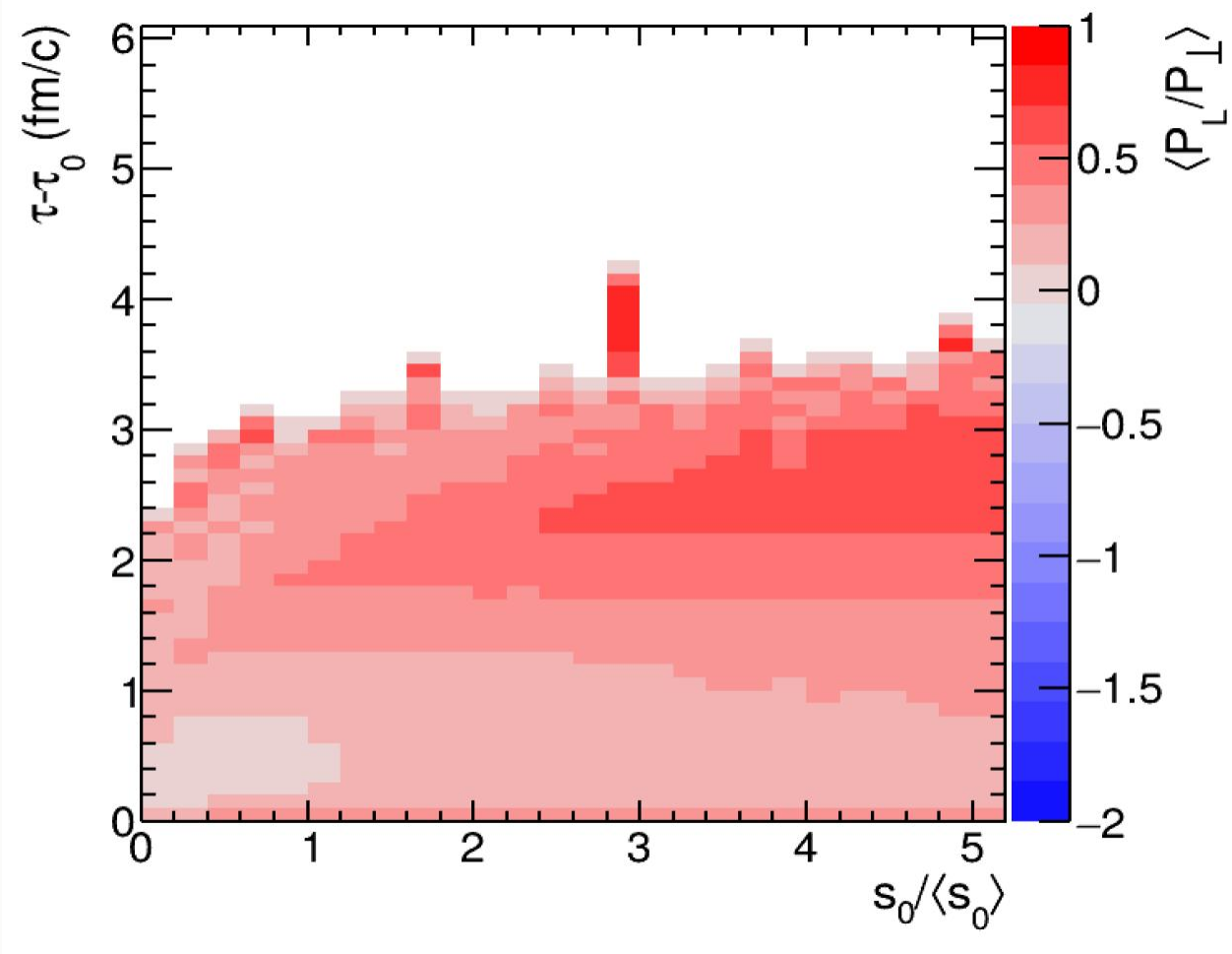

$\langle 1-\Theta(P_L/P_T)\rangle$

VH, small-mass, $(P_L/P_T)_0$=0.4, τ0=0.12 fm/c, (η/s)min=0.16

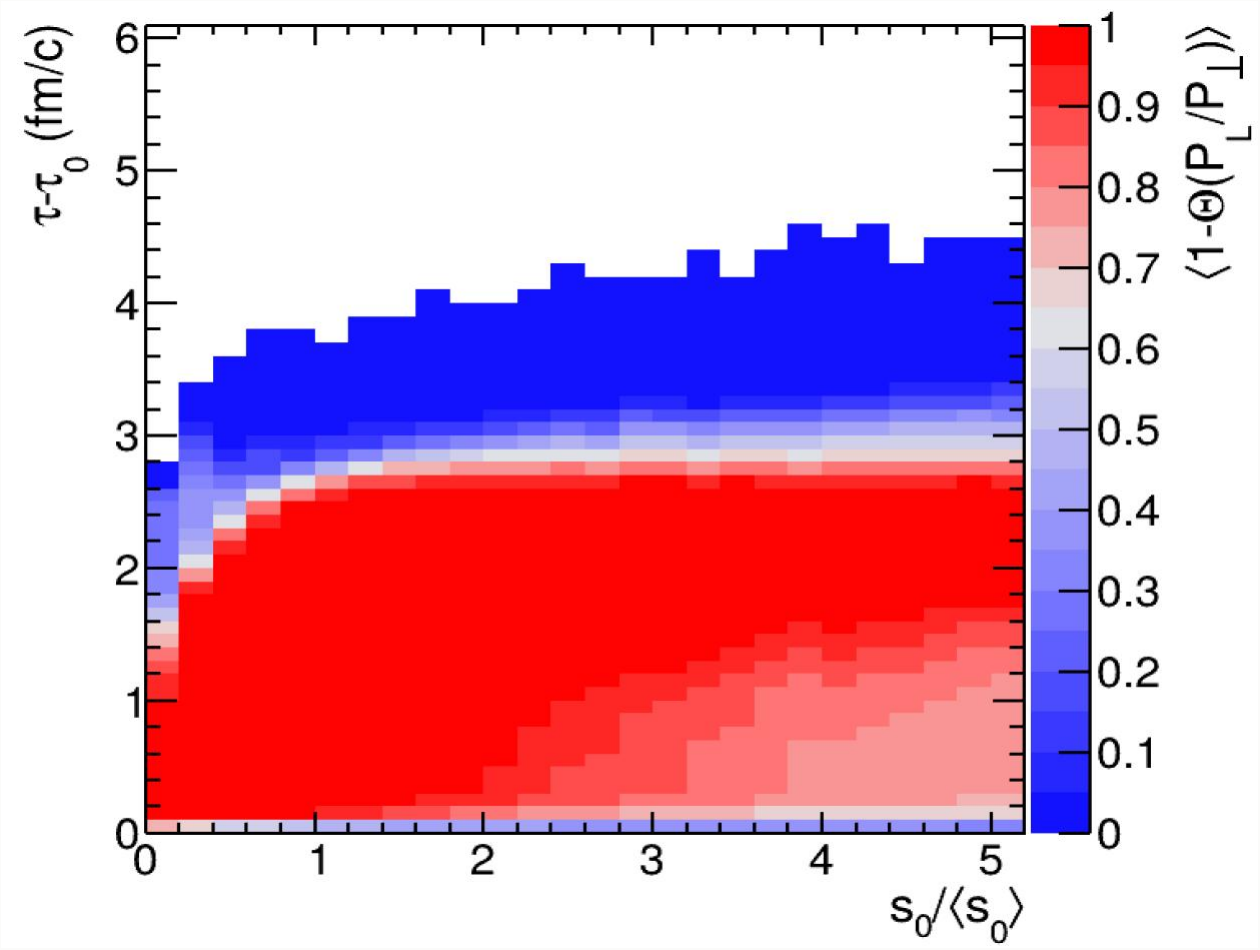

VH, m(T), $(P_L/P_T)_0$=0.4, τ0=0.12 fm/c, (η/s)min=0.16

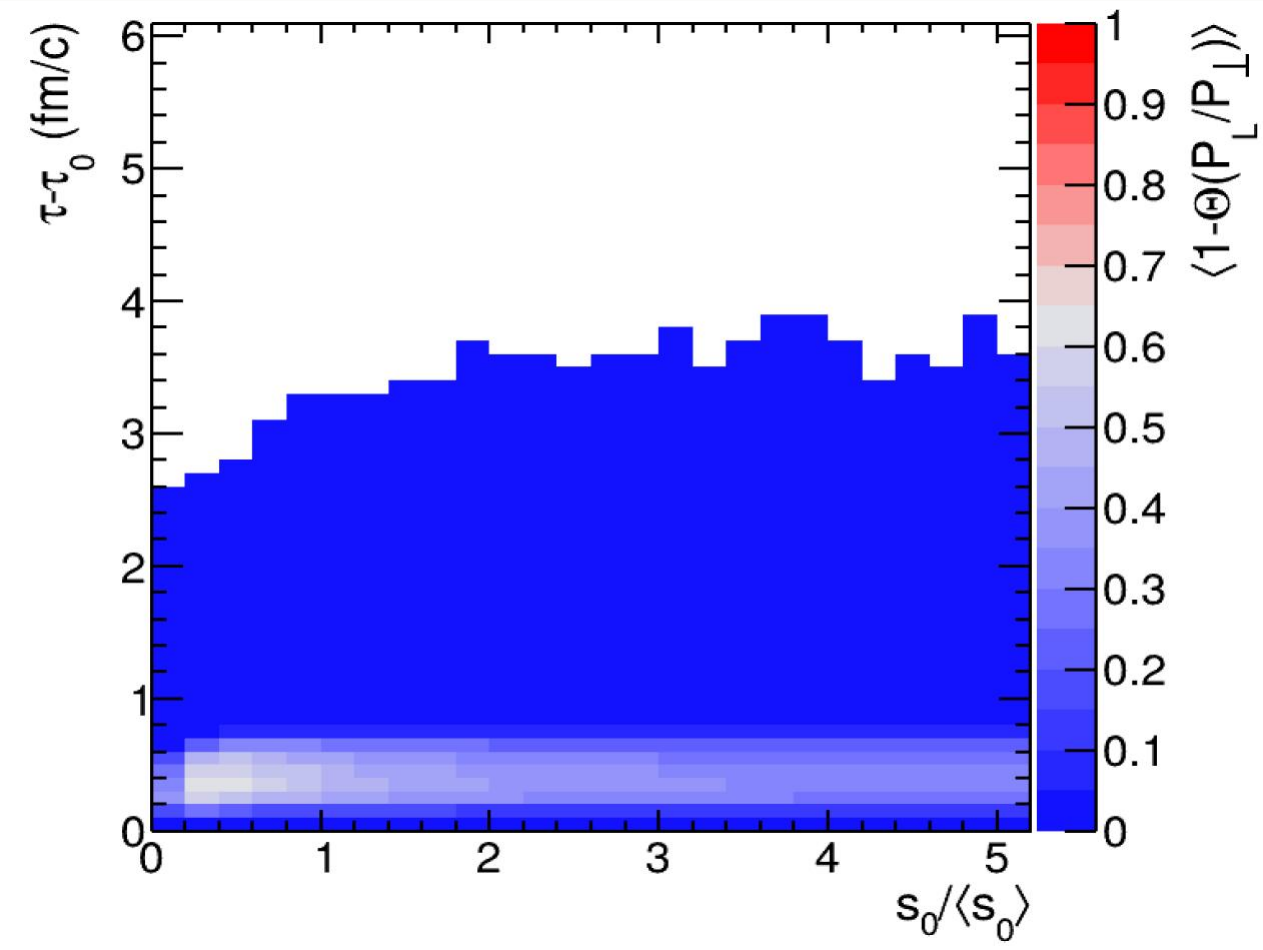

$\langle 1-\Theta(P_L/P_T)\rangle$

VAH, small-mass, $(P_L/P_T)_0$=0.4, τ0=0.12 fm/c, (η/s)min=0.16

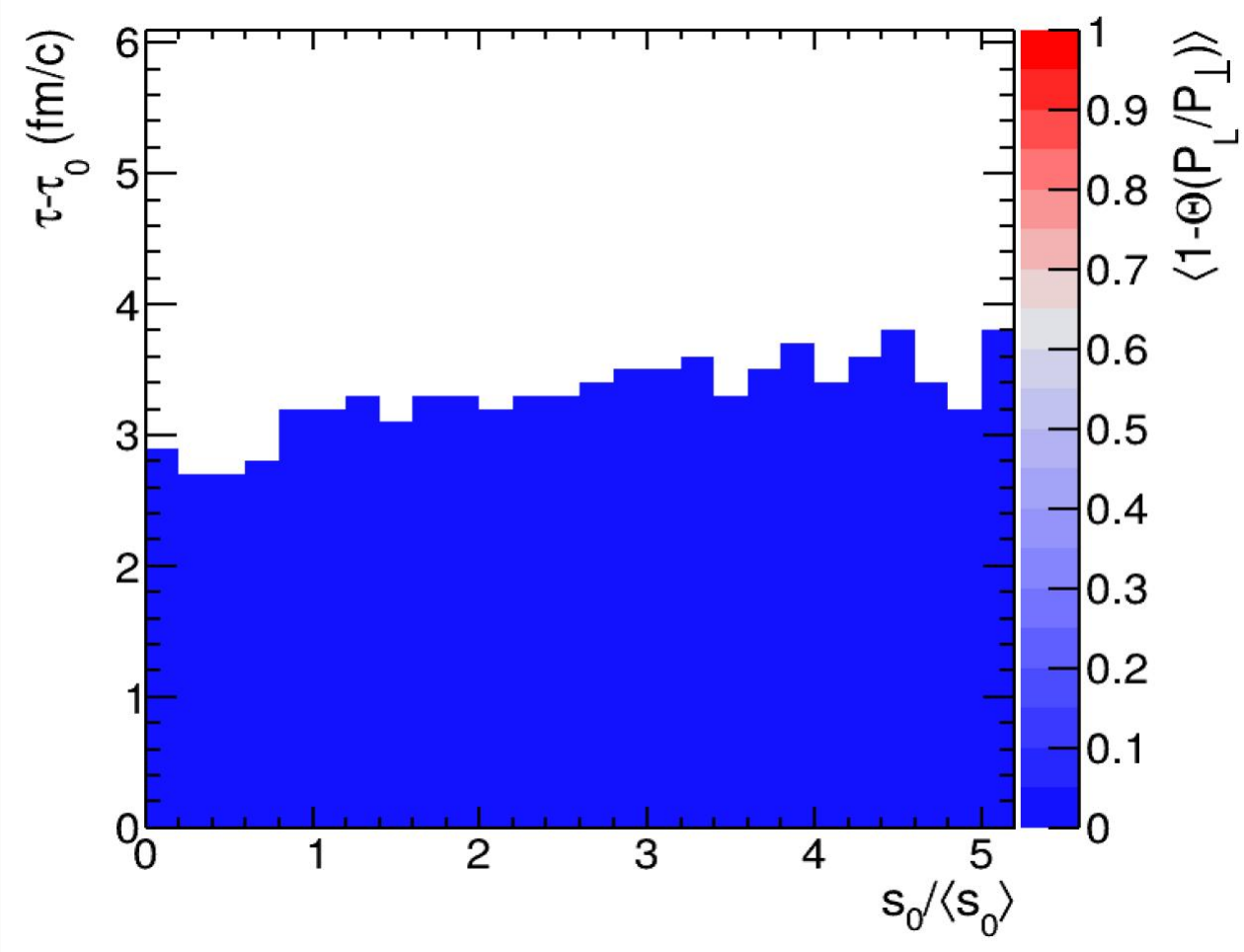

VAH, m(T), $(P_L/P_T)_0$=0.4, τ0=0.12 fm/c, (η/s)min=0.16

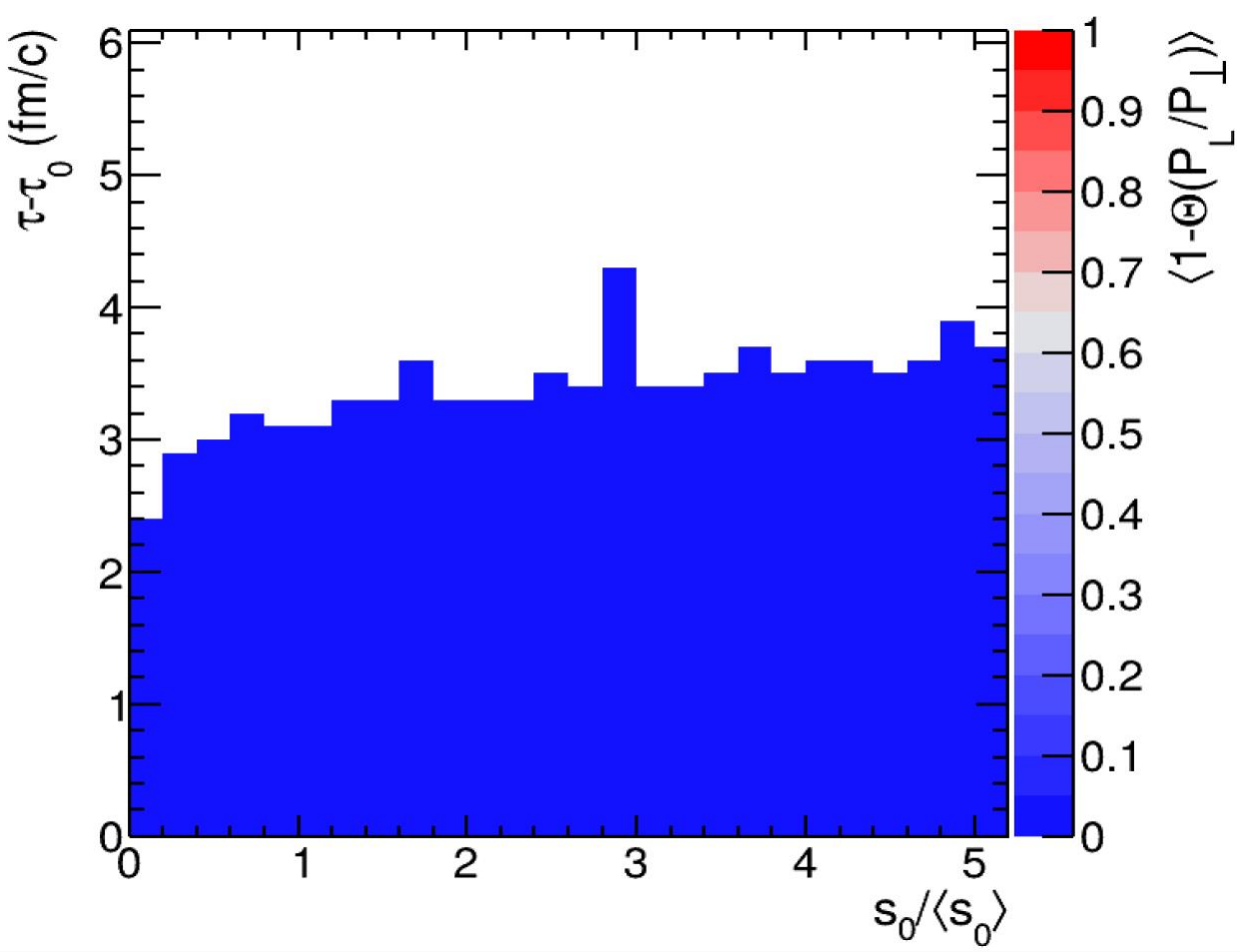

$\langle Re_\pi^{-1} \rangle$

VH, small-mass, $(P_L/P_T)_0$=0.4, τ0=0.12 fm/c, (η/s)min=0.16

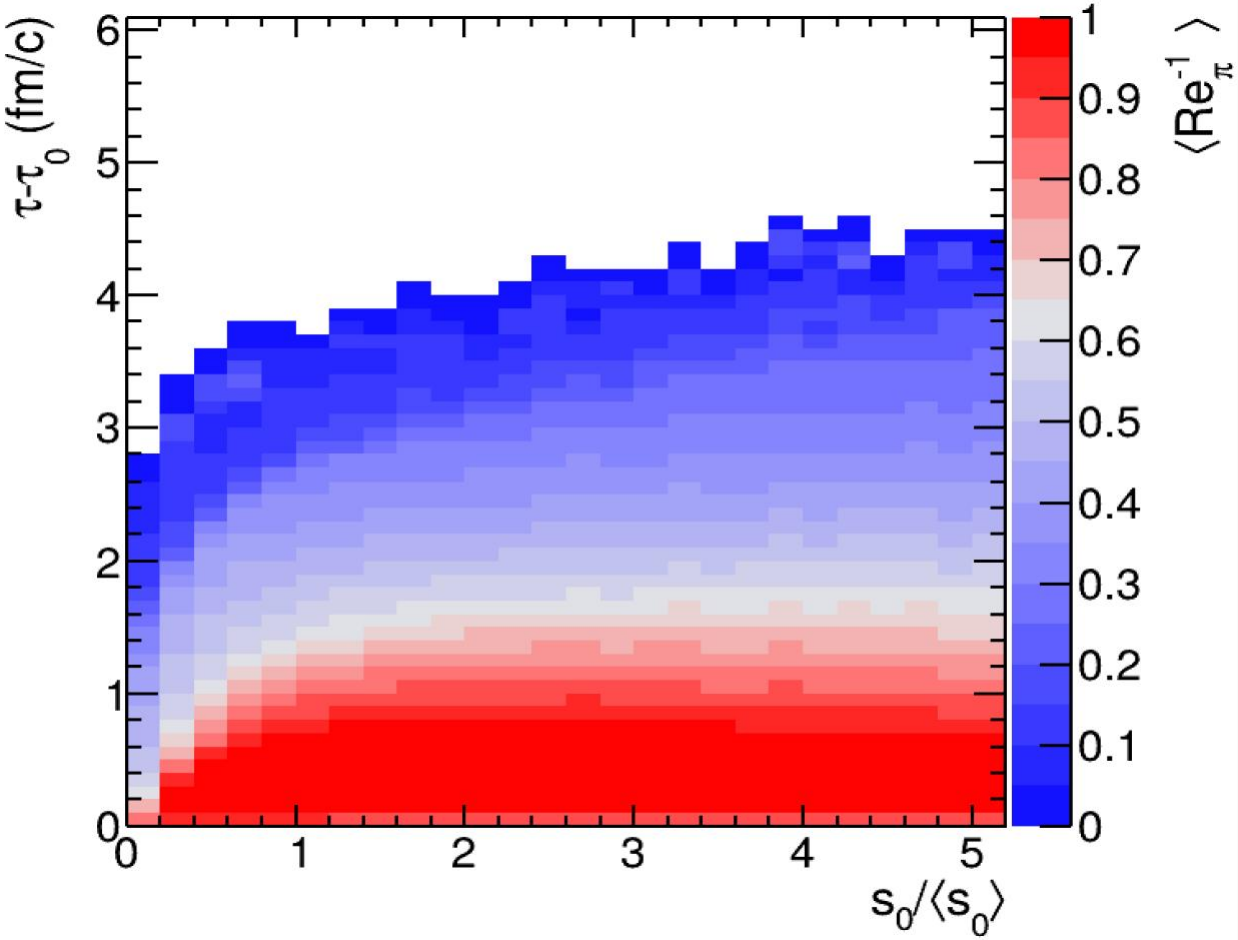

VH, m(T), $(P_L/P_T)_0$=0.4, τ0=0.12 fm/c, (η/s)min=0.16

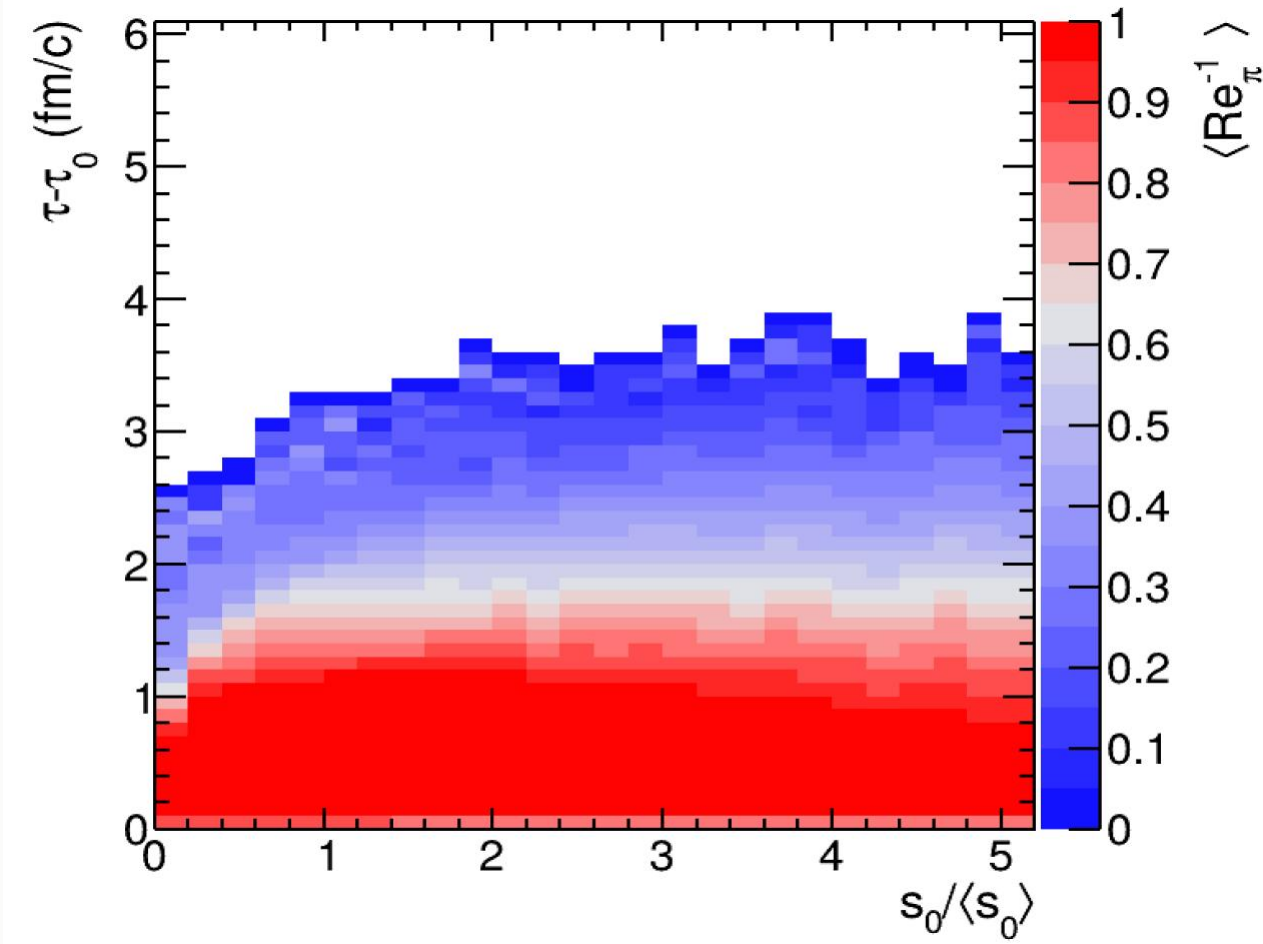

$\langle Re_\pi^{-1} \rangle$

VAH, small-mass, $(P_L/P_T)_0$=0.4, τ0=0.12 fm/c, (η/s)min=0.16

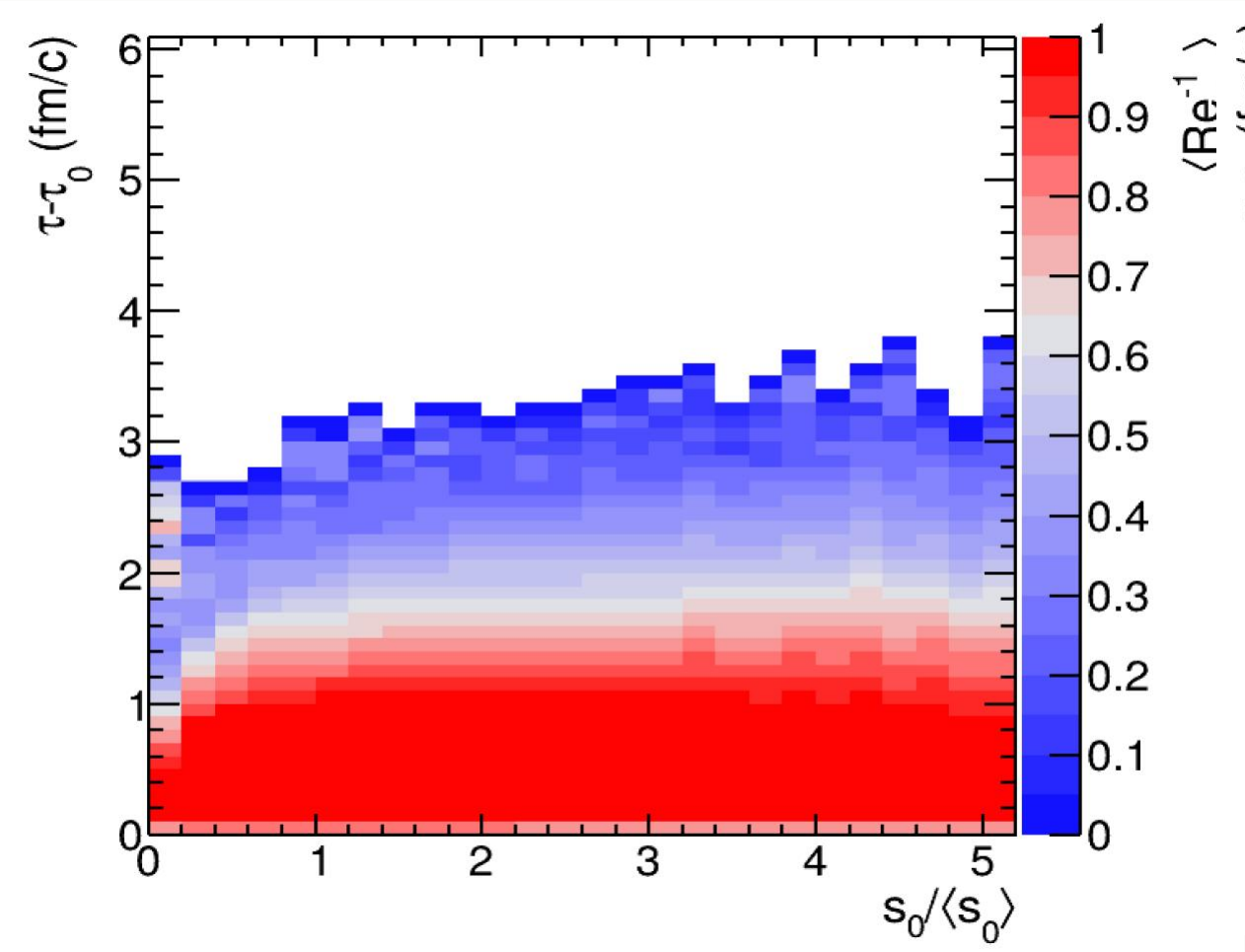

VAH, m(T), $(P_L/P_T)_0$=0.4, τ0=0.12 fm/c, (η/s)min=0.16

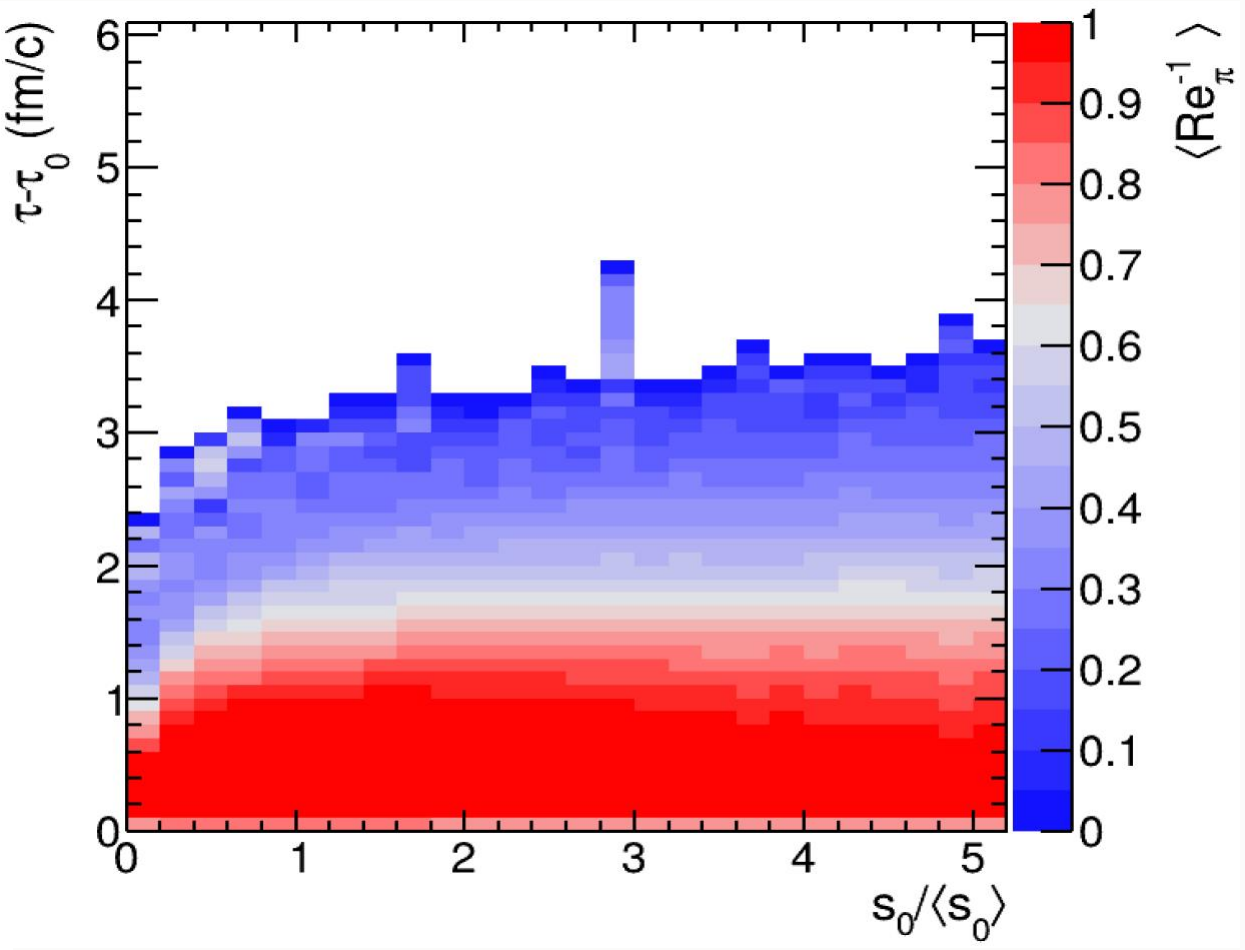

$\langle Re_{\delta\pi}^{-1} \rangle$

VAH, small-mass, $(P_L/P_T)_0$=0.4, τ0=0.12 fm/c, (η/s)min=0.16

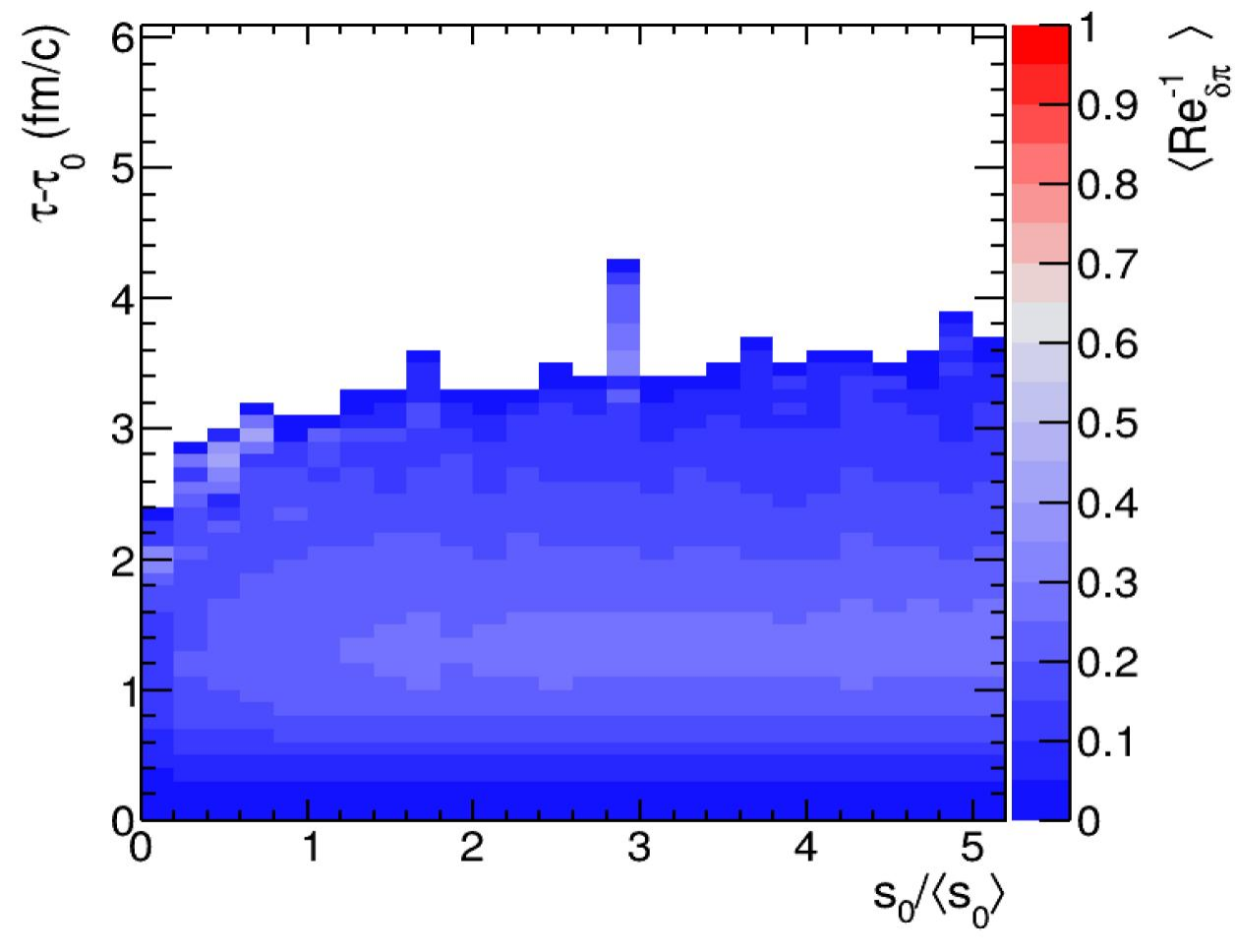

VAH, m(T), $(P_L/P_T)_0$=0.4, τ0=0.12 fm/c, (η/s)min=0.16